

PROGRESSION OF BREAST CANCER METASTATIC
DISEASE AND SUBSEQUENT OSTEOLYTIC BONE
DEGRADATION MEDIATED BY ONCOSTATIN M

By

Ken Tawara

A thesis

submitted in partial fulfillment

of the requirements for the degree of

Master of Science in Biology

Boise State University

May 2011

BOISE STATE UNIVERSITY GRADUATE COLLEGE

DEFENSE COMMITTEE AND FINAL READING APPROVALS

of the thesis submitted by

Ken Tawara

Thesis Title: Progression of Breast Cancer Metastatic Disease and Subsequent
Osteolytic Bone Degradation Mediated by Oncostatin M

Date of Final Oral Examination: 23 March 2011

The following individuals read and discussed the thesis submitted by student Ken Tawara, and they evaluated his presentation and response to questions during the final oral examination. They found that the student passed the final oral examination.

Cheryl L. Jorcyk, Ph.D. Chair, Supervisory Committee

Julia T. Oxford, Ph.D. Member, Supervisory Committee

Cynthia Keller-Peck, Ph.D. Member, Supervisory Committee

The final reading approval of the thesis was granted by Cheryl L. Jorcyk, Ph.D., Chair of the Supervisory Committee. The thesis was approved for the Graduate College by John R. Pelton, Ph.D., Dean of the Graduate College.

ACKNOWLEDGEMENTS

I would like to thank my thesis advisor and mentor, Dr. Cheryl Jorcyk, who provided me the great opportunity to work in a cancer biology lab in a capacity beyond that of a typical master's degree graduate student. In the lab, I was able to expand my skill sets beyond the laboratory, to improve my communication skills, manage supplies, learn the headaches of bookkeeping, and learn the responsibilities that come with reaching the rank of "Lab Guru." I am also very grateful for the opportunity to attend many conferences with the lab and give countless poster and oral presentations. These opportunities have given me a lot of confidence in public speaking that I previously did not have. Also, I am thankful for the opportunity of teaching a molecular cancer lab has given me great insight into how teaching can be very enjoyable and rewarding.

I would also like to thank my thesis committee members, Dr. Julia Oxford and Dr. Cynthia Keller-Peck, for guiding my project and giving me insight into new ways of finding the answers that I'm looking for. I would also like to thank the committee members for editing my manuscripts and providing me with help to make them as best as they can be. Finally, I would also like to thank Dr. Randy Ryan for providing the groundwork on Oncostatin M that made my project and the various projects in the lab possible.

ABSTRACT

Breast cancer is the most diagnosed cancer in women and is the second most common cancer-related death for women worldwide. While the primary tumor itself is not lethal, the metastases that disrupt vital organ functions pose a significant clinical challenge. Seventy percent of women with metastatic breast cancer have metastases to the bone, which is the most significant cause of morbidity for these patients. Oncostatin M (OSM) is a pleiotropic cytokine that plays a role in the immune system, wound repair, and haematopoiesis. OSM was previously considered for anticancer therapy due to its anti-proliferative effects against breast cancer cells *in vitro*. However, recent studies in the literature and from our lab suggest that OSM increases the metastatic potential of breast cancer cells. OSM has been shown to increase angiogenesis through the induction of VEGF and invasion through the release of MMP family of proteases. However, the exact role that OSM has on the metastatic cascade of breast cancer remains unclear. In this study, we attempted to elucidate the role of OSM on breast cancer metastases in an *in vivo* and in an *in vitro* mouse model of breast cancer. The results indicate that OSM increases pro-metastatic characteristics on 4T1.2 murine mammary cancer cells *in vitro*. OSM induced detachment and various factors that are thought to promote metastases and bone degradation such as VEGF, COX-2, IL-6, and HIF1 α . In an *in vivo* orthotopic 4T1.2 mouse model of breast cancer, OSM also increased the metastatic burden to the lung, spleen and the liver *in vivo*, while tumor

growth was unaffected. In an *in vitro* co-culture model of the metastatic bone microenvironment, OSM and murine mammary cancer cells synergistically increased osteoclast differentiation and activity. Furthermore, inhibition of VEGF, COX-2, IL-6, or HIF1 α attenuates osteoclast differentiation. Our data suggest that OSM might be a useful target for individualized anticancer therapies on cancer patients with high level of serum OSM concentrations and may help prevent metastases and bone destruction in breast.

TABLE OF CONTENTS

ACKNOWLEDGEMENTS	iii
ABSTRACT	iv
LIST OF FIGURES	x
INTRODUCTION	1
Cancer Metastasis	2
Oncostatin M and Its Pro-Metastatic Effects	3
Bone Homeostasis	5
OSM and IL-6 in the Bone Microenvironment	7
Bone Metastases	9
Mechanism of Tumor Metastasis to the Bone	11
OSM and IL-6 Production by Cancer Cells in the Bone Microenvironment May Facilitate Osteolysis	12
Mouse Models of Breast Cancer Metastases	13
Summary	15
MATERIALS AND METHODS	17
Cell Lines	17
Inhibitors, siRNA, and Antibodies	17
Enzyme Linked Immunosorbent Assay	18
Reverse-Transcriptase PCR Analysis	19
Cell Detachment and Proliferation	20

Western Blot	20
Animals and Tumor Cell Injections	21
Animal Sacrifice and Post-Sacrifice Analysis	22
Plasmid Construct Design	23
Transfections	24
Co-cultures for Generation of Conditioned Media	25
Bone Marrow Cell Extraction	25
Osteoclastogenesis Assay	26
Bone Resorption Assay (Mouse Calvaria)	27
Bone Resorption Assay (Osteologic Plates)	28
Statistical Analysis	29
RESULTS	30
Basal OSM and OSMR Expression Levels Are Higher in 4T1.2 Cells Than in 66c14 Cells	30
OSM Inhibited Proliferation of Both 66c14 and 4T1.2 Cells, but Induced Detachment of Only 4T1.2 Cells	31
OSM Induced the Expression of HIF1 α in Both 4T1.2 and 66c14 Cell Lines but Induced VEGF Expression Only in 4T1.2 Cells	32
OSM Induced COX-2 Expression in Both 4T1.2 and 66c14 Cell Lines	33
Recombinant OSM, Injected Interperitoneally, Increased Metastasis in an <i>in vivo</i> 4T1.2 Model of Mammary Cancer	33
4T1.2 and 66c14 cells Overexpressing mOSM Exhibited Similar <i>in vitro</i> Characteristics as Cells Treated with rmOSM	35
66c14 ^{OSM} Cells Have Increased Tumor Growth Rate and Reduced Metastasis <i>in vivo</i>	37
4T1.2 ^{OSM} Cells Failed to Produce Thriving Tumors and Had Minimal Metastases in the Lung	38

OSM Synergistically Induced Osteoclastogenesis with 66c14 Cells in the Presence of Non-Adherent Bone Marrow Cells	39
OSM Overexpressing 66c14 Cells Increased Osteoclast Differentiation in Bone Marrow Cells	41
m-CSF, VEGF, and HIF1 α May Play a Role in 66c14- and OSM-Mediated BM Osteoclast Differentiation	41
Both Osteoblasts and OSM Increased Osteoclast Differentiation in BM Cultures	43
OSM and 4T1.2 Cells Increased Bone Resorption of Mouse Calvaria	44
OSM and 4T1.2 Cells Promote Osteoclast Differentiation of RAW264.7 Monocytic Cells	45
Conditioned Media From 4T1.2 Cells Treated with OSM Increased Osteoclast Differentiation of RAW264.7 Cells	46
OSM Increased VEGF and IL-6 Secretion Independently of HIF1 α in 4T1.2 Cells	47
VEGF and IL-6 Neutralizing Antibodies Inhibited OSM-Mediated Osteoclast Differentiation in 4T1.2 + RAW264.7 Cell Co-Cultures	48
OSM and Murine Breast Cancer Cells Increased RAW264.7 Cell-Derived Osteoclast-Mediated Bone Resorption	49
DISCUSSION	51
OSM Increases Pro-Metastatic Markers in 4T1.2 and 66c14 Cells <i>in vitro</i> Which Lead to Increased Metastases <i>in vivo</i>	51
Overexpressing OSM in 66c14 and 4T1.2 Cells <i>in vitro</i> Leads to Similar Characteristics as Exogenous OSM but Cause Drastic Changes <i>in vivo</i>	57
OSM in Conjunction with 66c14, but Not 4T1.2 Mammary Tumor Cells, Increases Osteoclast Differentiation of Non-Adherent Bone Marrow Cells	62
4T1.2 Cells Need Osteoblasts to Increase Osteoclastogenesis and Osteoclast Activity of Non-Adherent Bone Marrow Cells	65
4T1.2 Cells in Conjunction with OSM Increased Osteoclastogenesis in RAW264.7 Cells	67

Conclusion	72
REFERENCES	73
APPENDIX A	88
Figures	
APPENDIX B	157
Interleukin-6 Review Manuscript	

LIST OF FIGURES

Figure A.1:	Schematic Diagram of Generalized Metastatic Steps Necessary for Cancer Cells from Primary Tumors to Reach Secondary Sites	89
Figure A.2:	OSM Induces Pro-Metastatic Effects in Mammary Cancer Cells	91
Figure A.3:	CXCR4/CXCL12-Mediated Chemokine Attraction to the Bone	93
Figure A.4:	66c14 and 4T1.2 Mouse Mammary Carcinoma Cells Metastasize to Different Organs When Injected Orthotopically into Balb/c Mouse	95
Figure A.5:	The Metastatic 4T1.2 Cells Have More Intrinsic OSM Signaling	97
Figure A.6:	OSM Inhibits Proliferation of 66c14 and 4T1.2 Cells but Only Induces Tumor Cell Detachment of 4T1.2 Cells	99
Figure A.7:	OSM Increases VEGF Secretion by 4T1.2 but Not 66c14 Cells, While HIF1 α Expression is Induced by OSM in Both 66c14 and 4T1.2 Cells	101
Figure A.8:	OSM Increases COX-2 Expression in 66c14 and 4T1.2 Cells	103
Figure A.9:	Injection of Recombinant Mouse OSM (rmOSM) Increases Metastases but Not Tumor Growth <i>in vivo</i> in an Orthotopic 4T1.2 Mouse Model	105
Figure A.10:	In the 4T1.2 Mouse Models, the Size of Metastases Differs Depending on rmOSM Treatment, While the Number of Lung Metastases Changes with Tumor-Ulcerative Status	107
Figure A.11:	OSM-Treated Mice Have More Bone Metastases and Potentially Reduced Bone Integrity	109
Figure A.12:	Mouse OSM Expression Plasmid Design	111
Figure A.13:	Overexpression of OSM in 66c14 and 4T1.2 Cells Transfected With the pcDNA3.1+OSM Construct	113

Figure A.14: OSM-Overexpressing 66c14 and 4T1.2 Cells Depict Similar Characteristics to Parental Cells Treated with rmOSM	115
Figure A.15: OSM-Overexpressing 66c14 Cells Grow Much Faster than Vector Control Cells <i>in vivo</i> in an Orthotopic 66c14 Mouse Model	117
Figure A.16: OSM-Overexpressing 66c14 Cells Have Reduced Numbers of Metastases, but Larger Total Metastatic Volume Compared to 66c14+Vector Cells <i>in vivo</i> in an Orthotopic 66c14 Mouse Model	119
Figure A.17: OSM-Overexpressing 4T1.2 Cells Fail to Grow and Metastasize <i>in vivo</i> in an Orthotopic 4T1.2 Mouse Model	121
Figure A.18: 4T1.2 ^{OSM} -Injected Mice Have a Much Higher Survival Rate	123
Figure A.19: Schematic Demonstrating Preparation of Pre-Osteoclasts for Osteoclastogenesis Experiment	125
Figure A.20: 66c14 Mouse Breast Cancer Cells and OSM Synergistically Increase Osteoclastogenesis with Non-Adherent Bone Marrow (BM) Cells ...	127
Figure A.21: Representative Images of TRAP+ Cells Detected in Osteoclastogenesis Assays	129
Figure A.22: As with the Addition of Recombinant OSM, 66c14 ^{OSM} Cells Increase Osteoclast Differentiation of BM Cells in the Presence of RANKL	131
Figure A.23: 66c14 Cells Express Pro-Osteoclastic Markers Analyzed via ELISA on Osteoclastogenesis Culture Supernatants, While Expression of RANKL Is Unchanged As Analyzed by Western Blot	133
Figure A.24: Suppression of HIF1 α by the HIF1 α Inhibitor YC-1 Inhibits 66c14+OSM-Mediated Osteoclast Differentiation of BM Cells	135
Figure A.25: Schematic Diagram of Osteoclastogenesis Co-Culture Experiments with Osteoblasts	137
Figure A.26: Osteoblasts, in Conjunction with OSM, Increase the Number of Multi-Nucleated TRAP+ Cells in Osteoclastogenesis Experiments	139
Figure A.27: Osteoclast Activity is Higher in Cultures Containing 4T1.2 Cells	141

Figure A.28: Schematic of Osteoclastogenesis Co-Culture Experiments Including RAW264.7 Cells	143
Figure A.29: RAW264.7 Monocytic Cell Lines Undergo Osteoclastogenesis in Response to OSM-Stimulated 4T1.2 Cells but Not 66c14 Cells ...	145
Figure A.30: Conditioned Media from OSM-Treated Cancer Cells Increases Osteoclastogenesis of RAW264.7 Cells and Is Mediated by HIF1 α	147
Figure A.31: 4T1.2 Cells Produce VEGF and IL-6 in Response to OSM	149
Figure A.32: Neutralizing Antibodies to VEGF and IL-6 Inhibit Osteoclastogenesis in RAW264.7 Cells	151
Figure A.33: Conditioned Media from 66c14 but Not 4T1.2 Cells Treated with OSM Significantly Increases RAW264.7 Cell-Derived Osteoclast Activity	153
Figure A.34: Model of Osteoclastogenesis	155

INTRODUCTION

Breast cancer is the most commonly diagnosed cancer in women worldwide, and approximately 400 thousand women succumb to the metastatic disease each year (1). In the United States, the mortality rate for metastatic breast cancer is about 40 thousand women per year (2). Despite significant recent advancements in understanding the metastatic process, many of the specific factors involved are still unknown. Metastasis of breast cancer cells to sites such as bone, lung, brain, liver, and other vital organs poses a major clinical challenge and generally leads to a poor prognosis. Bone is the most common site of metastasis for metastatic breast cancer patients, occurring with approximately 70% probability, and is the most significant cause of morbidity for these patients (3).

The process of metastases is not only variable between patients with different types of breast cancer, but the course of metastatic disease is also unpredictable even between patients with the same type of primary breast tumor. It is now thought that a part of this variability between patients could be explained by the differences in the levels of pro-inflammatory cytokines (4-6). In particular, interleukin-6 (IL-6) and IL-6-related cytokines may play a major role in the progression of cancer metastasis, patient morbidity, and mortality (7-9). OSM, belonging to the IL-6 family of cytokines, has also been implicated in playing a role in the progression of metastatic disease (10-13).

In this study, we attempted to explicate the role of OSM in cancer progression, metastases, and osteolysis in an *in vitro* and *in vivo* model of mouse mammary cancer.

Cancer Metastasis

During the progression of malignant disease, morbidity and mortality do not occur due to the primary tumor in the majority of the cases. Metastasis of the primary tumor cells to secondary vital organs leads to disruption of the normal physiological functions of the organs. For example, metastasis of cancer cells to the lung can lead to disruption of the normal respiratory process, while metastasis to the brain can cause disruption of the cognitive and autonomic physiological processes. As cells accumulate mutations, the normal cells become hyperplastic and eventually detach from their surroundings and become mobile by releasing proteases that degrade the extracellular matrix. Overall, the cell can gain a more mesenchymal phenotype. This process has been described as the epithelial to mesenchymal transition (EMT), which has recently been thought to be an important first step in the metastatic cascade (14). Once the cancer cells become mobile, they can eventually intravasate into the local blood or lymphatic system, thus causing the cancer cell to enter the circulatory system or lymph system respectively. Most cancer cells that do enter the circulatory system do not survive due to the body's innate immune response which kills a large portion of cancer cells (15, 16). Some of the cells are able to extravasate from the circulatory system at a secondary site and then grow a secondary tumor (Figure A.1).

While the exact mechanisms describing the extravasation process are widely unknown, it has been thought that the microenvironment of the secondary site can

provide a favorable location for the cancer cell to survive. For example, the lung provides ample oxygen, while other organs such as the liver provide a high amount of glucose, and the bone contains a large supply of growth factors embedded in the bone matrix; all of which help the cancer cells grow faster (17). The mechanism governing the homing aspect of the cancer cells is thought to be due to a chemokine-mediated stimulation of cancer cell mobility, causing the cells to move towards the highest concentration gradient of chemokines. This effect has been demonstrated by the high expression of C-X-C chemokine receptor type 4 (CXCR4), C-C chemokine receptor type 10 (CCR10), and other chemokine receptors on breast cancer cells leading the cells to respond to specific chemokine ligands expressed at secondary sites, and thus aiding in the overall metastatic cascade (18). Once these cancer cells reach the metastatic site, they have to successfully evade the immune system in order to avoid natural killer cells, cytotoxic T-cell, dendritic cell, or macrophage cell-mediated necrosis or apoptosis (19-23). In a recent study, it has been demonstrated that regulatory T-cells co-migrate with cancer cells to the secondary metastatic site to suppress the local innate immune response (24). Potent immune-activating pro-inflammatory cytokines such as oncostatin M (OSM) and IL-6 have also been demonstrated to promote tumor survival, invasion, and metastasis (13, 25).

Oncostatin M and Its Pro-Metastatic Effects

OSM is a pleiotropic cytokine of the IL-6 family generally considered a pro-inflammatory cytokine that has important functions in the immune system cascade (11, 26). In addition, OSM has demonstrated pro-differentiating activities for

haematopoietic stem cells and is an important cytokine for fetal liver development to support fetal hepatic cell-mediated hematopoiesis (27). Although the roles of OSM in inflammation, immune system functioning, as well as in hematopoiesis are well characterized, its roles in bone metabolism and breast cancer metastasis are not well understood. Early results from *in vitro* analysis of the effect of OSM on human breast cancer cells indicate that OSM is a potent inhibitor of breast cancer cell proliferation (28). Thus, OSM was previously considered a potential breast cancer therapeutic drug. Current research indicates, however, that OSM may increase the metastatic potential of human breast cancer cells via induction of increased mobility and invasiveness, and the upregulation of various genes related to angiogenesis such as vascular endothelial growth factor (VEGF) (12, 13, 29) (Figure A.2). OSM also induces the expression of various oncogenes including c-fos, c-myc, transforming growth factor alpha, and epidermal growth factor receptor (10). Furthermore, OSM has been shown to stimulate the secretion of factors related to bone metastasis and osteolysis such as VEGF, receptor activator of nuclear factor kappa-B ligand (RANKL), and cyclooxygenase-2 (COX-2) (30, 31).

OSM has been thought to promote the phenotypic transition of breast, lung, and pancreatic cancer cells from an epithelial to a mesenchymal phenotype, leading to reduced substrate attachment, increased *in vitro* invasion, and an upregulation of metalloproteinases that degrade the local extracellular matrix (12, 13, 32, 33).

Cytokines such as OSM, IL-6, and other gp-130-related factors have important effects in maintaining bone integrity and is normally carefully regulated. However, during

disease states such as osteoarthritis and bone metastases, the balance of OSM and other IL-6/gp130 cytokines is severely disrupted, leading to bone degradation (34).

Bone Homeostasis

Bone homeostasis is maintained by a variety of cell types that control remodeling of the bone matrix. Two important cell types that mediate bone homeostasis are osteoblasts and osteoclasts. Osteoblasts contribute to the bone matrix by production of type I collagen, deposition of hydroxyapatite crystals into the collagen matrix, and regulation of osteoclast activity (35, 36). Osteoblasts are of mesenchymal origin and differentiate from pre-osteoblasts primarily via bone morphogenic proteins (BMP) that induce runt-related transcription factor 2 (Runx2), leading to increased alkaline phosphatase activity (35). Conversely, osteoclasts resorb bone matrix (37) and differentiate from the hematopoietic cell lineage upon stimulation in a differentiation process called osteoclastogenesis.

Osteoclastogenesis is mediated by cytokines such as receptor activator of NF- κ B ligand (RANKL), macrophage-colony stimulating factor (M-CSF), and parathyroid hormone related protein (PTHrP) (37-40). RANKL, a membrane-bound ligand, is produced primarily by osteoblasts (41). Osteoclastogenesis is regulated primarily via osteoblast-produced RANKL and osteoprotegerin (OPG) expression, a decoy receptor to RANKL that suppresses RANKL activity (42). Osteoblasts that express RANKL have cell-to-cell contact with osteoclasts via ligand-receptor binding between RANKL and RANK (receptor activator of NF- κ B) (43). RANKL functions to promote osteoclast differentiation and activity through stimulation of various pathways including the

phosphatidylinositol-3 kinase (PI3K) pathway and the mitogen activated protein kinase (MAPK) pathway. The MAPK pathway leads to the activation of c-fos, nuclear factor of activated T-cells-2 (NFAT2), and other transcription factors (44, 45). Cleavage of RANKL from the cell membrane by proteinases such as matrix metalloproteinase-7 (MMP7) yields the soluble form of RANKL (sRANKL), which has a physiological function that is still disputed, although both anti- and pro-osteoclastogenic effects have been reported (41, 46-48).

To make room for the new bone being deposited by the osteoblasts, osteoclasts need to differentiate and resorb bone in a controlled manner. As osteoclasts differentiate in response to pro-osteoclastic factors, the single nucleated pre-osteoclastic cells undergo cell fusion to create multi-nucleated cells (45). Some large osteoclasts can contain upwards of thirty or more nuclei. These multinucleated osteoclasts then create a segregated zone; a sealed area between the osteoclast and the bone matrix. Osteoclasts subsequently release hydrogen ions into the segregated zone, solubilizing the hydroxyapatite crystals and promoting acid-activated proteinases such as cathepsin K to degrade the collagen matrix (45, 49). Osteoblasts generate new matrix to fill the vacant area. The rate at which osteoclasts differentiate and resorb bone is carefully regulated by osteoblast-produced RANKL and OPG. Other cells in the bone matrix such as osteocytes, terminally-differentiated osteoblasts, are able to regulate the generation and resorption of bone matrix by affecting osteoblast and osteoclast activity (50). Osteocytes inhibit osteoclast activity by releasing factors such as transforming growth factor-beta (TGF β). When osteocytes are mechanically stimulated by a shock to the bone resulting in dynamic fluid movement in their mechanoreceptor, they promote

alkaline phosphatase activity in osteoblasts by cell-to-cell contact, increasing bone mineralization and turnover (51-54). In this manner, damaged sections of the bone are removed and replaced with new bone matrix by osteoblasts.

In normal bone, homeostasis is constantly maintained and bone integrity is preserved by a continuous cycle of bone renewal. However, when cancer cells metastasize to the bone, the complex and balanced interplay of the cells becomes disrupted, leading to a pathologic condition that compromises bone integrity. One of the many characteristics that bone-homing cancer cells have in common is the release of copious levels of cytokines such as OSM and IL-6, as well as high expression levels of chemokine receptors such as CXCR4, which are important in facilitating bone invasion and growth of metastatic lesions (55-57).

OSM and IL-6 in the Bone Microenvironment

IL-6, much like OSM, is a major pleiotropic, pro-inflammatory cytokine which plays a role in immune response, hematopoiesis, cell differentiation, wound repair, and bone remodeling (58, 59). Reactive stromal cells in the bone, which are primarily mesenchymal stem cells in the bone marrow, are thought to regulate bone metabolism in response to various stimuli (60, 61). Inflammation in the bone caused by injury or disease increases the expression of IL-6 and OSM by reactive stromal cells of the bone and infiltrating monocytes and macrophages, promoting bone remodeling as seen by higher osteoclast activity (62). IL-6 and OSM production is stimulated in response to prostaglandin E2 (PGE2), interleukin-1 beta (IL-1 β), lipopolysaccharides, TGF β) and other various mediators of inflammation (63-68). IL-6 binds to its heterotrimeric

receptor, consisting of two gp130 subunits and an IL-6 receptor subunit, on target cells and activates the signal transducers and activators of transcription (STAT), mitogen-activated protein kinase (MAPK), and phosphatidylinositol-3 kinase (PI3K) (69-72). On the other hand, OSM binds to the OSMR β gp130 heterodimer but this also leads to STAT3, MAPK, and PI3K activation (73-75). OSM and IL-6 signaling through the Jak/STAT3 pathway can lead to expression of RANKL from osteoblast/stromal cells, causing direct stimulation of osteoclast differentiation and activity, resulting in bone destruction (76, 77).

Studies using IL-6 knockout mice have demonstrated that IL-6 is necessary for upregulating osteoclast activity and bone resorption *in vivo*. IL-6 knockout mice were shown to be protected from increased osteoclast activity and differentiation when their bones were injected with the arthritis-inducing antigen heat-killed *Mycobacterium tuberculosis* (78). IL-6 knockout bones that received antigen injections had less RANKL and interleukin-17 (IL-17) expression as well as reduced osteolysis and cartilage destruction near the site of injection compared to wild-type mice. IL-17 is a pro-inflammatory and pro-osteoclastogenic cytokine implicated in arthritis and tumorigenesis that is produced in CD4⁺ helper and tumor infiltrating T-cells when activated by IL-6 (79, 80). Additional mouse studies have demonstrated that inhibition of IL-6 activity, with an IL-6 receptor (IL-6R) antagonist that inhibits downstream receptor signaling, reduced bone resorption (81). These results suggest that IL-6 plays a major role in the upregulation of additional pro-osteoclastic factors essential for osteoclast activity. Similar studies using OSM and OSMR knockout mice reveal that

OSM signaling is important to the maintenance of hematopoietic stem cells in the bone marrow, which may result in reduced osteoclast differentiation and activity (82, 83).

Regulation of OSM and IL-6 expression is important in preventing excessive bone resorption and maintaining bone integrity. 17- β -estradiol has also been shown to suppress the activity of IL-6, OSM, and other STAT3-dependant cytokines by inhibiting STAT3 via upregulation of the protein inhibitor of activated STAT3 (PIAS3) (84). In addition, testosterone also decreases IL-6 expression and OSM activity by inhibiting NF- κ B activity and the hypothalamic-pituitary-adrenal axis; normally a potent stimulator of IL-6 production. Both of these result in testosterone-mediated bone-preserving effects (85-87). On the other hand, cytokines such as OSM and TNF α also inhibit aromatase activity, leading to a reduction in the overall 17- β -estradiol concentration in local organs such as adipose tissue and bone (88). This may point to a mechanism where both OSM and 17- β -estradiol competitively inhibit each other. Therapies that involve suppression of testosterone or 17- β -estradiol are effective against androgen-dependent prostate and breast cancer respectively, however bone density decreases significantly with these therapies leading to an increased chance of developing osteoporosis and pathological fractures (89). This loss of bone density may be due to the increase in OSM and IL-6 in the bone from the suppression of androgen hormones.

Bone Metastases

Various types of cancers metastasize to the bone, including breast, prostate, lung, thyroid, kidney, multiple myeloma, melanoma, and neuroblastoma (90-94). Not all

types of bone metastases affect the bone in the same way, though for all cancer types, bone is only compromised at the site of metastasis. For example, breast cancer predominantly causes osteolytic lesions, resulting in an upregulation of osteoclast activity and subsequent decreased bone density and integrity that may lead to fractures (91, 95). Conversely, prostate cancer results in primarily osteoblastic lesions that are caused by cytokine-induced upregulation of osteoblast activity and subsequent increased bone density (95). These types of bone metastases cause thickening of the bone, resulting in the possibility of nerve compression, vertebral fusion, and spinal cord compression depending on the location of the metastases. In contrast to what is found in normal bone where collagen fibers are highly organized and tightly packed, bone created by osteoblastic lesions contain disorganized, loosely packed collagen fibrils (40). This leads to a high degree of bone brittleness, increase in potential fractures, and pain as the normal bone is replaced by abnormal bone created by the osteoblastic lesions. A subset of prostate cancers may also cause osteolytic lesions due to the expression of different cytokines that promote osteoclast activity rather than osteoblast activity (96). Multiple myeloma causes only osteolytic lesions. Other cancers, including lung, kidney, melanoma, neuroblastoma, and thyroid carcinomas, result in primarily osteolytic lesions, but osteoblastic lesions occur occasionally (94, 95, 97, 98).

Metastasis of the primary tumor to the bone occurs in about 60-75% of patients with breast cancer, prostate cancer, neuroblastoma, or multiple myeloma (90-92, 99). Metastasis to the bone from other cancers such as lung, kidney, and thyroid only occur in 30-50% of patients (93). Molecular mechanisms involved in the capacity of a cancer cell to metastasize to the bone are not completely understood. However, inflammatory

cytokines such as OSM and IL-6 appear to play a role in several steps of the metastatic process.

Mechanism of Tumor Metastasis to the Bone

It is not well understood how cancer cells locate the bone, grow, and thrive in an environment vastly different from their host environment. After the initial stages of metastases are complete and the cancer cells are in the circulatory system, there are certain signals thought to be expressed by the bone, which attract cancer cells to that location. In particular, it is thought that cancer cells are attracted to bone marrow due to the relatively high levels of CXCL12 expression by osteoblasts which attracts any CXCR4 positive cells (100). In most cases, bone metastatic cells tend to overexpress CXCR4 levels, which promotes cell metastasis to the bone. For that reason alone, therapeutics are being considered to block the CXCR4/CXCL12 axis to help prevent possible bone metastases (101).

Addition of cytokines such as OSM makes the CXCR4/CXCL12 axis more potent, possibly leading to increased bone metastasis. Cytokines such as OSM and IL-6, that activate NF- κ B through the STAT3 or c-Jun pathway, can increase the expression of CXCR4 in breast cancer cells, leading to increased cell mobility (102). Once the cancer cells have localized to the bone marrow, they can mediate increased levels of CXCL12 production by the bone stromal cells and osteoblasts in a OSM-dependant manner, further promoting cancer cell migration to the bone (103). The increased CXCL12 production can then in turn activate other CXCR4 receptors in the area and stimulate local production of IL-6 (104). In this way, bone metastases can increase the

likelihood that other circulating tumor cells will home to bone by increasing the level of CXCR4 and CXCL12 activity in the bone marrow (Figure A.3).

Once cancer cells colonize to bone, they have to deal with the challenges of cell survival and growth in a foreign environment. It is well known that the bone is a reservoir of a complex mixture of growth factors (105) that are released as the bone is degraded by metastatic lesions. The mixture of growth factors include TGF β , insulin like growth factor 1, insulin like growth factor 2, platelet derived growth factor, bone morphogenic proteins, fibroblast growth factors, and other factors that when released, can significantly improve tumor cell survival and growth (17). These factors promote expression of pro-survival signals in the cancer cells such as B-cell lymphoma 2 (Bcl-2) and inhibit apoptotic signals such as caspases. These factors also support further osteoclast differentiation and activity, leading to increased release of more growth factors, which stimulate increased cancer cell growth and accelerated bone destruction. Thus, a vicious positive feedback loop is established. The accelerated bone destruction can quickly incapacitate a patient and lead to rapid loss of bone integrity causing fractures, massive pain, and loss of mobility.

OSM and IL-6 Production by Cancer Cells in the Bone Microenvironment May Facilitate Osteolysis

OSM and IL-6 produced by cancer cells initiate a variety of downstream signaling cascades that can lead to bone destruction. Although many cancer cell types that metastasize to the bone endogenously produce and secrete high levels of cytokines such as OSM and IL-6, others stimulate the surrounding stromal cells to release copious

amounts of these cytokines. A proposed mechanism for cancer cell-induced osteoclastogenesis and osteoclast activity is that the cancer cells are able to promote an inflammatory response in osteoblasts (106, 107). The activation of inflammatory signals from osteoblasts in response to cancer cell-conditioned medium *in vitro* has been shown to cause an upregulation of PGE₂, promoting the production of OSM and IL-6, which activates osteoclasts via stimulation of RANKL and PTHrP production (18, 62, 63). This effect was seen in breast cancer cells, oral squamous carcinoma cell lines, and in neuroblastoma cells (55, 106, 108).

In a recent study, conditioned media from human breast cancer cells (MDA-MB-231) induced an inflammatory response in osteoblasts by NF- κ B activation within the osteoblasts (107). The amplified activity of NF- κ B has been shown to stimulate COX2/prostaglandin E2 synthase activity, which can result in PGE₂ production (109). High levels of PGE₂ have also been shown to promote potent, pro-osteoclastic effects by stimulating osteoblasts and immune cells to secrete various factors such as RANKL, IL-6, and OSM causing a positive feedback loop (68, 110, 111). However, to date, the mechanism involving OSM and cancer metastasis to the bone and subsequent cancer-mediated osteoclast differentiation and osteolysis is unclear at best.

Mouse Models of Breast Cancer Metastases

In order to study metastasis and cancer progression in a living system, animal models are frequently used. The species *mus musculus* is the most commonly used animal for the *in vivo* studies of cancer and metastatic events. There are many types of mice available for the study of metastatic disease. Transgenic or knockout mice with

defective tumor suppressor genes or overexpressed oncogenes lead to spontaneous development of carcinogenesis, which allows study of the initiation of tumorigenesis (112). Alternatively, carcinogens can also be used to study spontaneous carcinogenesis or for the development of screening tools for testing potential genotoxic agents in mice with defective DNA repair genes (113).

To study the progression of cancer using human cancer cell lines in mice, athymic or immune deficient mice are needed to prevent immune rejection of the xenografted human tumor (114). Although the study of human cancer in animal models may provide the most clinically relevant data for cancer treatment, some data suggests that the lack of an immune system in this model may skew the results. Recent publications state the importance of the immune system in the progression of metastatic disease, concluding that it may have a dual role in promoting and inhibiting metastases (115). Also, cytokines such as OSM, IL-6, and their downstream signaling molecules are heavily involved in the immune cascade which makes the use of immuno-compromised mice inappropriate.

An alternative to using immuno-compromised mice is to establish cancer cell lines harvested from spontaneous tumors developed in immuno-competent inbred mouse strains. Cancer cells developed in this manner make the cells immuno-compatible with the host inbred mouse strain, and are said to be syngeneic (116). Syngeneic mouse tumor models have recently been shown to be a valuable experimental model for testing immuno-modulating drugs and potential therapeutic agents (117, 118). For these reasons, our laboratory uses syngeneic mouse mammary cancer cell lines that were originally derived from a Balb/c inbred mouse.

66c14 and 4T1.2 cells are clonal subpopulations derived from a single spontaneous mouse mammary tumor in a Balb/c mouse which were selected for specific metastatic profiles. When injected orthotopically into a mouse's mammary fat pad, 66c14 cells only metastasize to the lung and lymph nodes, whereas 4T1.2 cells metastasize to the lung, liver, brain, and bone (119) (Figure A.4).

In our *in vivo* model, we inject these cancer cells orthotopically into the 4th mammary fat pad of Balb/c mice. This type of anatomically correct grafting of foreign cells, also called orthotopic transplantation or injection, allows the mammary carcinoma cells to grow in their native organ and subsequently grow a tumor. The tumor cells then invade into the surrounding extra cellular matrix, and metastasize into various other organs in a manner that mimics a natural progression of the disease in a mammalian organism model. This is distinct from other methods of transplanting cancer cells into mice, such as intra-cardiac or tail-vein injections, that bypasses the need to first grow a tumor and metastasize. These routes of cancer cell injection bypass the intravasation step of the metastatic cascade and prevent the study of the entire metastatic cascade. In this study, 4T1.2 or 66c14 cells are orthotopically injected to the 4th mammary fat pad of Balb/c mice to study the effect of OSM on the entire metastatic cascade.

Summary

The work presented in this study can be divided into 3 main goals. i). To characterize the effect of exogenous OSM on 4T1.2 and 66c14 cells *in vitro* and *in vivo*. ii). To generate OSM overexpressing 4T1.2 and 66c14 mouse mammary cancer cell lines and characterize the effect of endogenously over-expressed OSM on cancer cells'

behavior both *in vitro* and *in vivo*. iii). To determine some of the mechanisms governing the pro-osteoclastic effects observed when OSM is added in conjunction with 4T1.2 and 66c14 cells to pre-osteoclast cells. Results gained from this study will help elucidate the role of OSM in the metastatic cascade, as well as in breast cancer bone metastases. The results presented here will also lead to further studies on OSM-mediated effects on the ability of cancer cells to induce osteoclast differentiation. Furthermore, the results present a rationale for the development of therapeutics that inhibits OSM signaling to reduce cancer metastases and bone destruction.

MATERIALS AND METHODS

Cell Lines

4T1.2 and 66c14 mouse mammary adenocarcinoma cells were obtained from Robin L. Anderson at the Peter Macillan Cancer Institute (Melbourne, Australia). RAW264.7 mouse monocytic cell lines and UMR106 rat osteoblastic cell lines were obtained from American Type Culture Collection (Rockville, MD). All tissue culture media and supplements were obtained from Hyclone (Logan, UT). 4T1.2 and 66c14 cells were cultured in alpha MEM media supplemented with 10% fetal bovine serum (FBS), 1X sodium pyruvate, and 1X penicillin-streptomycin. RAW264.7 and UMR106 cells were maintained in DMEM media supplemented with 10% FBS, 1X sodium pyruvate, and 1X penicillin-streptomycin. All cells were maintained at 37°C, 5% carbon dioxide, and 95% humidity.

Inhibitors, siRNA, and Antibodies

Recombinant mouse proteins, mCSF, OSM, and RANKL and antibodies against VEGF and IL-6 were purchased from R&D systems (Minneapolis, MN). A biotinylated mOSM antibody was also purchased from R&D systems. A chemical inhibitor to HIF1 α , 5-[1-(phenylmethyl)-1H-indazol-3-yl]-2-furanmethanol (YC-1), and a chemical inhibitor to COX-2, (N-[2-(cyclohexyloxy)-4-nitrophenyl]-methanesulfonamide

(NS398) were purchased from Cayman chemicals (Ann Arbor, MI). HIF1 α siRNA and COX-2 siRNA were purchased from Applied Biosystems (Carlsbad, CA). Control non-targeting siRNA was purchased from Dharmacon Thermo Scientific (Lafayette, CO). Rabbit polyclonal antibodies against mouse HIF1 α , COX-2, and RANKL were purchased from Novus Biologicals (Littleton, CO). Goat polyclonal antibody against mouse parathyroid hormone related protein (PTHrP) was purchased from Santa Cruz Biotech (Santa Cruz, CA).

Enzyme Linked Immunosorbent Assay

To measure secreted OSM in conditioned media, a standard direct ELISA was developed. Conditioned media from mouse mammary cancer cells was incubated overnight in 96-well ELISA plates (Thermo Fisher Milford, MA). Plates were washed with PBS containing 0.05% Tween-20 (PBS-T) and blocked using PBS containing 1% IgG-free BSA (Jackson Immunological West Grove, PA). mOSM biotinylated antibody was used as the detection antibody (1 μ g/ml diluted in PBS) and 100 μ l was added per well and incubated overnight. Plates were washed again with PBS-T and incubated with streptavidin-horse radish peroxidase (HRP) at 1:200 dilution (R&D systems). After a final wash, 100 μ l of 1-Step Ultra TMB-ELISA substrate (Thermo Pierce Rockford, IL) per well was added and incubated for 30 minutes. The reaction was stopped using 2N sulfuric acid (50ng/ml), and read and corrected at 450nm and 570nm, respectively.

In order to measure mouse VEGF, mCSF, RANKL, IL-6, OPG, TGF β , and TNF α in conditioned media, DuoSet ELISA kits for each of the factors were purchased

from R&D systems and used according to manufacturer instructions. The ELISA plates, color substrates, wash buffers, and BSA from above were also used with this kit.

Reverse-Transcriptase PCR analysis

In order to quantify differences in the level of OSMR expression between cell lines, a RT-PCR was carried out. 4T1.2 and 66c14 cells were grown to 70% confluency and RNA was extracted using the RNA-STAT 60 (Tel-test) reagent purchased from Tel-test (Friendswood, Tx). RNA-STAT 60 reagent was used (1ml/5x10⁵ cells) and allowed to solubilize the cells for 20 minutes. Chloroform (200 µl/1ml of RNA-STAT 60) was added followed by vortexing for 10 seconds, and centrifugation at 12,000rpm. The upper aqueous layer was transferred to a new tube containing isopropanol (0.5ml/1ml of RNA STAT60) used, followed by vortexing for 10 seconds and incubation on ice for 15 minutes. The mixture was centrifuged at 12,000rpm and the supernatant discarded. The pellet was washed by adding 1ml of 75% ethanol, mixed and centrifuged at 12,000rpm and the supernatant discarded. This wash step was repeated two additional times. The RNA was allowed to air-dry in a sterile environment and resuspended with 0.1% TE buffer.

cDNA was generated from this RNA using the reverse transcriptase kit (Ambion) with the two-step RT reaction protocol. The cDNA generated from the RT reaction was used in a PCR reaction at (25 µl) containing 2.5 µl of 10x PCR buffer, 2.5mM DNTP's, 10mM primers, 5U goTaq polymerase, (Promega, Madison, WI) and 2 µl cDNA. The following primers for mOSMR were used:

Fwd primer: TAGACTGAACATATCCAACACCA

Rev primer: TCCATGGATTGGCTCATCTGGCA

Amplifications were carried out as follows: initial denaturation at 94°C for 2 minutes, followed by 30 cycles of 94°C for 1 min, 60°C for 1 min, 72°C for 1 min, then a final extension of 72°C for 10 minutes. The PCR products were electrophoresed on a 1% Tris-Agarose gel containing 0.5 µg/ml of ethidium bromide at 100 volts for 45 minutes. The gels were imaged using a Kodak Image station and exposed for 40 seconds. Band densities were calculated using the ImageJ software (NIH), and data was presented as a percentage difference in OSMR expression.

Cell Detachment and Proliferation

4T1.2 or 66c14 cells were seeded in 24-well plates (1×10^3) with 1ml of complete media, and treated with +/- 25 ng/ml of OSM. Detached cells were collected from the supernatant and were counted after 48 hours of OSM treatment. Cell viability was assessed with trypan blue stain (Hyclone) viable, unstained cells were counted on a hemocytometer. To assess proliferation, attached cells were trypsinized using 0.25% trypsin, and counted every 2 days, 8 days total, using a hemocytometer. (The average of 3-4 squares counted were multiplied by 10^4 .)

Western Blot

4T1.2 and 66c14 cells were grown to 50% confluency for HIF1 α Western blots and 75% confluency for COX-2, RANKL or PTHrP Western blots. The cells were treated with 25 ng/ml of OSM in serum free media. The cells were then lysed using an RIPA buffer (25 mM Tris-HCl (pH 7.6), 150 mM NaCl, 1% NP-40, 1% sodium

deoxycholate, 0.1% SDS) containing 10 µl/ml of protease inhibitor cocktail (SIGMA, p-8340), and electrophoresed on a 7.5% bis-acrylamide gel. The proteins were transferred to a nitrocellulose membrane using a Bio-Rad (Hercules, CA) Mini-Gel Transblot apparatus.

The membrane was blocked overnight in 5% non-fat dry milk (NFDm) in TBS with 0.05% Tween-20 (TBS-T). The primary antibodies against HIF1 α , COX-2, RANKL, and PTHrP were added at 1:1000 dilution in TBS-T+5% NFDm, applied to the membrane at room temperature for 1 hour under gentle agitation and washed for 3 x 10 minutes in TBS-T. The secondary antibody, anti-rabbit-HRP or anti-goat-HRP (Jackson Immunologicals, West Grove, PA) was used at 1:5000 concentration in TBS-T+5% NFDm and incubated for 45 minutes under gentle agitation and washed for 5 x 10 minutes in TBS-T. Enhanced chemiluminescence reagents were applied for 1 minute (Thermo Pierce) and the membranes exposed to an X-ray film (Thermo Pierce) for 1-15 minutes. Band thickness and pixel density were calculated using the Image J software, and data shown as a percentage difference in protein levels.

Animals and Tumor Cell Injections

Six-week-old female BALB/c mice were obtained from the National Cancer Institute's Animal Production Area, Frederick, MD. Each mouse was anesthetized by i.p. injection of 6.25 mg/kg of sodium pentobarbital, or inhalation of 2.5% isoflurane. 1×10^5 4T1.2 or 66c14 cancer cells, or various stably transfected cell lines were injected orthotopically into the 4th mammary fat pad of Balb/c inbred mice. For groups that received rmOSM injections, OSM was injected into the mice intraperitoneally (IP) after

tumors became palpable (50ng/g twice a week), while control mice received PBS injections. All animal studies were conducted in accordance with the protocol approved by the Institutional Animal Care and Use Committee (IACUC) at the VA Medical Center (Boise, ID).

Starting at 2 weeks post injection, tumor length and width were measured with mechanical calipers, 3 times a week and tumor volume extrapolated using the following equation (tumor volume = (length x width²) /2). Survival endpoint was defined by the IACUC as tumor size greater than 20mm in diameter, 10% or more weight loss, or appearance of cachexia.

Animal Sacrifice and Post-Sacrifice Analysis

Mice were sacrificed via CO₂ asphyxiation, followed by cervical dislocation. The brain, lung, spleen, liver, and kidneys were collected and preserved in 10% formalin. The femur, tibia, hip and spine were collected and preserved in 10% formalin. Any metastases to the organs were noted, and the numbers of metastases on the lungs were counted using a 40X dissecting scope. Digital X-ray radiographs of the bone were taken with the X-ray operating at 60kVp and 50mV. The femur, tibia, and spine were separated and embedded into paraffin using the following procedures. Bones were soaked in 10% ethylenediaminetetraacetic acid (EDTA) for 2 weeks to decalcify the bones. Bones were then placed in increasing concentrations of ethanol diluted in ddH₂O from 15%, 30%, 50%, 70%, 80%, 90% 95%, to 100%, with at least 2 hours incubation in between. Then bones were placed in a solution of 50% ethanol and 50% tert-butanol for 2 hours, followed by 100% tert-butanol for another 2 hours. Finally, bones were

placed in a mixture of 50% tert-butanol and 50% liquid paraffin for 2 hours, and then the bones were left in 100% paraffin overnight at 55°C. The paraffin embedded bones were placed in molds and allowed to harden. Paraffinized bones were sectioned to 4 micron thickness and stained with hematoxylin and eosin (H&E). The sections were also stained with a tartrate resistant acid phosphate (TRAP) stain kit using the slide staining protocol as per manufacturer's instructions (Sigma St. Louis, MO). The bone sectioning and staining were done by Bengt Phung (College of Idaho Caldwell, ID). The H&E stained bone sections were sent to a veterinary pathologist, Dr. Kathleen Potter (Washington State University, Pullman, WA) for analysis.

Plasmid Construct Design

For the creation of a mOSM overexpressing plasmid, a 888 bp full-length mouse OSM cDNA fragment was generated by RT-PCR of mouse thymus RNA and cloned into pcDNA3.1+ (Invitrogen, Carlsbad, CA) plasmid with EcoRI ends yielding a 904 bp insert (Figure A,12). The work for creating the full-length mouse OSM cDNA fragment was done by Lynda Zhang (Boise State University, Boise, ID), and the cDNA was inserted to pcDNA3.1+ plasmid by Dr. Sujatha Kadaba (Boise State University, Boise, ID). The plasmids were sequenced by Idaho State University (Pocatello, Idaho). All plasmids were purified using the Pureyeild Maxiprep kit (Promega Madison, WI) before use for transfections.

Transfections

Stable transfection of cells was performed using the Lipofectamine LTX +PLUS transfection reagent kit (Invitrogen). Cells were grown to 60-70% confluency on a 6-well plate. One μg of pcDNA3.1+mOSM, or pcDNA3.1 empty vector was mixed with 6 μl of Lipofectamine LTX, 2 μl of PLUS reagent, and 100 μl of serum-free alpha-MEM media. These mixtures were incubated for 30 minutes at room temperature and added to each wells on a 6-well plate. The cells were transfected for 72 hours, trypsinized, serially diluted in G418 selection media and added to 96-well plates. For 66c14 cell transfections, 650 $\mu\text{g}/\text{ml}$ of G418 in complete alpha-MEM was used to select the transfected cells. For 4T1.2 cell transfections, 450 $\mu\text{g}/\text{ml}$ of G418 in complete alpha-MEM was used to select the transfected cells. Single colonies were grown in 96-well plates for 2 weeks in selection media, and the conditioned media was collected tested for OSM expression by ELISA. OSM overexpressing 4T1.2 cells were designated 4T1.2^{OSM}, and OSM overexpressing 66c14 cells were designated 66c14^{OSM}.

For transient knockdown of factors using siRNA, cells were plated into 6-well or 24-well plates at 50% confluency. HIF1 α siRNA, COX-2 siRNA or control siRNA were used at a final concentration of 25 nM and the cells were transfected with Hiperfect Transfection reagent (Qiagen Valencia, CA). For siRNA treatment in a 24-well plate format, each well received 100 μl of serum free media containing 3 μl Hiperfect Transfection reagent and 25 picomoles of siRNA (5 μl of stock siRNA at 5 μM). The mixture was incubated at room temperature for 10 minutes, and 100 μl of the mixture was added to each well containing cells with 1ml of complete media. The cells

were allowed to incubate in the transfection media for 18-48 hours at 37°C, 5% CO₂, and 95% humidity before experimentation. For short term experiments, transfections lasted overnight (about 18 hours), and for long-term experiments (6 days or longer), transfections lasted 48 hours.

Co-Cultures for Generation of Conditioned Media

In order to study changes in mRNA expression, protein expression, and function, single cultures and co-cultures of various cells were treated, followed by collection of conditioned media for analysis and additional assays. At harvest, cells were no more than 85% confluent. 4T1.2, 66c14, RAW264.7 and UMR106 cells were treated with +/- OSM, +/- HIF1 α siRNA, +/-COX-2 siRNA and +/- YC-1 48-72 hours and their conditioned media and cell lysates were collected after analysis and subsequent assays. Additionally co-cultures of RAW264.7+4T1.2 or +66c14 cells and UMR106+4T1.2 or +66c14 were also treated as described above and the conditioned media and cell lysates were also collected. The conditioned media was then used for either osteoclastogenesis assays, bone resorption assays or the expressions of various factors were tested by ELISA. Cell lysates were either further processed for RNA extraction for RT-PCR, or used for Western blots.

Bone Marrow Cell Extraction

4-10 week old female Balb/c were sacrificed via cervical dislocation. The hind legs were removed, using sterile technique, and the muscles and tendons were carefully cleaned off from the femur and the tibia. The ends of the bones were cut off to expose

the bone marrow, and using a 23-gauge needle and syringe filled with α -MEM containing 10% FBS, the marrow was flushed out from the bones and pushed through a 40 μ m cell strainer. The cell mixture was then centrifuged at 90G to pellet the cells, and the supernatant was removed. Red blood cells were then lysed and removed using a 4 minute incubation in a ammonium chloride lysis buffer (144mM NH_4Cl , 17mM Tris-HCL pH7.4). After the 4 minute incubation, the lysis buffer was diluted with serum free DMEM or α -MEM media to increase the total volume by 4-fold. The cell mixture was centrifuged, the supernatant removed, and the cells were resuspended in α -MEM, plus 15% FBS. The cells were subsequently incubated at 37°C, 95% humidity, and 5% CO_2 for 48 hours. The adherent cells were discarded. The non-adherent cells were collected from the supernatant and used in subsequent osteoclastogenesis and bone resorption assays.

Osteoclastogenesis Assay

1×10^4 RAW264.7, or 1×10^5 bone marrow cells were added to each well in duplicate into a 24-well plate. In addition, 1×10^3 4T1.2 or 66c14 cells were added as well as +/- 25 ng/ml rmOSM, +/- 10 ng/ml rmRANKL, and 5 ng/ml of mCSF. Additionally, +/-HIF1 α siRNA, +/-COX-2 siRNA, +/- antiVEGF antibody, +/- anti IL-6 antibodies and +/-YC-1 were also added to the osteoclastogenesis co-cultures. Alternatively, conditioned media from 4T1.2 and 66c14 cells co-cultured with UMR106 cells treated with +/-OSM, +/- HIF1 α siRNA, +/- antiVEGF antibody, and +/- anti IL-6 antibodies were collected from cells and added to the wells containing bone marrow cells or RAW264.7 cells. The co-cultures were maintained for 7-10 days with out any

changes in the media and osteoclasts were stained using the tartrate resistant acid phosphate stain kit (Sigma St. Louis, MO). The cells were fixed using 300 μ l /well of a TRAP compatible fixing solution (65% acetone, 25% citrate buffer, and 10% of 37% formaldehyde) for 10 minutes.

In order to formulate the TRAP staining solution compatible for tissue culture staining, reagents were added in the following order to make enough solution for a single 24-well plate. 135 μ l of fast garnet GBC base solution was mixed with 135 μ l of sodium nitrite solution and incubated for 2 minutes at room temperature. The mixed solution was added to 12ml of ddH₂O. Then 135 μ l of naphthol AS-BI phosphoric acid solution was added to the H₂O solution. Finally, 500 μ l of acetate solution was added, followed by 270 μ l of tartrate solution. After rinsing the fixing solution out of the wells with ddH₂O three times, 450 μ l of the stain solution was added to each well and incubated at 37°C for 20 minutes. TRAP positive cells that were stained purple were counted and quantified per well.

Bone Resorption Assay (Mouse Calvaria)

4-10 week old female Balb/c mice were sacrificed via cervical dislocation. The calvaria from the mice were removed and the outer membrane on the skull was scraped off. The calvaria were halved and each piece was placed in one well of a 24-well plate. The calvaria were immersed in α -MEM with 10% FBS containing 1×10^5 non-adherent bone marrow cells with 5 ng/ml of mCSF. These cells were co-cultured with or without 1000 4T1.2 or 66c14 cells, +/- 25ng/ml rmOSM, and +/- 10ng/ml RANKL. The co-cultures were incubated for 10 days. To analyze, the supernatants were diluted serially

3 times with ddH₂O and assayed for released calcium levels using the calcium arsenazo III assay (Thermo scientific 51036). Calcium arsenazo reagent (200 µl) was added to each well of a 96-well plate along with 2 µl of the samples and 2 µl of the calcium standards, added in duplicate. The samples were then mixed and incubated for 1 minute and the absorbance was read at 650nm using a plate reader. Calcium levels present in α -MEM were subtracted in the final result.

Bone Resorption Assay (Osteologic Plates)

One thousand RAW264.7 cells with 5 ng/ml of mCSF suspended in 150 µl of α -MEM were placed in each well of a 16-well osteologic multi-test plate (354608, BD scientific, Franklin Lakes, NJ). One hundred and fifty microliters of conditioned media previously collected from co-cultured 4T1.2 and 66c14 cells with UMR106 cells treated with +/- 25ng/ml rmOSM, +/- NS398 were also added to the appropriate wells in the multi-test plate and were incubated at 37C, 5% CO₂, 95% humidity. Every 2-3 days for 10 days the media was replaced as needed with 150 µl fresh media with 5 ng/ml m-CSF, and 150 µl conditioned media. The wells were removed from the slides and were immersed in 5% bleach (0.3% sodium hypochlorite) to remove the cells. The multi-test plates were then washed thoroughly with ddH₂O. The plates were stained via the Von Kossa silver stain. The multi-test plates were immersed in 5% Silver Nitrate for up to 6 hours, or until the color was dark brown. The test plates were washed thoroughly with ddH₂O, the deposited silver was then fixed with 2% sodium thiosulfate, and the test plates were washed again with ddH₂O. The plates were allowed to dry and high

resolution images were taken by photo-microscopy. Pits were then analyzed using the Image J software, and area absorption was recorded.

Statistical Analysis

Data is displayed as means +/- standard error of the mean (SEM). Analyses of the data were performed using Student's t-test or analysis of variance where appropriate. Survival data was analyzed using the Log-Rank test. Contingency table analysis was done using the Fisher's exact test due to the relatively small sample size. Significance was assumed when $p < 0.05$.

RESULTS

Basal OSM and OSMR Expression Levels Are Higher in 4T1.2 Cells Than in 66c14 Cells

In order to characterize the basal levels of OSM and OSMR signaling, we analyzed the differences in OSM and OSMR expression levels between the 66c14 and 4T1.2 cell lines. To measure OSM expression, conditioned media was collected from 66c14 and 4T1.2 cells after 72 hours in a culture and analyzed for secreted levels of mouse OSM by ELISA. 66c14 cells secreted a total of 38 pg/ml of OSM over a 72 hour period, while 4T1.2 cells secreted a total of 105 pg/ml (Figure A.5A). The basal expression levels of OSM between the cell lines differ with the more metastatic 4T1.2 cells secreting almost 3-fold higher levels of OSM.

To determine basal levels of OSMR, we extracted mRNA from both cell lines, made cDNA, performed RT-PCR, and analyzed the products by electrophoresis. The OSMR band was much brighter for 4T1.2 cells than the 66c14 cells, and Image J was used to calculate the band intensity. There was a similar trend to what was seen with OSM levels, as 4T1.2 cells expressed 2.5-fold more OSMR than 66c14 cells (Figure A.5C). Overall, these results show that the more metastatic 4T1.2 cells have higher OSM and OSMR expression levels. This suggests possible increased autocrine OSM

signaling with 4T1.2 cells. These differences in OSM signaling may contribute to the different metastatic characteristics exhibited by the two cell lines.

OSM Inhibited Proliferation of Both 66c14 and 4T1.2 Cells, but Induced Detachment of Only 4T1.2 Cells

66c14 and 4T1.2 cells have different metastatic profiles (119), and we surmised this may be due, in part, to their differences in OSM and OSMR expression levels. Addition of recombinant OSM was tested to assess its ability to induce changes in certain metastatic characteristics such as tumor cell proliferation and detachment. To study the proliferation profile of these cells when they were treated with OSM, 25 ng/ml of OSM was added to the number of cell cultures and the cells were counted every other day for 7 days. OSM inhibited proliferation of both cell lines by about 20% and no significant differences in proliferation rate were detected between the cell lines (Figure A.6 A&B).

To study the ability of OSM to cause tumor cell detachment in the cell lines, OSM (25ng/ml) was added to sub-confluent cell culture flasks for 24 hours. 4T1.2 cells treated with OSM resulted in 2.5-fold more detached cells compared to untreated cells (Figure A.6D). In contrast, OSM did not seem to affect 66c14 cell detachment (Figure A.6C). In the population of detached 4T1.2 cells, less than 1% of the total cells counted were dead, as assessed by trypan blue staining, (data not shown) indicating that OSM did not affect cell viability. Overall, this data suggest that while OSM inhibits proliferation, it increases the propensity of the more aggressive 4T1.2 cells to detach.

**OSM Induced the Expression of HIF1 α in Both 4T1.2 and 66c14 Cell Lines
but Induced VEGF Expression Only in 4T1.2 Cells**

VEGF and HIF1 α are markers that implicate the induction of angiogenesis, increased pro-survival mechanisms, and the promotion of metastasis (120, 121). To determine ability of OSM to upregulate VEGF expression, sub-confluent cultures of either 66c14 or 4T1.2 cells were treated with OSM (25 ng/ml) for 72 hours. The supernatant was collected and the concentration of VEGF was determined via ELISA. Approximately 2,400 pg/ml of VEGF were secreted in 72 hours by 66c14 cells, regardless of OSM treatment (Figure A.7A). 4T1.2 cells, on the other hand, secreted very low levels of VEGF (50 pg/ml), and the addition of OSM increased VEGF secretion by about 16-fold (Figure A.7B). The significant difference between 66c14 and 4T1.2 VEGF secretion profiles suggests that 66c14 cells have high constitutive expression of VEGF, while 4T1.2 cells respond to OSM by upregulating VEGF.

To assess the ability of OSM to induce HIF1 α expression, we treated 4T1.2 and 66c14 cells with OSM (25ng/ml) at 50% confluency for 4 hours following an overnight serum-free starvation. Cell lysates were collected for Western blot analysis to determine HIF1 α expression in the cells. Both 66c14 and 4T1.2 cells showed OSM induced HIF1 α expression by over 10-fold (Figure A.7C), while in 4T1.2 cells, HIF1 α increased by 2.5-fold (Figure A.7D). These differences in fold changes may be due to 66c14's very low basal expression of HIF1 α , as the total OSM-stimulated HIF1 α levels appeared to be similar to each other by Western blot analysis (Figure A.7E). Taken together, OSM increased VEGF expression in 4T1.2 but not 66c14 cells and induced HIF1 α expression in both cell lines. These results suggest that OSM may

increase VEGF- and HIF1 α -promoted tumor-mediated angiogenesis and metastases *in vivo* in response to OSM.

OSM Induced COX-2 Expression in Both 4T1.2 and 66c14 Cell Lines

COX-2 expression has been linked to metastases, and its product, prostaglandin E2, is a potent pro-inflammatory factor, capable of causing inflammation-mediated angiogenesis (12). The effect of OSM on COX-2 expression was evaluated on 4T1.2 and 66c14 cells. Cell cultures were treated with OSM (25ng/ml) for 0-24 hours. Cells lysates were collected at different time points and assessed by Western blot analysis to determine COX-2 expression levels. OSM induced a 3.5-fold increase in COX-2 expression in 66c14 cells, which peaked at 12 hours and dropped slightly at 24 hours (Figure A.8A). On the other hand in 4T1.2 cells, OSM-induced COX-2 expression peaked earlier at 6 hours with a 3-fold induction, and expression of COX-2 remained steady through 24 hours (Figure A.8B). The more metastatic 4T1.2 cells responded earlier to OSM by producing COX-2 earlier, which may suggest the induction of pro-inflammatory effects via the COX-2 product, PGE2.

Recombinant OSM, Injected Intraperitoneally, Increased Metastasis in an *in vivo* 4T1.2 Model of Mammary Cancer

4T1.2 cells clearly demonstrated an increased response to OSM compared to 66c14 cells as shown by increased detachment, VEGF secretion, and a faster time to peak expression of COX-2. Thus, to test the effect of OSM on cancer cell growth and metastases *in vivo*, the more OSM-sensitive 4T1.2 cells were studied in a murine model

of mammary carcinoma. Considering the *in vitro* results, it was expected that mice treated with recombinant OSM would result in increased metastases and reduced tumor growth.

4T1.2 cells (1×10^5) were injected orthotopically into the 4th mammary fat-pad of five 4-week old female Balb/c mice. As soon as the tumor was palpable, rmOSM was injected twice a week interperitoneally (I.P.) at 50 ng/g, which correlates to 1 μ g of OSM for a 20 gram mouse. OSM did not significantly alter tumor growth *in vivo* compared to PBS injected control mice (Figure A.9A). The tumors were allowed to grow for 38 days and the mice sacrificed. OSM also did not alter the primary tumor burden at 38 days, as both groups had tumors that were 18% of body weight (Figure A.9B). However, OSM did increase the number of metastatic lesions seen in the lung by about 2-fold (Figure A.9C). In addition, the ratio of mice with metastases to the spleen and liver was higher in OSM-treated mice (Figure A.9D), Eighty percent of mice that received OSM injections but only 30% of control mice had metastases to the spleen. Additionally, 90% of mice that received OSM injections had metastases to the liver, while only 40% of control did.

When the sizes of metastases to the lung were analyzed, the mice that had OSM injections generally had smaller metastases than the control mice (Figure A.10 A&B). Mice that received OSM treatment had 2.5-times more “small metastases” (<0.5 mm) compared to control mice. On the other hand, mice that received OSM injections had 2-fold less “large metastases” (>0.5mm) compared to controls. Some mice also developed ulcerating tumors, and the mice that had ulcers on their tumor had almost double the number of lung metastases compared to mice that did not have ulcers (Figure

A.10C). There was no significant correlation between tumor ulceration rates and OSM treatment (data not shown).

To analyze bone metastases, X-ray radiographs and H&E histological stains were performed. Typical bone metastases appear as shadows in X-ray radiographs (Figure A.11B left) and in H&E stain as a tight cluster of cells with little space between the cells in H&E stains (Figure A.11B right). The H&E stained sections were analyzed by a veterinary pathologist, Dr. Kathleen Potter (Washington State University, Pullman, WA), for detection of metastases to the bone. Overall, the number of mice that had metastases to the bone was higher in mice that received OSM injections but this data was not statistically significant (Figure A.11A). A trend was also observed upon TRAP staining where the intensity of the TRAP stain was stronger in the bones of mice that received OSM injections. This may indicate increased osteoclast number and activity in OSM treated mice, however due to the sample size being too low, this was not statistically significant (Figure A.11C). Overall, injection of recombinant OSM had no effect on tumor growth or tumor burden while metastases increased. OSM may also have increased the number of active osteoclasts present in the bone, which would allow for the increased bone resorption needed for the osteolytic lesions seen in this model (30).

4T1.2 and 66c14 Cells Overexpressing mOSM Exhibited Similar *in vitro* Characteristics as Cells Treated with rMOSM

As the first step in characterizing the effects of endogenously produced OSM, we generated OSM overexpressing 4T1.2 and 66c14 cells. A 888bp mOSM cDNA was

generated by reverse transcriptase-PCR using RNA isolated from mouse thymus. The mOSM cDNA was inserted into the pcDNA-3.1 expression vector and the resultant plasmid and was used for transfections (Figure A.12).

To determine the amount of mOSM secreted by the stably transfected cells, the cells were grown in serum-free media for 48 hours and their conditioned media was analyzed by ELISA. In general, cells transfected with the mOSM-overexpressing construct displayed increased OSM secretion. In 66c14 cells, the highest producing colony was colony 61, which was later renamed 66c14^{OSM}. Colony 61 produced 100-fold more mOSM at (5 ng/ml after 48 hours) compared to untransfected cells and 50-fold more OSM compared to control cells transfected with the vector alone (Figure A.13A). With 4T1.2 cells, the maximal amount of mOSM expression achieved was 600 pg/ml by colony 51. This colony was chosen because it had a lower standard error in the ELISA data (Figure A.13B).

To test the functionality of the mOSM produced by the transfected 66c14 and 4T1.2 cells, OSM-induced tumor cell detachment and VEGF secretion was assessed. These experiments also allowed comparison between endogenous and exogenous OSM signaling. 66c14 colony 61 displayed 4-fold more detached cells compared to vector control and 4.5-fold more detached cells compared to untransfected 66c14 cells (Figure A.14A). The 4T1.2, colony 51 showed a 65-fold increase in detached cells as compared to vector control and untransfected cells (Figure A.14B).

Secreted VEGF levels, as measured by ELISA, were not altered in 66c14 colony 61 cells, as compared to controls. This is probably due to the fact that these cells have a very high basal expression of VEGF and the production pathway is likely saturated

leaving little room for extra OSM would to have any effect (Figure A.14C). On the other hand, 4T1.2 colony 51 cells produced a high level of secreted VEGF, which was 9-fold higher compared to vector control or untransfected cells (Figure A.14D). Overall, these results suggest that the *in vitro* effects between endogenously produced OSM and exogenously added recombinant OSM are similar.

66c14⁺OSM Cells Have Increased Tumor Growth Rate and Reduced Metastasis *in vivo*.

It has been previously shown *in vivo* that 66c14 cells are generally not a very aggressive cell line and their metastatic capacity is low compared to 4T1.2 cells (119). Previous *in vivo* experiments using 66c14 cells in a mouse model of mammary cancer revealed that I.P. injection of recombinant OSM did not effect tumor growth or metastases (data not shown). For that reason, we expected that OSM-overexpressing 66c14 cells will also behave similarly *in vivo* to the previous experiments and have similar tumor growth rates and metastases as mice with 66c14+vector tumors.

To study the effect of OSM-overexpressing 66c14 cells *in vivo*, 1×10^5 66c14⁺OSM or 66c14+Vector cells were injected into the 4th mammary fat pad of eleven 4-week old Balb/c female mice. 66c14⁺OSM tumors grew significantly faster than the 66c14+Vector tumors and reached nearly 6000 mm³ in tumor volume by the end of the experiment (Figure A.15). Total tumor burden was also 300% higher in 66c14⁺OSM tumor bearing mice compared to 66c14+vector tumor bearing mice (Figure A.16A). However, when comparing the total number of lung metastases, 66c14⁺OSM tumors surprisingly produced only 1-2 metastases per lung while the

66c14+Vector tumors produced over 10 metastases per lung on average (Figure A.16B). On the other hand, when total metastatic lesion volume was compared, 66c14^{OSM} mice had a 6-fold higher lung metastatic lesion volume compared to the 66c14+vector mice (Figure A.16C).

This discrepancy appeared to be due to a significant difference in the size of lung metastases. 66c14+vector mice had lung metastases that were on average smaller than 1 mm in diameter, while 66c14^{OSM} mice had lung metastases that were on average 2.25 mm in diameter (Figure A.16D). These differences in tumor diameter translate to a 6-fold increase in volume. In 66c14 tumor bearing mice, the results indicate that endogenously or locally produced OSM decreases metastatic events and increases proliferation dramatically causing both the tumor and the metastases to grow rapidly.

4T1.2^{OSM} Cells Failed to Produce Thriving Tumors and Had Minimal Metastases in the Lung

To study the effect of OSM overexpressing 4T1.2 cells *in vivo*, and to test the effect of endogenously/locally produced OSM, 1×10^5 4T1.2^{OSM} or 4T1.2+Vector cells were injected into the 4th mammary fat pad of 10 4-week old female Balb/c mice. 4T1.2^{OSM} tumors grew at the same rate as the 4T1.2+Vector tumors until day 16, at which point, 4T1.2^{OSM} tumors shrank in size to undetectable levels while 4T1.2+Vector tumors continued to grow (Figure A.17A). Mice with 4T1.2^{OSM} tumors had significantly lower tumor burden at less than 1% of bodyweight compared to 22% of bodyweight for 4T1.2+Vector tumor bearing mice (Figure A.17B). Similarly,

4T1.2⁺OSM tumor bearing mice had no lung metastases where as 4T1.2+Vector tumor bearing mice averaged 10 metastatic lesions per mice (Figure A.17C).

In order to assess mouse survival, an endpoint criterion was defined as tumors reaching 20 mm in diameter, 10% loss of bodyweight, or apparent cachexia. Figure A.18A shows some of the physical manifestations of the endpoint with large 20mm tumors on the left and cachexia which may indicate presence of excessive metastases (Figure A.18A, right panel). 4T1.2⁺OSM tumor bearing mice survived much longer, with 90% of mice still alive at day 72 and showing no sign of metastatic disease. In contrast, 4T1.2+vector tumor bearing mice had a much reduced survival rate with 100% of the mice meeting the endpoint criteria by day 57 (Figure A.18B). Overall, these results are significantly different from previous *in vivo* experiments using exogenously injected recombinant OSM in 4T1.2 tumor bearing mice where OSM increased metastases. This suggests that significant differences in signaling may exist between exogenous and endogenous or local production of OSM. Specifically, the timing and amount of OSM in the tumor and metastatic microenvironment may be important for tumor proliferation and metastasis.

OSM Synergistically Induced Osteoclastogenesis with 66c14 Cells in the Presence of Non-Adherent Bone Marrow Cells

Previous studies indicated that OSM plays a major role in bone inflammation, osteoclastic bone resorption, and loss of bone structural integrity (30, 122). Furthermore, in our *in vivo* experiment, there was some indication that OSM injections increased TRAP+ staining in the bone, suggesting increased osteoclast number and

activity (Figure A.11C). To investigate the role of OSM and osteoclast differentiation, we co-cultured non-adherent bone marrow (BM) cells containing osteoclast progenitors with 4T1.2 or 66c14 cells in the presence or absence of OSM. RANKL (10ng/ml) was also added to the co-culture to increase the baseline osteoclastogenesis rate (Figure A.19). Both 66c14 and 4T1.2 cells express the OSMR as show in figure A.5B&C, but in previously published work, pre-osteoclast cells from the bone marrow do not express OSMR (123).

When 66c14 murine mammary cancer cells were co-cultured with non-adherent bone marrow (BM) cells in the presence of OSM, the number of TRAP-positive (TRAP+) cells were 2-fold higher (Figure A.20A) compared to 4T1.2 cell co-cultures (Figure A.20B) or BM cells alone (Figure A.20C). The addition of RANKL with OSM induced a large increase in the number of TRAP+ cells in the 66c14 + BM co-cultures (Figure A.20A), and the levels of TRAP+ cells were 4-fold higher compared to the 4T1.2 co-culture or BM alone with OSM and RANKL. In the co-cultures containing 4T1.2 cells, the change in the level of osteoclast differentiation compared to BM alone was not significant (Figure A.20B&C).

Figure A.21 depicts representative images of osteoclastogenesis and the largest osteoclasts were seen in the 66c14 +OSM co-cultures with BM with RANKL. These results indicate that while OSM and 66c14 cells increase osteoclastogenesis dramatically, OSM and 4T1.2 cells need osteoblasts to increase osteoclastogenesis. This result is paradoxical as the more metastatic 4T1.2 cells do not induce osteoclastogenesis, while the 66c14 cells which do not metastasize to the bone, increase osteoclastogenesis. This suggests that 4T1.2 cell-mediated osteoclastogenesis may not

be working through BM cells or they need to signal through other cells in the culture to support osteoclast differentiation.

OSM Overexpressing 66c14 Cells Increased Osteoclast Differentiation in Bone Marrow Cells

To determine if endogenously produced OSM in 66c14^{OSM} and 4T1.2^{OSM} cells increases osteoclast differentiation in the same manner as exogenously added OSM, the transfected cells were used in the same osteoclast differentiation experiment as described above. 66c14^{OSM} cells produced 8-fold more TRAP⁺ cells compared to vector control, while 4T1.2^{OSM} cells had no significant difference in the total number of TRAP⁺ cell counts compared to its vector control (Figure A.22A). When counting only multinucleated cells, an indication of more progressed osteoclastogenesis, the results mirror the total TRAP⁺ cell counts. 66c14^{OSM} cells produced 15-fold more multi-nucleated TRAP⁺ cells compared to vector control cells (Figure A.22B). The results of these osteoclastogenesis assays are similar between endogenously produced OSM and exogenously added OSM. This suggests that at least for osteoclast differentiation, endogenous or exogenous OSM signaling may be analogous to each other.

m-CSF, VEGF, and HIF1 α May Play a Role in 66c14- and OSM-Mediated BM Osteoclast Differentiation

To ascertain which pro-osteoclastic factors are produced during osteoclastogenesis in response to OSM and cancer cells, and to see if osteoblasts will

have an effect on the production of these factors, various ELISAs were performed on collected conditioned media from the co-culture experiments. Osteoclastic factors that were assessed include, VEGF, m-CSF, TNF α , OPG, and TGF β .

OSM did not appear to regulate the secretion of TNF α , TGF β , and OPG (data not shown). While there was no significant difference between +/- OSM treatments, the levels of both secreted m-CSF and VEGF were highest in the co-cultures containing 66c14 cells (Figure A.23A&B). In fact, m-CSF levels were 9-fold higher in 66c14+BM co-cultures compared to 4T1.2 co-cultures or BM alone (Figure A.23A). VEGF levels were 1.5-fold higher in 66c14 cells compared to 4T1.2 cells, and 4-fold higher when compared to BM cells alone.

The addition of osteoblasts into the co-culture did not significantly alter the amount of m-CSF produced, but it did increase the level of VEGF in the BM cultures as well as in the 4T1.2+BM co-cultures by about 10-50% (Figure A.23B). Also, a Western blot analysis of RANKL showed that, OSM did not significantly alter RANKL expression levels in 4T1.2 or 66c14 cells and was not affected by blocking HIF1 α or COX2 expression by siRNA (Figure A.23C). Finally, parathyroid-hormone related protein levels were measured in the cancer cells with the same conditions, but PTHrP protein was not detected via Western blot analysis (data not shown).

Previous experiments indicated that OSM significantly increases HIF1 α levels in 66c14 and 4T1.2 cells (Figure A.7C-E). In order to determine if HIF1 α is important in osteoclast differentiation of BM cells, a chemical inhibitor to HIF1 α (YC-1) or a HIF1 α siRNA was used in the same osteoclastogenesis experiments. YC-1

significantly inhibited 66c14+OSM mediated osteoclast differentiation by 60% but had no effect on osteoclastogenesis in 4T1.2+BM or BM alone co-cultures (Figure A.24A).

To determine if tumor cell-expressed HIF1 α , versus BM-cell expressed HIF1 α was important for OSM-induced tumor cell-mediated osteoclastogenesis, 66c14 cells were cultured separately and treated with +/- OSM and +/- HIF1 α siRNA. The conditioned media from treated 66c14 cells was then applied to the BM cells. Conditioned media from 66c14 cells treated with OSM increased the osteoclast differentiation rate by 3.5-fold (Figure A.24B). However, when the conditioned media from 66c14 cells treated with the HIF1 α siRNA was added to the BM cells, there was a 50% reduction on the osteoclast differentiation rate, suggesting that OSM induces secretion of pro-osteoclastic factors in 66c14 cells through HIF1 α . Conditioned media from 4T1.2 cells treated with +/-OSM or HIF1 α siRNA did not have any effect on osteoclast differentiation in non-adherent BM cell cultures (data not shown).

Both Osteoblasts and OSM Increased Osteoclast Differentiation in BM Cultures

Breast cancer cells have been shown to generate an inflammatory response in the bone microenvironment and increase osteoclast differentiation (57, 111). Furthermore osteoclastogenesis cannot happen in normal bone without osteoblast activity (43). To determine the effect of osteoblasts in osteoclastogenesis, UMR106 osteoblastic cells were added to tumor + BM co-cultures as a source of and in place of using recombinant RANKL (Figure A.25). Without osteoblasts, there was no osteoclastogenesis in any of the co-cultures (Figure A.26 A&B). There was no difference in the number of TRAP+ cells between 66c14+BM+UMR106 co-cultures in

the presence of or absence of OSM, but in the absence of OSM, there was a 2.5-fold increase in the 4T1.2+BM+UMR106 co-culture (Figure A.26A). In a co-culture with BM+UMR106 cells, there was a modest 3-fold increase of TRAP+ cells when treated by OSM. On the other hand, OSM paradoxically decreased TRAP+ cells in the 4T1.2+UMR106 co-cultures by 60%.

When counting multi-nucleated cells, almost all of the TRAP+ multinucleated cells were seen in (+OSM, +osteoblast) co-cultures, and no significant differences between the cancer cells or BM alone were detected, although the cultures containing 4T1.2 cells were consistently higher by 20-30% (Figure A.26B). This suggests that OSM and osteoblasts promote the formation of multi-nucleated cells through cell fusion, which may explain the decrease in the total number of TRAP+ cells in the co-cultures containing 4T1.2 cells.

To see if there was a difference in the level of soluble RANKL produced in these osteoclastogenesis co-cultures, a RANKL ELISA was used. Only the cultures with osteoblasts had an appreciable level of RANKL in the conditioned media (Figure A.26C). The highest level of soluble RANKL was seen in 66c14 co-cultures with about a 2-fold increase over 4T1.2 co-cultures and BM cultures. These results suggest that while osteoblasts are important in osteoclastogenesis, the mechanism of tumor cell- and OSM-mediated osteoclast activity may be independent of RANKL.

OSM and 4T1.2 Cells Increased Bone Resorption of Mouse Calvaria

Osteoclast differentiation rates do not suggest anything about the activity of these osteoclasts. It is possible that the same conditions which stimulate osteoclast

differentiation would not stimulate osteoclast activity. To assess the ability of cancer cells and OSM to induce osteoclast activity, cancer cells and OSM were added to cultures containing live mouse calvaria, or skull bones from young mice, along with BM cells, RANKL, and m-CSF. After 10 days of incubation at 37°C, free calcium in the conditioned media, which correlates to overall bone resorption levels, was analyzed using the calcium arsenazo III assay.

66c14 cell-treated calvaria had little to no increase in calcium levels in response to OSM treatment, but the addition of RANKL increased the calcium levels modestly by about 10% (Figure A.27A). 4T1.2 cell-treated calvaria had a 35% increase in released calcium when treated with OSM, while the addition of RANKL increased calcium levels by an additional 10%. Cultures containing bone alone also responded to OSM with a 10-20% increase in released calcium levels. Representative images are depicted in figure A.27B. 4T1.2 cell-treated calvaria with OSM showed the most fragmentation of the bone, suggesting the highest level of bone resorption. These results may indicate that while 4T1.2 plus OSM cells do not increase osteoclast differentiation of BM cells, they may contribute to an increased osteoclast activity.

OSM and 4T1.2 Cells Promote Osteoclast Differentiation of RAW264.7 Monocytic Cells

There are at least 2 different origins for osteoclasts that colonize in the bone. One source is BM hematopoietic stem cells that require m-CSF, an early mediator of osteoclastogenesis, to differentiate. The other source is peripheral blood mononuclear cells (PBMCs), which mainly consist of monocytic cells, found in the blood and spleen,

that are less dependant on m-CSF for differentiation into mature osteoclasts (124, 125). RAW264.7 is a monocytic cell line which is often used as a substitute model for primary PBMCs extracted from live specimens. To assess the ability of OSM and tumor cells to induce osteoclast differentiation of PBMCs, a similar osteoclastogenesis experiment was performed using RAW264.7 cells instead of BM cells (Figure A.28).

OSM did not have any effect on both 66c14+RAW264.7 and RAW264.7 co-cultures (Figure A.29A&B). The addition of HIF1 α or COX-2 siRNAs also had little effect on the co-cultures. Overall, the number of TRAP+ cells in these co-cultures averaged 20-35 cells per well. In 4T1.2+RAW264.7 co-cultures, on the other hand, OSM significantly increased osteoclast differentiation by 10-fold, which was attenuated by 70% HIF1 α siRNA, COX-2 siRNA, or YC-1 (Figure A.29C). In addition, the total number of TRAP+ cells in the 4T1.2+OSM co-cultures reached about 500 cells per well, suggesting 4T1.2 cells mediate osteoclast differentiation on the PBMCs. These results may indicate that the more metastatic 4T1.2 cells recruit PBMCs from the blood stream to generate osteoclasts in order to initiate bone metastases.

Conditioned Media from 4T1.2 Cells Treated with OSM Increased Osteoclast Differentiation of RAW264.7 Cells

To assess the effect of secreted factors from murine cancer cells on monocytic osteoclast differentiation, the cancer cells were cultured separately from RAW264.7 cells and were treated with +/- OSM and +/- HIF1 α siRNA. Conditioned media from 66c14 +/- OSM cells did not have any significant effects on osteoclastogenesis of RAW264.7 cells (data not shown). Conditioned media from 4T1.2 +OSM culture had

4-fold more TRAP+ cells than cultures not treated with OSM (Figure A.30).

Conditioned media from 4T1.2 cells treated with both OSM and the HIF1 α siRNA, as compared to the control siRNA, demonstrated 60% less activity in differentiating RAW264.7 cells into osteoclasts. This result suggests that HIF1 α - and OSM-mediated secretion of pro-osteoclastic factors may play a role in osteoclast differentiation.

Interestingly, there was a 5-fold reduction in the total numbers of TRAP+ cells when 4T1.2 conditioned media was added to RAW264.7 cells compared to co-culturing RAW264.7 and 4T1.2 cells. This may indicate that while secreted factors from cancer cells are important in osteoclastogenesis, there may be membrane bound factors that also stimulate osteoclast differentiation, suggesting that cell-to-cell contact is important.

OSM Increased VEGF and IL-6 Secretion Independently of HIF1 α in 4T1.2 Cells

VEGF and IL-6 are common pro-osteoclastic factors that have possible implications in cancer cell-mediated osteoclastogenesis, and are potentially regulated by HIF1 α (78, 126). To determine the changes in VEGF and IL-6 concentrations in osteoclastogenesis co-cultures, these secreted factors from co-cultures treated with or without OSM were investigated by ELISA. OSM increased secreted VEGF from 4T1.2 tumor cells alone by 2-fold. Addition of the HIF1 α siRNA has no effect, suggesting that OSM mediated upregulation of VEGF is independent of HIF1 α (Figure A.31A). However, when the 4T1.2 cells were co-cultured with the RAW264.7 cells, VEGF levels increased without OSM by about 3-fold and increased 2-fold further with the addition of OSM. Furthermore, the addition of the HIF1 α siRNA inhibits OSM-stimulated VEGF secretion in the 4T1.2+RAW264.7 co-culture by 50%.

4T1.2 cells also increased IL-6 secretion by 4-fold in response to OSM, but the addition of HIF1 α siRNA or co-culturing with RAW264.7 cells had no effect (Figure A.31B.) RAW264.7 cells alone produce minimal amount of VEGF or IL-6. This suggests that HIF1 α siRNA mediated inhibition of osteoclast differentiation may be due in part from the reduction in VEGF secretion in the co-cultures but not IL-6 secretion.

VEGF and IL-6 Neutralizing Antibodies Inhibited OSM-Mediated Osteoclast Differentiation in 4T1.2 + RAW264.7 Cell Co-Cultures

In the previous experiment, we showed that OSM increased the secretion of the osteoclastogenic factors VEGF and IL-6 by 4T1.2 cells. We hypothesized that the inhibition of these factors with neutralizing antibodies would attenuate OSM-mediated increases in osteoclastogenesis. When anti-VEGF and anti-IL-6 neutralizing antibodies were added directly to the standard osteoclastogenesis experiment, they both inhibit OSM-mediated osteoclast differentiation by 50% (Figure A.32A). When RAW264.7 cells were cultured without any 4T1.2 cells, neither OSM nor the anti-VEGF and anti-IL-6 neutralizing antibodies had any effect.

To assess whether the secreted VEGF and IL-6 came from 4T1.2 or RAW 264.7 cells, the 4T1.2 cells were cultured separately and treated +/- OSM and with or without the neutralizing antibodies. The conditioned media from the 4T1.2 cultures were then added directly to RAW264.7 cells. Conditioned media from OSM-treated 4T1.2 cells increased osteoclast differentiation by almost 2-fold. On the other hand, the 4T1.2 cell conditioned media treated with anti-VEGF and anti-IL-6 neutralizing antibodies,

reduced osteoclast differentiation by 50% (Figure A.32B). Due to the fact that the deficit of VEGF or IL-6 via the neutralizing antibodies reduced osteoclast differentiation levels down to -OSM treatment levels, suggesting that both VEGF and IL-6 are needed for optimal osteoclastogenesis.

OSM and Murine Breast Cancer Cells Increased RAW264.7 Cell-Derived Osteoclast-Mediated Bone Resorption

To assess the ability of the tumor cell to increase osteoclast activity in osteoclasts derived from RAW264.7 cells, conditioned media from 4T1.2, 66c14, 4T1.2+UMR106, or 66c14+UMR106 cells treated with +/- OSM were added to differentiated RAW264.7 cells in osteologic substrates. The osteologic substrates are coated with an artificial bone-like matrix that contains calcium crystals interlocked with collagen fibers. The cultures were incubated for 10 days, and the resorbed area was analyzed using the Image J software. In the osteologic wells that received conditioned media from 66c14 and 66c14+UMR106 (osteoblastic) cells, OSM induced osteoclast activity by 2-fold (Figure A.33A). The COX-2 inhibitor was also added, and it decreased osteoclast activity down to control levels in all conditions. In osteologic wells that received conditioned media from 4T1.2 cells treated with OSM, there was a small 30% increase, and this data point is not significant (Figure A.33B). The addition of NS398 failed to inhibit osteolytic activity. When conditioned media from 4T1.2+UMR106 co-cultures were applied to the osteologic wells, OSM and NS398 had no significant effect (Figure A.33B).

Figure A.34C depicts resorbed pits on a typical Von Kossa stained osteologic substrate. As was previously shown, BM derived osteoclast activity increased in response to 4T1.2 cells (Figure A.27A), while RAW264.7 derived osteoclast activity increased in response to 66c14. Thus, while both BM cells and RAW264.7 are “pre-osteoclasts” and are supposedly the same type of cell once fully differentiated, there appears to be a difference between the fully differentiated osteoclasts in terms of response to different cancer cells.

DISCUSSION

Breast cancer remains one of the leading causes of death for women in the United States, and a vast majority of patients experience metastases involving the skeletal system with high morbidity and mortality. The multi-step process involved in progression of breast cancer metastasis to the bone and other organs remains largely unknown. However, metastatic cells are widely known to be heterogeneous, where different factors may be upregulated in different breast cancer patients. It is thought that these differences lie in the cytokines and growth factors, and for that reason, research on cytokines in the IL-6 family is increasing. This study attempts to elucidate the role of OSM, a highly pleiotropic IL-6 family cytokine, in breast cancer pathogenesis and induction of osteoclast differentiation and activity.

OSM Increases Pro-Metastatic Markers In 4T1.2 and 66c14 Cells *in vitro* Which Lead to Increased Metastases *in vivo*

4T1.2 and 66c14 cells differ significantly in their metastatic profile despite having the same clonal origin. 4T1.2 cells metastasize similarly to human breast cancer cells and target the lung, liver, brain and bone where as 66c14 cells target only the lung and lymph nodes (Figure A.4) (119). It is now commonly thought that the metastatic profile of various cancer cell lines and their pathogenesis differ due to their inherent differences in the expression of numerous cytokines. We show that 4T1.2 cells have

both higher secreted OSM levels and higher expression of OSM receptor levels as compared to 66c14 cells. This suggests an increase in tumor cell autocrine OSM signaling as well as paracrine signaling of OSM from 4T1.2 cells to the surrounding tissue. 4T1.2 cells having a higher overall OSM signaling may help increase OSM mediated pro-inflammatory and pro-invasion factors such as IL-6 by activating NF- κ B (104, 127). This total increased activity of OSM and OSM-mediated secondary inflammation by 4T1.2 cells may be in part the mechanism which 4T1.2 cells are more metastatic than 66c14 cells.

Although OSM has been shown to have growth inhibitory effects on various types of breast cancer cells (28), this does not preclude OSM from inhibiting tumor metastasis. Other pro-metastatic cytokines such as transforming growth factor beta (TGF β) can have growth inhibitory activities on certain types of breast cancer cells, while the metastatic capacity is increased (128). Therefore, this may lead to the speculation that pro-metastatic cytokines like OSM and TGF β that inhibit cancer cell growth, may be shifting the gene expression of cancer cells from proliferation to expression of factors that upregulate angiogenesis, detachment, and mobility.

Both 4T1.2 and 66c14 cells experience growth inhibition when treated with OSM, while the magnitude of growth inhibition on 4T1.2 cells is slightly greater. Additionally, 4T1.2 cells display increased detachment when treated with OSM, and in comparison, 66c14 cells had no induction of detachment when treated with OSM. These results suggest that 4T1.2 cells display increased pro-metastatic phenotype in response to OSM due to their higher cell detachment levels. However, it is unclear why OSM causes detachment on one cell line and not the other.

One of the main mechanisms for cancer cell detachment from the substrate is to degrade the extracellular matrix (ECM) that binds the cancer cells. Proteases that degrade the ECM released from cancer cells and from other sources are known in certain conditions to cause detachment in epithelial cells (129). OSM has also been shown to increase the secretion of proteases such as matrix metalloproteinase 9 (MMP9) from human cancer cells (130). Secretion of proteases from 4T1.2 cells treated with OSM may be responsible for their ability to detach, while in 66c14 cells, OSM alone may not be enough to cause protease secretion. In arthritis, chondrocytes and synovial fibroblasts need both OSM and TNF α to initiate matrix metalloproteinase (MMP) production and cause protease mediated destruction of the extra cellular matrix (131). Thus, it is possible that 66c14 cells similarly may need additional factors to release the necessary proteases to degrade the ECM and detach from the substrate.

OSM has been shown to induce various cytokines and growth factors such as VEGF, COX-2, and HIF1 α in human breast cancer cells. Stimulation of these factors lead to the upregulation of angiogenesis, increased mobility, and degradation of the extracellular matrix; all of which are hallmarks of metastatic potential (12, 13, 29). VEGF has been shown to stimulate blood vessel growth, confer drug resistance against chemotherapeutics, and increase metastases (132, 133). In addition, HIF1 α is implicated in angiogenesis, osteoclast formation, and the enhancement of osteolytic bone metastases (120, 134, 135).

We carried out Western blots and ELISA tests to determine if OSM induces VEGF, HIF1 α and/or COX-2 on our murine breast cancer cell lines. Our results showed that although 4T1.2 upregulated VEGF when treated with OSM, 66c14 cells

showed little difference between the treatments and VEGF seemed to be constitutively expressed. Our results also showed that 66c14 cells are much more sensitive than 4T1.2 cells to OSM in terms of HIF1 α induction. However, this may just be an artifact in the data that measures % induction of HIF1 α , as the Western blot shows that the basal level of HIF1 α in 4T1.2 is much higher than in 66c14 cells. This may suggest that total HIF1 α signal intensity is the same between the cells when these cells are treated with OSM.

COX-2 is a key intracellular enzyme in the biosynthesis of prostaglandin E₂, and has been shown to increase bone metastases, while breast cancer patients taking COX-2 inhibitors have less risk of developing bone metastases (136, 137). A time course analysis of COX-2 production showed that 4T1.2 cells reach peak COX-2 levels in the cells in half the time than 66c14 cells in response to OSM. The faster response time to OSM in terms of COX-2 expression may be due in part from the higher level of OSMR in 4T1.2 cells which allows increased OSM signaling. Combined, this may at least in part explain 4T1.2 cell's propensity to metastasize more aggressively to bone and target organs than 66c14 cells.

Recent research and data show that interaction between inflammation and cancer may be a critical component in cancer progression and metastasis (138, 139). High levels of systemic OSM is well known to cause inflammation in a wide range of target organs, including the bone, and cause joint destruction and osteolysis (131, 140). In order to assess the impact of exogenous injection of OSM has on cancer progression and metastasis, we injected rmOSM into Balb/c mice that had 4T1.2 cells implanted into their 4th mammary fat pad. Since OSM is a pro-inflammatory cytokine, we

expected that increased generalized inflammation caused by OSM injections would increase the level of metastases *in vivo*. We also expected that the rate of tumor growth and the overall tumor burden would be lower in the group of mice which received OSM injections as OSM decreased 4T1.2 cell growth *in vitro*. However, we saw that the overall tumor burden and rate of tumor growth was almost exactly the same between the treatments groups (Figure A.9A&B). It is possible that even with the concentration of 50ng/g of OSM being injected I.P., the OSM did not significantly perfuse the tumor due to vascular defects that are common in fast growing tumors (141, 142). Thus, there was not enough OSM to effectively inhibit tumor proliferation. On the other hand, when metastases to the lung were analyzed, the group that received OSM had significantly more metastases to the lung than mice that did not receive OSM (Figure A.9C). In addition, the mice that received OSM also had a higher incidence of metastases to the liver, spleen (Figure A.9D), and the bone (Figure A.11A) compared to control mice. Even though OSM injections did not affect the growth of the primary tumor, the increase in the amount of metastases was significant. This suggests that higher levels of serum OSM concentrations may lead to increased metastases. In a recent study on human patients, it was demonstrated that IL-6 concentration in the serum correlated to increased prostate cancer progression and metastases (143). OSM injections also led to smaller metastases in the lung. In this case OSM may be acting on these metastases more efficiently to reduce their size by inhibiting their cell proliferation. However, the reduction in the size of the metastases did not reduce the morbidity rate in the mice.

In this study we noticed that some mice experienced skin ulceration on the site of the primary tumor but did not appear to be correlated to tumor size. Tumors

significantly disrupt the homeostasis of the surrounding tissue, and the reduced nutrient and oxygen availability can lead to focal necrosis and ulcer formation on the skin (144). We compared the numbers of lung metastases between mice that had ulcerating tumors, with local infections, to mice that did not have any ulcerating primary tumors. Because infection and open wounds increase inflammation, we expected that these effects would increase the number of metastases to the lung. Indeed, the mice that had ulcerated tumors had about 2-fold more metastases to the lung compared to mice that did not (Figure A.10C).

Published reports have indicated that OSM increases osteoclast differentiation and activity. In normal bone homeostasis, increased osteoclast activity leads to increased bone resorption (30), and this may be occurring in a bone metastatic environment as well. To assess the general level of osteoclast number and activity, we stained sections of the bone with a TRAP stain, and saw a general trend where the mice that received OSM had stronger TRAP+ staining compared to control mice, which would indicate increased osteoclast number and activity (Figure A.11C).

While injection of OSM was able to increase metastatic burden in mice injected with 4T1.2 cells, a similar experiment where OSM was injected into mice implanted with 66c14 cells demonstrated no difference in metastatic burden between the groups (data not shown). Similarly, mice injected with 66c14 cells did not display any differences in OSM mediated changes in tumor growth rates. Other than the lung, no metastases to any organs were detected nor was there a difference between the groups in terms of total number or size of lung metastases (data not shown). The failure of 66c14 cells to respond to OSM *in vivo* in any capacity suggests that either OSM concentration

was too low and was not able to simulate the 66c14 cells in a sufficient manner due to their low expression of the OSM receptor, or that OSM was not sufficiently perfused through the tumor.

We have shown that secreted VEGF levels from 66c14 cells are very high no matter the conditions. This high level of VEGF may lead to abnormal, rapidly branching blood vessels. The high level of local VEGF seen in many types of cancer, including breast cancer, has been thought to create poorly perfused, leaky, immature blood vessels that not only provide insufficient nutrients, but also reduced perfusion of exogenous agents into the tumor (145). Reduction of VEGF by using anti-VEGF therapies in human cancer patients has had modest anti-cancer effects at best, and at times worsened prognosis due to the restoration of normal vascularization in the tumor, leading to acceleration in tumor growth (146). As such, the high levels of VEGF production by 66c14 cells may be detrimental to the cell's ability to sufficiently grow and metastasize *in vivo* due to their possibly dysfunctional tumor infiltrating vasculature.

Overexpressing OSM in 66c14 and 4T1.2 Cells *in vitro* Leads to Similar Characteristics as Exogenous OSM but Cause Drastic Changes *in vivo*

The previous set of experiments focused primarily on exogenous OSM where the cytokine was either added directly to the tissue culture plate or injected into the mice. In order to study the effects of higher endogenous or local production of OSM, we developed cells that overexpress OSM. An expression vector containing the mouse OSM cDNA was designed and transfected into both 4T1.2 and 66c14 cells to generate cell lines that express high levels of OSM compared to the parental cell lines (Figure

A.13A&B). In order to compare between exogenous and endogenous signaling, as well as the functionality of OSM in these over-expressing cells, their level of tumor cell detachment and VEGF production was assessed.

Unlike the previous experiment where exogenous OSM added to 66c14 cells failed to induce cell detachment, overexpression of OSM in 66c14 cells seem to significantly increase detachment (Figure A.14A). This suggests that there might be some differences between how OSM is signaling exogenously vs. endogenously. Endogenous production of OSM may act in an intracrine manner where OSM that has not been secreted may bind to OSM receptors inside the cytoplasm, translocate to the membrane, and initiate signaling. In a recent study it has been shown that the blockade of intracrine signaling of VEGF inhibited colorectal cancer growth, survival, and sensitized the cells to chemotherapeutics (147). Also, the authors contended that intracrine signaling also promoted different VEGF mediated effects that are distinct from paracrine signaling. Thus, very high levels of endogenous production of OSM may have a more potent OSM mediated signaling of downstream pathways than exogenously added OSM. On the other hand, cell detachment levels between OSM overexpressing 4T1.2 cells and wild type 4T1.2 cells stimulated with exogenous OSM were similar. Aside from the differences in detachment in 66c14 cells, there does not seem to be any other differences between exogenously added OSM vs endogenously overexpressed OSM *in vitro*.

To test the effect of endogenous or local production of OSM *in vivo*, OSM overexpressing 66c14 and 4T1.2 cells were implanted into Balb/c mice. Unlike the previous *in vivo* experiment, where the 66c14 *in vivo* experiment showed no difference

between the +/- OSM injection groups, the mice that received 66c14^{OSM} cells had a surprisingly faster tumor growth rate compared to mice that had received 66c14+vector cells (Figure A.15). However, the total number of metastases were much lower in 66c14^{OSM} tumor bearing mice, while the size of these metastases were larger in these mice compared to the mice with 66c14+vector tumors (Figure A.16B-D). These data suggest that endogenously generated OSM allows faster tumor growth *in vivo* which is contrary to what was seen *in vitro* when 66c14 tumor bearing mice were injected with OSM.

A possible explanation for this could be that OSM stimulates the release of factors that help regulate angiogenesis and allows maturation of blood vessels. OSM stimulates HIF1 α and subsequent signaling from HIF1 α may lead to expression of other pro-angiogenic factors such as angiopoietin, platelet derived growth factor, placental growth factor and other angiogenic factors (120, 121, 148). In particular, angiopoietins 1 and 2 are important pro-angiogenic factors that are responsible for maturation of blood vessels (149). It is possible that because of the increased maturity of blood vessels in the tumors of 66c14^{OSM} injected mice, the vessels are less leaky, leading to less metastases, while allowing increased perfusion of nutrients, which stimulates growth of the tumor. A second explanation is that the integration of the expression construct into the mouse genome may have disrupted or modified the function of a gene that regulates proliferation. The integration of the expression construct to a growth regulatory gene could disrupt its function and increase cell growth. To eliminate this possibility, other OSM-overexpressing clones could have been tested *in vivo*, but unfortunately they were not saved.

Significant differences were also present between mice treated with exogenous OSM in 4T1.2 tumor bearing mice, and mice injected with 4T1.2^{OSM} cells. Unlike the previous experiment where there was no difference in the tumor growth rate between the groups in mice injected with +/- OSM, 4T1.2^{OSM} cells had significantly reduced tumor growth rate compared to 4T1.2+vector control cells. Up to about 16 days post tumor cell implantation, the 4T1.2^{OSM} and 4T1.2+Vector tumors grew at the same rate and the tumor sizes between the two groups were very similar. However, after 16 days, the 4T1.2^{OSM} tumor shrank in size, leading to a significant reduction in overall tumor burden (Figure A.17A-B). In addition, none of the mice injected with 4T1.2^{OSM} cells developed any metastases to the lung or any other organs (Figure A.17C). This is most likely due to the decreased tumor proliferation and lack of any metastatic cells. Due to the significant reduction in both tumor and metastatic burden, the survival rate of mice injected with 4T1.2^{OSM} cells was much higher than mice injected with 4T1.2+vector cells (Figure A.18B). It is possible that with 4T1.2^{OSM} cells, the local concentration of OSM increased too much *in vivo* in the tumor and promoted a potent anti-proliferative effect after a certain amount of time. The inhibition in tumor growth may not have occurred until day 16 when the accumulated concentration of OSM was not high enough to inhibit tumor growth. However, the specific mechanism that governs this effect remains unclear.

Even though 4T1.2 and 66c14 cells were originally derived from the same clonal murine mammary cancer, their response to OSM, and their behavior *in vivo* and *in vitro* is very different from each other (119). Increased systemic distribution of OSM in mice by OSM injections increased metastases in 4T1.2 tumor bearing mice but not in

66c14 tumor bearing mice. Increased endogenous production of OSM by 66c14^{OSM} cells increased tumor growth but inhibited metastases *in vivo*, while 4T1.2^{OSM} overexpressing cells failed to sustain tumor growth, and metastases were not found in any organs. These differences between systemic distribution vs local endogenous production of OSM may shed some light into how OSM mediates metastases. Previous studies show that OSM is produced not only in the tumor cells but by also infiltrating immune cells such as neutrophils and may be the cause of OSM mediated metastases (11, 150).

Production of OSM from the spleen and from immune cells, such as dendritic cells, may potentiate metastasis from the primary tumors and cause cachexia in cancer patients (9, 67). It is possible that the innate immune system is generating a systemic inflammatory response to factors produced by the tumor cells which increases patient morbidity and mortality. This was seen where sharp increases in serum IL-6, which is closely related to OSM, were correlated to late stage cachexia in cancer patients. (151-153). Thus, OSM signaling through increased serum concentrations of OSM via exogenous injection may have played an important role in the stimulation of cancer metastases in 4T1.2 tumor cell bearing mice. On the other hand, 66c14 cells may require a mixture of local and systemic OSM production to stabilize the vasculature to support increased tumor growth. This would suggest that suppression of OSM signaling may reduce metastases in 4T1.2 cells. Preliminary results in our lab using 4T1.2 cells transfected with mouse OSM shRNA indicate that decreased OSM secretion from 4T1.2 cells decreased metastases *in vivo*.

OSM in Conjunction with 66c14, but Not 4T1.2 Mammary Tumor Cells, Increases Osteoclast Differentiation of Non-Adherent Bone Marrow Cells

Due to previous reports of 4T1.2 cells' propensity to metastasize to the bone (119), and their increased reaction to OSM treatment, we have expected that the 4T1.2 cells would be able to stimulate osteoclast differentiation when treated with OSM. Previous studies indicated that OSM increases bone loss via increased osteoclast activity (30, 122), and suggest that OSM is important to the generation of osteolytic lesions necessary for bone metastases. To test if OSM stimulates cancer cells to secrete pro-osteoclastic factors and promote osteoclast differentiation *in vitro*, cancer cells were co-cultured with non-adherent bone marrow cells that contain osteoclast progenitors and were treated with OSM. Although co-cultures containing 4T1.2 cells treated with OSM increased production of TRAP positive osteoclast cells, the numbers of the TRAP+ cells were not any higher than with bone marrow cells alone (Figure A.20B-C). On the other hand, 66c14 cells treated with OSM stimulated osteoclast differentiation 2-4 times what was seen with 4T1.2 co-cultures or with bone marrow cells alone (Figure A.20A).

We also tested OSM overexpressing cells in osteoclastogenesis assays to test if there was a difference in endogenously produced OSM vs exogenously added OSM. The results mirrored the experiment with exogenously added OSM where 66c14^{OSM} cells increased osteoclastogenesis in BM cultures significantly more than 4T1.2^{OSM} cells or BM cells. This suggests that while 4T1.2 cells are able metastasize to the bone, their primary mechanism to stimulate osteoclast differentiation may be through additional cells in the bone microenvironment such as osteoblasts. Indeed, some studies conclude that cancer cells signal through osteoblasts to induce osteoclast differentiation

and activity in bone metastases (57, 154). Other possibilities include that 4T1.2 cells stimulate osteoclastogenesis from cells other than BM cells, or that OSM is not related to 4T1.2 mediated osteoclast differentiation.

To answer why 66c14 cells contribute BM cell differentiation to osteoclasts at a faster rate compared to 4T1.2 cells, m-CSF and VEGF ELISAs were performed on conditioned media from the osteoclastogenesis experiments. In Figure A.23A, we can clearly see that co-cultures containing 66c14 cells produced significantly more m-CSF compared to 4T1.2 cells, while BM cells alone barely produced any m-CSF. The addition of osteoblasts into the co-culture did not significantly affect m-CSF levels. Similarly, osteoclastogenesis co-cultures containing 66c14 cells produced the most VEGF out of any culture conditions. However, these effects were not mediated by OSM. These results suggest that because 66c14 cancer cells constitutively express a large amount of m-CSF, they are able to effectively induce osteoclast differentiation in BM cells. A study that utilizes the human breast cancer cell line MDA-MB-231, which also constitutively express m-CSF, has also been shown to increase osteoclast differentiation in a bone marrow derived cell line UMAS-33 (155).

The non-adherent bone marrow cells contain hematopoietic stem cells that are thought to be an early precursor to osteoclasts. These cells are yet sensitive to RANKL, and only a few factors like m-CSF are able to induce differentiation (45). This suggests that 4T1.2 cells are not able to induce osteoclastogenesis efficiently in bone marrow cultures because, unlike 66c14 cells, 4T1.2 cells do not produce a high amount of m-CSF. Additionally, 4T1.2 cells do not produce as much VEGF as 66c14 cells do, which is also thought to support osteoclast survival and maturation (156). Finally, the

difference in osteoclastogenic capacity between 66c14 and 4T1.2 cells was not due to RANKL, as neither OSM nor HIF1 α /COX2 siRNA significantly affected RANKL expression and both cell lines expressed similar amounts of RANKL.

Previous reports suggest that hypoxia and HIF1 α stimulates osteoclast formation (135, 157), and our data demonstrates that OSM induces HIF1 α expression in the cancer cells. Therefore, we hypothesized that OSM may be signaling through HIF1 α to increase osteoclastogenesis. The YC-1 chemical inhibitor to HIF1 α significantly reduced the OSM-mediated increase in TRAP+ cells in co-cultures containing 66c14 cells. In order to determine if suppression of HIF1 α mediated osteoclastogenesis was important for 66c14 cells, BM cells, or both, we created conditioned media from 66c14 cells alone treated with HIF1 α siRNA and +/- OSM. Conditioned media from 66c14 cells were then applied to cultures that contained only bone marrow cells. Because the siRNA never touched the BM cells, the HIF1 α levels in the BM cells would not be affected. Conditioned media from HIF1 α siRNA-treated 66c14 cells induced significantly less TRAP+ cells compared to conditioned media from control siRNA treated 66c14 cells. This suggests that suppression of HIF1 α in 66c14 cells reduced the secretion of pro-osteoclastic factors from 66c14 cells.

While HIF1 α appears to be important for OSM and 66c14 mediated osteoclastogenesis of BM cells, the specific secreted factor that HIF1 α is upregulating remains unknown. ELISA analyses were done on 66c14 conditioned media with other pro-osteoclastic factors that are HIF1 α regulated such as TGF β and TNF α . The results yielded no difference with OSM or HIF1 α siRNA treatments (data not shown) and they are unlikely candidates for HIF1 α -mediated osteoclastogenesis in the 66c14 + bone

marrow model. According to our data, the OSM signaled HIF1 α -regulated pro-osteoclastic factor is none of the common pro-osteoclastic factors which include m-CSF, RANKL, VEGF, TGF β , or TNF α . It is likely that the candidate HIF1 α regulated pro-osteoclastic is a novel factor that has not been associated with HIF1 α , osteoclastogenesis, and OSM. Further studies using high throughput assays are needed to elucidate the candidate gene.

4T1.2 Cells Need Osteoblasts to Increase Osteoclastogenesis and Osteoclast Activity of Non-Adherent Bone Marrow Cells

Recent studies into the bone microenvironment and bone metastases indicated that cancer cells may induce an inflammatory response on osteoblasts, which leads to an increase in osteolytic signaling causing bone destruction (106, 107). To study the effect that osteoblasts have on osteoclastogenesis, we added UMR106 osteoblastic cells, in place of RANKL, into our co-cultures using the same osteoclastogenesis assay as previously described. We hypothesized that the cancer cells will induce osteoblasts to increase osteoclast differentiation. Our results show that without the presence of osteoblasts or RANKL, osteoclast differentiation does not occur even in the presence of cancer cells and OSM. The addition of osteoblasts to the co-cultures caused a sharp increase in the number of TRAP⁺ cells even without the presence of OSM. OSM increased TRAP⁺ cell number in co-cultures of BM and osteoblasts, but is decreased when 4T1.2 cells were added to co-cultures. No changes in total TRAP⁺ cells in co-cultures containing 66c14 cells were seen.

OSM appears to play a role in increasing osteoclast fusion in pre-osteoclastic cells, reducing the total number of TRAP+ cells, while increasing the number of multi-nucleated TRAP+ cells (30). Further analysis of our data indicates that the addition of OSM increased the number of multi-nucleated TRAP+ cells. Without the presence of OSM, there were almost no multi-nucleated TRAP+ cells indicating that OSM and osteoblasts are needed to create multi-nucleated cells. The cultures containing 4T1.2 cells had the highest number of multinucleated TRAP+ cells, while cultures containing 66c14 or BM cells were about the same as each other. This adds to the idea that 66c14 cells probably stimulate early stages of osteoclastogenesis with their high levels of m-CSF. 4T1.2 cells, on the other hand, may stimulate later stages of osteoclastogenesis. This would suggest that 4T1.2 cells should generate more soluble RANKL, a later mediator of osteoclast differentiation. However, an ELISA on soluble RANKL indicated that while the addition of osteoblasts increased RANKL secretion, co-cultures containing 4T1.2 cells produced as much RANKL as cultures containing BM cells. Nevertheless, with the increase in multinucleated TRAP+ cells in cultures containing 4T1.2 cells, it is also likely that 4T1.2 cells may stimulate osteoclast activity as well.

To test the hypothesis that 4T1.2 cells stimulate osteoclast activity, we designed an experiment that would test osteoclast activity by measuring released calcium from mouse calvaria. Live mouse calvaria were obtained from Balb/c mice and added to a co-culture containing bone marrow cells, OSM, and the murine mammary cancer cells. It was assumed that the live calvaria would contain the osteoblasts necessary to respond to the mammary cancer cells. As bone degrades, calcium is released into the surrounding medium, and is thought to be the cause of hypercalcemia in patients with

bone metastases (158-160). By measuring the calcium concentration in the conditioned media, we expect that the higher the bone degradation, the more calcium is released.

Released calcium levels were the highest in co-cultures containing 4T1.2 cells and OSM (Figure A.27B). Co-cultures containing 66c14 cells or bone alone had lower free calcium levels. Co-cultures containing 66c14 cells also did not have an apparent increase in free calcium levels in response to OSM, while cultures containing bone + BM cells did respond to OSM. The addition of RANKL increased free calcium levels in cultures containing 4T1.2 cells and bone but not in cultures containing 66c14 cells. This data suggests that in the more metastatic 4T1.2 cells, but not in 66c14 cells, OSM is able to upregulate osteoclast activity, increase bone resorption, and cause calcium to be released into the media. Furthermore, the reduced free calcium levels in cultures containing 66c14 cells vs bone alone may indicate that 66c14 cells may have an inhibitory effect on osteoclast activity. Other studies suggest that breast cancer cell subtypes that cause osteoblastic lesions also inhibit osteoclast activity and stimulate osteoblast activity, which reduce serum calcium levels (161-163). This also supports the notion that osteoclast differentiation and activity may be stimulated in different ways where increased osteoclast differentiation does not necessarily translate to increased osteoclast activity and vice versa.

4T1.2 Cells in Conjunction with OSM Increased Osteoclastogenesis in RAW264.7

Cells

Osteoclasts that colonize the bone for normal bone metabolism can come from two known sources. One source is the bone marrow, while the other source is the

peripheral blood mononuclear (PBMC). Unlike the haematopoietic stem cells in the bone marrow, which need early mediators of osteoclast differentiation such as m-CSF, PBMCs are thought to be more differentiated and do not require m-CSF to undergo osteoclastogenesis (124, 125). Recent research into peripheral blood mononuclear cells using a specific cell surface marker CD133 indicated that the levels of CD133+ RNA and cell numbers are elevated in patients with bone metastases regardless of the type of the primary cancer (164, 165). Thus, it is possible that PBMC derived osteoclasts are more important in the initiation and maintenance of bone metastases compared to osteoclasts derived from the bone marrow. To test the osteoclastogenesis of PBMCs, we established co-cultures including the mouse monocytic cell line RAW264.7, which are similar to PBMCs and are able to differentiate into osteoclasts (125).

The results from the RAW264.7 co-culture osteoclastogenesis assay, was in essence, a complete reversal of the results from the BM co-culture osteoclastogenesis assay. In this case, 66c14 cells were completely unable to increase osteoclast differentiation in co-cultures beyond the levels seen with cultures containing RAW264.7 cells. In addition, OSM or any of the HIF1 α or COX-2 inhibitors were unable to induce any difference in the number of TRAP+ cells in these conditions. In these co-cultures, the range of total TRAP+ cell numbers were about 20-35 cells. On the other hand, in co-cultures containing 4T1.2 cells, OSM increased osteoclast differentiation by over 12-fold, while inhibitors to COX2 and HIF1 α attenuated OSM mediated osteoclast differentiation. OSM and 4T1.2 cell-mediated induction of osteoclastogenesis increased the total TRAP+ cells to almost 500 cells per well. Taken together our results demonstrated that the more metastatic 4T1.2 cells increase

osteoclast differentiation on PBMCs but not BM cells. Recent studies indicated PBMCs isolated from patients with osteolytic bone metastases, regardless of cancer type, undergo spontaneous osteoclastogenesis (166, 167). Similar studies that demonstrate spontaneous osteoclastogenesis of BM cell were not found. This suggests that PBMC derived osteoclasts are more important than BM derived osteoclasts for the initiation and maintenance of bone metastases.

To test if 4T1.2 cells, like 66c14 cells, secrete pro-osteoclastic factors in response to OSM mediated by HIF1 α , the conditioned media was created using the same procedure with the 66c14 cells. 4T1.2 cells were treated with HIF1 α siRNA and +/- OSM, and the supernatant conditioned media was added to RAW264.7 cells. Conditioned media from OSM treated 4T1.2 cells increased osteoclastogenesis by about 4-fold, while the conditioned media from HIF1 α treated 4T1.2 cells had attenuated osteoclast differentiation rates. This suggests that like 66c14 cells, 4T1.2 cells also secrete pro-osteoclastic factors in response to OSM in a HIF1 α -dependant manner. However, the level of osteoclastogenesis is 5-fold lower than when the cells were co-cultured, suggesting that cell to cell contact between cancer cells and RAW264.7 cells are needed for optimal osteoclast differentiation. A recent study into prostate cancer cell mediated osteoclast differentiation demonstrated that physical cell-to-cell contact between osteoblasts and other cells stimulates osteoclastogenesis (168). Myeloma cells have also been known to form cell-to-cell contacts with PBMC derived osteoclasts to increase cancer cell survival and osteoclast activity (169).

To test which OSM-mediated pro-osteoclastic factor is positively correlated to HIF1 α siRNA, conditioned media from cultures containing 4T1.2 cells treated with

OSM were analyzed for VEGF and IL-6 levels. VEGF and IL-6 are both potent pro-osteoclastic factors that have implications in bone metastases (58, 81, 170, 171). OSM increased VEGF levels in 4T1.2 cells but HIF1 α siRNA did not affect VEGF levels. On the other hand, when the 4T1.2 cells are co-cultured with RAW264.7 cells, the levels of VEGF secretions increased further in the absence of OSM, and with the addition of OSM, it increased another 2-fold. HIF1 α siRNA attenuated OSM mediated VEGF secretion in the co-cultures. This suggests that while OSM-mediated VEGF induction is independent of HIF1 α when the 4T1.2 cells are not co-cultured, co-culturing not only increases VEGF but the OSM-mediated increase in VEGF is mediated by HIF1 α . When looking at IL-6 levels, OSM increased IL-6 in 4T1.2 and in co-cultures at about the same levels, while HIF1 α siRNA had no effect on IL-6 production (Figure A.31B). Thus, it is likely that the HIF1 α siRNA-mediated reduction in osteoclastogenesis may be partly mediated by the reduction in VEGF levels in the co-culture. This does not discount the possibility that OSM mediated secretion of IL-6 is also supporting osteoclastogenesis.

To test whether VEGF and IL-6 is important on osteoclast differentiation in RAW264.7 cells, neutralizing antibodies to IL-6 and VEGF were used in the osteoclastogenesis co-culture to see if they attenuate the number of TRAP+ cells. In the co-culture with 4T1.2 cells and RAW264.7 cells, OSM increased osteoclast differentiation while IL-6 or VEGF neutralizing antibodies suppressed osteoclastogenesis back down to the -OSM levels (Figure A.32 A). This suggests that both VEGF and IL-6 are needed for optimal osteoclast differentiation and the deficit of either VEGF or IL-6 significantly inhibits osteoclastogenesis.

To test whether VEGF and IL-6 production by 4T1.2 cells, but not RAW264.7 cells, is important, we created conditioned media from 4T1.2 cells alone treated with +/- anti-VEGF or +/- anti-IL-6 neutralizing antibody in the absence or presence of OSM. The conditioned media was then added to RAW264.7 cultures to see if the absence of OSM-mediated 4T1.2-produced VEGF or IL-6 in the co-culture would inhibit OSM stimulated osteoclastogenesis. Again as before, the neutralizing antibody against VEGF or IL-6 suppressed osteoclast differentiation back down to -OSM levels, which suggest that neither tumor cell produced VEGF nor IL-6 alone would be able to increase osteoclastogenesis.

There was a disconnect between osteoclast differentiation and activity where increased osteoclast differentiation did not necessarily translate to increased bone resorption. In order to test whether 66c14 or 4T1.2 cells increase osteoclast activity in differentiated RAW264.7 cells, conditioned media from the cancer cells, UMR106 osteoblastic cells, or the co-culture of them treated with OSM or COX-2 inhibitors were generated. Surprisingly, the conditioned media from 66c14 cells treated with OSM increased RAW264.7 osteoclast activity more than the 4T1.2 cell derived conditioned media. The NS398 COX-2 inhibitor reduced osteoclast activity in cultures containing the 66c14 conditioned media, but did not affect the 4T1.2 cell's ability to increase the level of bone resorption. However the conditioned media from cells containing UMR106 cells had minimal impact on osteoclast activity.

These results again stress the possibility that osteoclast activity is not directly linked to osteoclast differentiation. 66c14 cells increased bone marrow osteoclastogenesis when stimulated by OSM, but had no effect on bone resorption on

the calvaria, while 4T1.2 cells had significant pro-osteolytic effects. Similarly, 4T1.2 cells were able to increase osteoclastogenesis in RAW264.7 cells but its pro-osteolytic effects on RAW264.7 derived osteoclasts were not as prominent as 66c14 cells. In this model, COX-2 and HIF1 α appeared to be important to 66c14 and 4T1.2-mediated increase in osteoclast differentiation. COX-2 mediated osteoclastogenesis is already a well-known mechanism of osteoclast differentiation as its product PGE₂ is a potent pro-osteoclastic factor (111). While some studies suggest that HIF1 α -mediated upregulation of angiopoietin like proteins and VEGF may be involved in osteoclast differentiation, the exact mechanisms governing HIF1 α -mediated osteoclastogenesis are not clear (172, 173). We found that HIF1 α may be mediating VEGF levels in the co-culture of 4T1.2 + RAW264.7 cells treated with OSM, but the exact mechanism is not known. On the other hand, 66c14 cells are upregulating a still unidentified pro-osteoclastic factor mediated by HIF1 α .

Conclusion

These highly variable effects by OSM on cancer pathogenesis make it unlikely that any anti-OSM therapies could be administered to patients with metastatic disease without further research. There is a need for a more complete understanding of OSM and its effects on various types of cancer cells and the progression of metastases. As cancer therapeutics move towards individualized therapies (174-176), and as the technology to characterize cancer cell behavior to various cytokines improves, anti OSM drugs may become a part of an individualized anti cancer regimen.

REFERENCES

1. Parkin DM, Bray F, Ferlay J, Pisani P. Global cancer statistics, 2002. *CA: a cancer journal for clinicians* 2005;55(2):74-108.
2. Jemal A, Siegel R, Xu J, Ward E. Cancer statistics, 2010. *CA: a cancer journal for clinicians* 2010;60(5):277-300.
3. Coleman RE. Skeletal complications of malignancy. *Cancer* 1997;80(8 Suppl):1588-94.
4. Dranoff G. Cytokines in cancer pathogenesis and cancer therapy. *Nature reviews* 2004;4(1):11-22.
5. Jager A, Sleijfer S, van der Rijt CC. The pathogenesis of cancer related fatigue: could increased activity of pro-inflammatory cytokines be the common denominator? *Eur J Cancer* 2008;44(2):175-81.
6. Argiles JM, Busquets S, Lopez-Soriano FJ. Cytokines in the pathogenesis of cancer cachexia. *Current opinion in clinical nutrition and metabolic care* 2003;6(4):401-6.
7. Knüpfner H, Preiß R. Significance of interleukin-6 (IL-6) in breast cancer (review). *Breast Cancer Research and Treatment* 2007;102(2):129-35.
8. Ashizawa T, Okada R, Suzuki Y, *et al.* Clinical significance of interleukin-6 (IL-6) in the spread of gastric cancer: role of IL-6 as a prognostic factor. *Gastric Cancer* 2005;8(2):124-31.
9. Barton BE, Murphy TF. CANCER CACHEXIA IS MEDIATED IN PART BY THE INDUCTION OF IL-6-LIKE CYTOKINES FROM THE SPLEEN. *Cytokine* 2001;16(6):251-7.
10. Douglas AM, Grant SL, Goss GA, Clouston DR, Sutherland RL, Begley CG. Oncostatin M induces the differentiation of breast cancer cells. *Int J Cancer* 1998;75(1):64-73.

11. Hurst SM, McLoughlin RM, Monslow J, *et al.* Secretion of oncostatin M by infiltrating neutrophils: regulation of IL-6 and chemokine expression in human mesothelial cells. *J Immunol* 2002;169(9):5244-51.
12. Holzer RG, Ryan RE, Tommack M, Schlekeway E, Jorcyk CL. Oncostatin M stimulates the detachment of a reservoir of invasive mammary carcinoma cells: role of cyclooxygenase-2. *Clin Exp Metastasis* 2004;21(2):167-76.
13. Jorcyk CL, Holzer RG, Ryan RE. Oncostatin M induces cell detachment and enhances the metastatic capacity of T-47D human breast carcinoma cells. *Cytokine* 2006;33(6):323-36.
14. Tester AM, Ruangpanit N, Anderson RL, Thompson EW. MMP-9 secretion and MMP-2 activation distinguish invasive and metastatic sublines of a mouse mammary carcinoma system showing epithelial-mesenchymal transition traits. *Clin Exp Metastasis* 2000;18(7):553-60.
15. Schmitz F, Heit A. Protective cancer immunotherapy: what can the innate immune system contribute? *Expert Opin Biol Ther* 2008;8(1):31-43.
16. Finn OJ. Bridging the innate and adaptive immune responses against cancer: 95th AACR meeting 2004. *Cancer Immunol Immunother* 2005;54(3):287-9.
17. Khan SN, Bostrom MP, Lane JM. Bone growth factors. *The Orthopedic clinics of North America* 2000;31(3):375-88.
18. Muller A, Homey B, Soto H, *et al.* Involvement of chemokine receptors in breast cancer metastasis. *Nature* 2001;410(6824):50-6.
19. Cooley S, Burns LJ, Repka T, Miller JS. Natural killer cell cytotoxicity of breast cancer targets is enhanced by two distinct mechanisms of antibody-dependent cellular cytotoxicity against LFA-3 and HER2/neu. *Experimental hematology* 1999;27(10):1533-41.
20. Costello RT, Fauriat C, Olive D. Natural killer cells and immunity against cancer. *Discovery medicine* 2004;4(23):333-7.
21. Luo Y, Yamada H, Evanoff DP, Chen X. Role of Th1-stimulating cytokines in bacillus Calmette-Guerin (BCG)-induced macrophage cytotoxicity against mouse bladder cancer MBT-2 cells. *Clinical and experimental immunology* 2006;146(1):181-8.
22. Pang PH, Chan KT, Tse LY, *et al.* Induction of cytotoxic T cell response against HCA661 positive cancer cells through activation with novel HLA-A *0201 restricted epitopes. *Cancer letters* 2007;256(2):178-85.

23. Shinagawa N, Yamazaki K, Tamura Y, *et al.* Immunotherapy with dendritic cells pulsed with tumor-derived gp96 against murine lung cancer is effective through immune response of CD8+ cytotoxic T lymphocytes and natural killer cells. *Cancer Immunol Immunother* 2008;57(2):165-74.
24. Olkhanud PB, Baatar D, Bodogai M, *et al.* Breast cancer lung metastasis requires expression of chemokine receptor CCR4 and regulatory T cells. *Cancer Res* 2009;69(14):5996-6004.
25. Sansone P, Storci G, Tavorari S, *et al.* IL-6 triggers malignant features in mammospheres from human ductal breast carcinoma and normal mammary gland. *The Journal of clinical investigation* 2007;117(12):3988-4002.
26. Brown TJ, Rowe JM, Liu JW, Shoyab M. Regulation of IL-6 expression by oncostatin M. *J Immunol* 1991;147(7):2175-80.
27. Miyajima A, Kinoshita T, Tanaka M, Kamiya A, Mukouyama Y, Hara T. Role of Oncostatin M in hematopoiesis and liver development. *Cytokine Growth Factor Rev* 2000;11(3):177-83.
28. Liu J, Spence MJ, Wallace PM, Forcier K, Hellstrom I, Vestal RE. Oncostatin M-specific receptor mediates inhibition of breast cancer cell growth and down-regulation of the c-myc proto-oncogene. *Cell Growth Differ* 1997;8(6):667-76.
29. Weiss TW, Speidl WS, Kaun C, *et al.* Glycoprotein 130 ligand oncostatin-M induces expression of vascular endothelial growth factor in human adult cardiac myocytes. *Cardiovasc Res* 2003;59(3):628-38.
30. Palmqvist P, Persson E, Conaway HH, Lerner UH. IL-6, leukemia inhibitory factor, and oncostatin M stimulate bone resorption and regulate the expression of receptor activator of NF-kappa B ligand, osteoprotegerin, and receptor activator of NF-kappa B in mouse calvariae. *J Immunol* 2002;169(6):3353-62.
31. Suda T, Udagawa N, Nakamura I, Miyaura C, Takahashi N. Modulation of osteoclast differentiation by local factors. *Bone* 1995;17(2 Suppl):87S-91S.
32. Argast GM, Mercado P, Mulford IJ, *et al.* Cooperative signaling between oncostatin M, hepatocyte growth factor and transforming growth factor-beta enhances epithelial to mesenchymal transition in lung and pancreatic tumor models. *Cells, tissues, organs* 2010;193(1-2):114-32.
33. Pollack V, Sarkozi R, Banki Z, *et al.* Oncostatin M-induced effects on EMT in human proximal tubular cells: differential role of ERK signaling. *American journal of physiology* 2007;293(5):F1714-26.
34. Sims NA, Walsh NC. GP130 cytokines and bone remodelling in health and disease. *BMB reports* 2010;43(8):513-23.

35. Jensen ED, Nair AK, Westendorf JJ. Histone deacetylase co-repressor complex control of Runx2 and bone formation. *Crit Rev Eukaryot Gene Expr* 2007;17(3):187-96.
36. Orimo H. The mechanism of mineralization and the role of alkaline phosphatase in health and disease. *Journal of Nippon Medical School = Nihon Ika Daigaku zasshi* 2010;77(1):4-12.
37. Teitelbaum SL. Bone resorption by osteoclasts. *Science (New York, NY)* 2000;289(5484):1504-8.
38. Ducy P, Schinke T, Karsenty G. The osteoblast: a sophisticated fibroblast under central surveillance. *Science (New York, NY)* 2000;289(5484):1501-4.
39. Tenta R, Sourla A, Lembessis P, Koutsilieris M. Bone-related growth factors and zoledronic acid regulate the PTHrP/PTH.1 receptor bioregulation systems in MG-63 human osteosarcoma cells. *Anticancer research* 2006;26(1A):283-91.
40. Eric AGB, Kristiann MD, Kenneth JP, Charles CC, Thomas JR, Laurie KM. Skeletal metastasis of prostate adenocarcinoma in rats: Morphometric analysis and role of parathyroid hormone-related protein. *Prostate* 1999;39(3):187-97.
41. Nakashima T, Kobayashi Y, Yamasaki S, *et al.* Protein expression and functional difference of membrane-bound and soluble receptor activator of NF-kappaB ligand: modulation of the expression by osteotropic factors and cytokines. *Biochemical and biophysical research communications* 2000;275(3):768-75.
42. Kearns AE, Khosla S, Kostenuik PJ. Receptor activator of nuclear factor kappaB ligand and osteoprotegerin regulation of bone remodeling in health and disease. *Endocrine reviews* 2008;29(2):155-92.
43. Martin TJ, Ng KW. Mechanisms by which cells of the osteoblast lineage control osteoclast formation and activity. *Journal of cellular biochemistry* 1994;56(3):357-66.
44. Takayanagi H, Kim S, Koga T, *et al.* Induction and Activation of the Transcription Factor NFATc1 (NFAT2) Integrate RANKL Signaling in Terminal Differentiation of Osteoclasts. *Developmental Cell* 2002;3(6):889-901.
45. Boyle WJ, Simonet WS, Lacey DL. Osteoclast differentiation and activation. *Nature* 2003;423(6937):337-42.
46. Hikita A, Yana I, Wakeyama H, *et al.* Negative Regulation of Osteoclastogenesis by Ectodomain Shedding of Receptor Activator of NF- $\hat{\text{I}}^{\text{B}}$ Ligand. 2006. p. 36846-55.

47. Kanzaki H, Han X, Lin X, Kawai T, Taubman MA. Is RANKL shedding involved in immune cell-mediated osteoclastogenesis? *Interface Oral Health Science* 2009; 2009. p. 403-5.
48. Lynch CC, Hikosaka A, Acuff HB, *et al.* MMP-7 promotes prostate cancer-induced osteolysis via the solubilization of RANKL. *Cancer cell* 2005;7(5):485-96.
49. Vaes G. Cellular biology and biochemical mechanism of bone resorption. A review of recent developments on the formation, activation, and mode of action of osteoclasts. *Clinical orthopaedics and related research* 1988(231):239-71.
50. Teti A, Zallone A. Do osteocytes contribute to bone mineral homeostasis? Osteocytic osteolysis revisited. *Bone* 2009;44(1):11-6.
51. Heino TJ, Hentunen TA, Vaananen HK. Osteocytes inhibit osteoclastic bone resorption through transforming growth factor-beta: enhancement by estrogen. *Journal of cellular biochemistry* 2002;85(1):185-97.
52. Taylor AF, Saunders MM, Shingle DL, Cimbala JM, Zhou Z, Donahue HJ. Mechanically stimulated osteocytes regulate osteoblastic activity via gap junctions. *American journal of physiology* 2007;292(1):C545-52.
53. Chan M, Lu X, Huo B, *et al.* A Trabecular Bone Explant Model of Osteocyte–Osteoblast Co-Culture for Bone Mechanobiology. *Cellular and Molecular Bioengineering* 2009;2(3):405-15.
54. Bonewald LF. Mechanosensation and Transduction in Osteocytes. *BoneKEY osteovision* 2006;3(10):7-15.
55. Ara T, Song L, Shimada H, *et al.* Interleukin-6 in the bone marrow microenvironment promotes the growth and survival of neuroblastoma cells. *Cancer Res* 2009;69(1):329-37.
56. Paule B, Clerc D, Rudant C, *et al.* Enhanced expression of interleukin-6 in bone and serum of metastatic renal cell carcinoma. *Human pathology* 1998;29(4):421-4.
57. Thomas RJ, Guise TA, Yin JJ, *et al.* Breast cancer cells interact with osteoblasts to support osteoclast formation. *Endocrinology* 1999;140(10):4451-8.
58. Naugler WE, Karin M. The wolf in sheep's clothing: the role of interleukin-6 in immunity, inflammation and cancer. *Trends in molecular medicine* 2008;14(3):109-19.
59. Naka T, Nishimoto N, Kishimoto T. The paradigm of IL-6: from basic science to medicine. *Arthritis research* 2002;4 Suppl 3:S233-42.

60. O'Connor JC, Farach-Carson MC, Schneider CJ, Carson DD. Coculture with prostate cancer cells alters endoglin expression and attenuates transforming growth factor-beta signaling in reactive bone marrow stromal cells. *Mol Cancer Res* 2007;5(6):585-603.
61. Wang L, Clutter S, Benincosa J, Fortney J, Gibson LF. Activation of transforming growth factor-beta1/p38/Smad3 signaling in stromal cells requires reactive oxygen species-mediated MMP-2 activity during bone marrow damage. *Stem cells (Dayton, Ohio)* 2005;23(8):1122-34.
62. Athanasou NA. Pathology of bone injury. *Diagnostic Histopathology* 2009;15(9):437-43.
63. Tosato G, Jones KD. Interleukin-1 induces interleukin-6 production in peripheral blood monocytes. 1990. p. 1305-10.
64. Holt I, Davie MW, Braidman IP, Marshall MJ. Prostaglandin E2 stimulates the production of interleukin-6 by neonatal mouse parietal bones. *Bone and mineral* 1994;25(1):47-57.
65. Eickelberg O, Pansky A, Mussmann R, *et al.* Transforming Growth Factor- β 1 Induces Interleukin-6 Expression via Activating Protein-1 Consisting of JunD Homodimers in Primary Human Lung Fibroblasts. 1999. p. 12933-8.
66. Zhang Y, Broser M, Rom W. Activation of the interleukin 6 gene by Mycobacterium tuberculosis or lipopolysaccharide is mediated by nuclear factors NF IL 6 and NF-kappa B. *Proceedings of the National Academy of Sciences of the United States of America* 1995;92(8):3632.
67. Suda T, Chida K, Todate A, *et al.* Oncostatin M production by human dendritic cells in response to bacterial products. *Cytokine* 2002;17(6):335-40.
68. Repovic P, Benveniste EN. Prostaglandin E2 is a novel inducer of oncostatin-M expression in macrophages and microglia. *J Neurosci* 2002;22(13):5334-43.
69. Heinrich PC, Behrmann I, Muller-Newen G, Schaper F, Graeve L. Interleukin-6-type cytokine signalling through the gp130/Jak/STAT pathway. *The Biochemical journal* 1998;334 (Pt 2):297-314.
70. Domingo-Domenech J, Oliva C, Rovira A, *et al.* Interleukin 6, a nuclear factor-kappaB target, predicts resistance to docetaxel in hormone-independent prostate cancer and nuclear factor-kappaB inhibition by PS-1145 enhances docetaxel antitumor activity. *Clin Cancer Res* 2006;12(18):5578-86.

71. Murakami M, Hibi M, Nakagawa N, *et al.* IL-6-induced homodimerization of gp130 and associated activation of a tyrosine kinase. *Science (New York, NY)* 1993;260(5115):1808-10.
72. Wegiel B, Bjartell A, Culig Z, Persson JL. Interleukin-6 activates PI3K/Akt pathway and regulates cyclin A1 to promote prostate cancer cell survival. *Int J Cancer* 2008;122(7):1521-9.
73. Soldi R, Graziani A, Benelli R, *et al.* Oncostatin M activates phosphatidylinositol-3-kinase in Kaposi's sarcoma cells. *Oncogene* 1994;9(8):2253-60.
74. Stancato LF, Sakatsume M, David M, *et al.* Beta interferon and oncostatin M activate Raf-1 and mitogen-activated protein kinase through a JAK1-dependent pathway. *Molecular and cellular biology* 1997;17(7):3833-40.
75. Zhang F, Li C, Halfter H, Liu J. Delineating an oncostatin M-activated STAT3 signaling pathway that coordinates the expression of genes involved in cell cycle regulation and extracellular matrix deposition of MCF-7 cells. *Oncogene* 2003;22(6):894-905.
76. Hashizume M, Hayakawa N, Mihara M. IL-6 trans-signalling directly induces RANKL on fibroblast-like synovial cells and is involved in RANKL induction by TNF-alpha and IL-17. *Rheumatology (Oxford, England)* 2008;47(11):1635-40.
77. Bishop KA, Meyer MB, Pike JW. A novel distal enhancer mediates cytokine induction of mouse RANK1 gene expression. *Molecular endocrinology (Baltimore, Md)* 2009;23(12):2095-110.
78. Wong PK, Quinn JM, Sims NA, van Nieuwenhuijze A, Campbell IK, Wicks IP. Interleukin-6 modulates production of T lymphocyte-derived cytokines in antigen-induced arthritis and drives inflammation-induced osteoclastogenesis. *Arthritis and rheumatism* 2006;54(1):158-68.
79. McGeachy MJ, Bak-Jensen KS, Chen Y, *et al.* TGF-beta and IL-6 drive the production of IL-17 and IL-10 by T cells and restrain T(H)-17 cell-mediated pathology. *Nature immunology* 2007;8(12):1390-7.
80. Wang L, Yi T, Kortylewski M, Pardoll DM, Zeng D, Yu H. IL-17 can promote tumor growth through an IL-6-Stat3 signaling pathway. *The Journal of experimental medicine* 2009;206(7):1457-64.
81. Moonga BS, Adebajo OA, Wang HJ, *et al.* Differential effects of interleukin-6 receptor activation on intracellular signaling and bone resorption by isolated rat osteoclasts. *The Journal of endocrinology* 2002;173(3):395-405.

82. Tanaka M, Hirabayashi Y, Sekiguchi T, Inoue T, Katsuki M, Miyajima A. Targeted disruption of oncostatin M receptor results in altered hematopoiesis. *Blood* 2003;102(9):3154-62.
83. Minehata K, Takeuchi M, Hirabayashi Y, *et al.* Oncostatin m maintains the hematopoietic microenvironment and retains hematopoietic progenitors in the bone marrow. *International journal of hematology* 2006;84(4):319-27.
84. Wang LH, Yang XY, Mihalic K, Xiao W, Li D, Farrar WL. Activation of estrogen receptor blocks interleukin-6-inducible cell growth of human multiple myeloma involving molecular cross-talk between estrogen receptor and STAT3 mediated by co-regulator PIAS3. *The Journal of biological chemistry* 2001;276(34):31839-44.
85. Coletta RD, Reynolds MA, Martelli-Junior H, Graner E, Almeida OP, Sauk JJ. Testosterone stimulates proliferation and inhibits interleukin-6 production of normal and hereditary gingival fibromatosis fibroblasts. *Oral microbiology and immunology* 2002;17(3):186-92.
86. Tuck SP, Francis RM. Testosterone, bone and osteoporosis. *Frontiers of hormone research* 2009;37:123-32.
87. Papadopoulos AD, Wardlaw SL. Testosterone suppresses the response of the hypothalamic-pituitary-adrenal axis to interleukin-6. *Neuroimmunomodulation* 2000;8(1):39-44.
88. Simpson E, Rubin G, Clyne C, *et al.* The role of local estrogen biosynthesis in males and females. *Trends in endocrinology and metabolism: TEM* 2000;11(5):184-8.
89. Hershman D, Narayanan R. Prevention and management of osteoporosis in women with breast cancer and men with prostate cancer. *Current Oncology Reports* 2004;6(4):277-84.
90. Coleman RE. Clinical Features of Metastatic Bone Disease and Risk of Skeletal Morbidity. 2006. p. 6243s-9s.
91. Coleman RE, Rubens RD. The clinical course of bone metastases from breast cancer. *British journal of cancer* 1987;55(1):61-6.
92. DuBois SG, Kalika Y, Lukens JN, *et al.* Metastatic Sites in Stage IV and IVS Neuroblastoma Correlate With Age, Tumor Biology, and Survival. 1999. p. 181-9.
93. Ricciardi S, de Marinis F. Treatment of bone metastases in lung cancer: the actual role of zoledronic acid. *Reviews on recent clinical trials* 2009;4(3):205-11.

94. Yang M, Jiang P, An Z, *et al.* Genetically Fluorescent Melanoma Bone and Organ Metastasis Models. 1999. p. 3549-59.
95. Guise TA, Mohammad KS, Clines G, *et al.* Basic mechanisms responsible for osteolytic and osteoblastic bone metastases. *Clin Cancer Res* 2006;12(20 Pt 2):6213s-6s.
96. Keller ET, Brown J. Prostate cancer bone metastases promote both osteolytic and osteoblastic activity. *Journal of cellular biochemistry* 2004;91(4):718-29.
97. Roodman GD. Mechanisms of bone metastasis. *N Engl J Med* 2004;350(16):1655-64.
98. Sohara Y, Shimada H, DeClerck YA. Mechanisms of bone invasion and metastasis in human neuroblastoma. *Cancer letters* 2005;228(1-2):203-9.
99. Coleman RE. Metastatic bone disease: clinical features, pathophysiology and treatment strategies. *Cancer Treatment Reviews* 2001;27(3):165-76.
100. Taichman RS, Cooper C, Keller ET, Pienta KJ, Taichman NS, McCauley LK. Use of the Stromal Cell-derived Factor-1/CXCR4 Pathway in Prostate Cancer Metastasis to Bone. 2002. p. 1832-7.
101. Hirbe AC, Morgan EA, Weilbaecher KN. The CXCR4/SDF-1 chemokine axis: a potential therapeutic target for bone metastases? *Current pharmaceutical design* 2010;16(11):1284-90.
102. Helbig G, Christopherson KW, 2nd, Bhat-Nakshatri P, *et al.* NF-kappaB promotes breast cancer cell migration and metastasis by inducing the expression of the chemokine receptor CXCR4. *The Journal of biological chemistry* 2003;278(24):21631-8.
103. Lee MJ, Song HY, Kim MR, Sung SM, Jung JS, Kim JH. Oncostatin M stimulates expression of stromal-derived factor-1 in human mesenchymal stem cells. *The international journal of biochemistry & cell biology* 2007;39(3):650-9.
104. Tang CH, Chuang JY, Fong YC, Maa MC, Way TD, Hung CH. Bone-derived SDF-1 stimulates IL-6 release via CXCR4, ERK and NF-kappaB pathways and promotes osteoclastogenesis in human oral cancer cells. *Carcinogenesis* 2008;29(8):1483-92.
105. Hauschka PV, Mavrakos AE, Iafrati MD, Doleman SE, Klagsbrun M. Growth factors in bone matrix. Isolation of multiple types by affinity chromatography on heparin-Sepharose. *The Journal of biological chemistry* 1986;261(27):12665-74.
106. Kinder M, Chislock E, Bussard KM, Shuman L, Mastro AM. Metastatic breast cancer induces an osteoblast inflammatory response. *Experimental cell research* 2008;314(1):173-83.

107. Chen YC, Sosnoski DM, Gandhi UH, Novinger LJ, Prabhu KS, Mastro AM. Selenium modifies the osteoblast inflammatory stress response to bone metastatic breast cancer. *Carcinogenesis* 2009;30(11):1941-8.
108. Deyama Y, Tei K, Yoshimura Y, *et al.* Oral squamous cell carcinomas stimulate osteoclast differentiation. *Oncology reports* 2008;20(3):663-8.
109. Lee KM, Kang BS, Lee HL, *et al.* Spinal NF-kB activation induces COX-2 upregulation and contributes to inflammatory pain hypersensitivity. *The European journal of neuroscience* 2004;19(12):3375-81.
110. Li X, Pilbeam CC, Pan L, Breyer RM, Raisz LG. Effects of prostaglandin E2 on gene expression in primary osteoblastic cells from prostaglandin receptor knockout mice. *Bone* 2002;30(4):567-73.
111. Kaji H, Sugimoto T, Kanatani M, Fukase M, Kumegawa M, Chihara K. Prostaglandin E2 stimulates osteoclast-like cell formation and bone-resorbing activity via osteoblasts: role of cAMP-dependent protein kinase. *J Bone Miner Res* 1996;11(1):62-71.
112. Fantozzi A, Christofori G. Mouse models of breast cancer metastasis. *Breast Cancer Res* 2006;8(4):212.
113. Umemura T, Kodama Y, Nishikawa A, *et al.* Nine-week detection of six genotoxic lung carcinogens using the rasH2/BHT mouse model. *Cancer letters* 2006;231(2):314-8.
114. Osborne CK, Coronado EB, Robinson JP. Human breast cancer in the athymic nude mouse: cytostatic effects of long-term antiestrogen therapy. *European journal of cancer & clinical oncology* 1987;23(8):1189-96.
115. de Visser KE, Eichten A, Coussens LM. Paradoxical roles of the immune system during cancer development. *Nature reviews* 2006;6(1):24-37.
116. Quinn BA, Xiao F, Bickel L, *et al.* Development of a syngeneic mouse model of epithelial ovarian cancer. *Journal of ovarian research* 2010;3:24.
117. Darro F, Decaestecker C, Gaussin JF, Mortier S, Van Ginckel R, Kiss R. Are syngeneic mouse tumor models still valuable experimental models in the field of anti-cancer drug discovery? *International journal of oncology* 2005;27(3):607-16.
118. Lee HJ, Tantawy MN, Nam KT, Choi I, Peterson TE, Price RR. Evaluation of an intraperitoneal ovarian cancer syngeneic mouse model using 18F-FDG MicroPET imaging. *Int J Gynecol Cancer* 2010;21(1):22-7.

119. Lelekakis M, Moseley JM, Martin TJ, *et al.* A novel orthotopic model of breast cancer metastasis to bone. *Clin Exp Metastasis* 1999;17(2):163-70.
120. Du R, Lu KV, Petritsch C, *et al.* HIF1alpha induces the recruitment of bone marrow-derived vascular modulatory cells to regulate tumor angiogenesis and invasion. *Cancer cell* 2008;13(3):206-20.
121. Toi M, Matsumoto T, Bando H. Vascular endothelial growth factor: its prognostic, predictive, and therapeutic implications. *The lancet oncology* 2001;2(11):667-73.
122. Brounais B, Chipoy C, Mori K, *et al.* Oncostatin M induces bone loss and sensitizes rat osteosarcoma to the antitumor effect of Midostaurin in vivo. *Clin Cancer Res* 2008;14(17):5400-9.
123. Heymann D, Rousselle AV. gp130 Cytokine family and bone cells. *Cytokine* 2000;12(10):1455-68.
124. Suzuki N, Yoshimura Y, Deyama Y, Suzuki K, Kitagawa Y. Mechanical stress directly suppresses osteoclast differentiation in RAW264.7 cells. *International journal of molecular medicine* 2008;21(3):291-6.
125. Cuetara BL, Crotti TN, O'Donoghue AJ, McHugh KP. Cloning and characterization of osteoclast precursors from the RAW264.7 cell line. *In vitro cellular & developmental biology* 2006;42(7):182-8.
126. Aldridge SE, Lennard TW, Williams JR, Birch MA. Vascular endothelial growth factor acts as an osteolytic factor in breast cancer metastases to bone. *British journal of cancer* 2005;92(8):1531-7.
127. Baker BJ, Park KW, Qin H, Ma X, Benveniste EN. IL-27 inhibits OSM-mediated TNF-alpha and iNOS gene expression in microglia. *Glia* 2010;58(9):1082-93.
128. Akhurst RJ, Derynck R. TGF-beta signaling in cancer--a double-edged sword. *Trends in cell biology* 2001;11(11):S44-51.
129. Hirayasu H, Yoshikawa Y, Tsuzuki S, Fushiki T. A lymphocyte serine protease granzyme A causes detachment of a small-intestinal epithelial cell line (IEC-6). *Bioscience, biotechnology, and biochemistry* 2008;72(9):2294-302.
130. Chen SH, Gillespie GY, Benveniste EN. Divergent effects of oncostatin M on astrogloma cells: influence on cell proliferation, invasion, and expression of matrix metalloproteinases. *Glia* 2006;53(2):191-200.

131. Hui W, Rowan AD, Richards CD, Cawston TE. Oncostatin M in combination with tumor necrosis factor alpha induces cartilage damage and matrix metalloproteinase expression in vitro and in vivo. *Arthritis and rheumatism* 2003;48(12):3404-18.
132. Borgstrom P, Gold DP, Hillan KJ, Ferrara N. Importance of VEGF for breast cancer angiogenesis in vivo: implications from intravital microscopy of combination treatments with an anti-VEGF neutralizing monoclonal antibody and doxorubicin. *Anticancer research* 1999;19(5B):4203-14.
133. Aesoy R, Sanchez BC, Norum JH, Lewensohn R, Viktorsson K, Linderholm B. An autocrine VEGF/VEGFR2 and p38 signaling loop confers resistance to 4-hydroxytamoxifen in MCF-7 breast cancer cells. *Mol Cancer Res* 2008;6(10):1630-8.
134. Hiraga T, Kizaka-Kondoh S, Hirota K, Hiraoka M, Yoneda T. Hypoxia and hypoxia-inducible factor-1 expression enhance osteolytic bone metastases of breast cancer. *Cancer Res* 2007;67(9):4157-63.
135. Arnett TR, Gibbons DC, Utting JC, *et al.* Hypoxia is a major stimulator of osteoclast formation and bone resorption. *Journal of cellular physiology* 2003;196(1):2-8.
136. Valsecchi ME, Pomerantz SC, Jaslow R, Tester W. Reduced risk of bone metastasis for patients with breast cancer who use COX-2 inhibitors. *Clinical breast cancer* 2009;9(4):225-30.
137. Singh B, Berry JA, Shoher A, Ayers GD, Wei C, Lucci A. COX-2 involvement in breast cancer metastasis to bone. *Oncogene* 2007;26(26):3789-96.
138. Coussens LM, Werb Z. Inflammation and cancer. *Nature* 2002;420(6917):860-7.
139. Mantovani A, Allavena P, Sica A, Balkwill F. Cancer-related inflammation. *Nature* 2008;454(7203):436-44.
140. Langdon C, Kerr C, Hassen M, Hara T, Arsenault AL, Richards CD. Murine oncostatin M stimulates mouse synovial fibroblasts in vitro and induces inflammation and destruction in mouse joints in vivo. *The American journal of pathology* 2000;157(4):1187-96.
141. Batchelor TT, Sorensen AG, di Tomaso E, *et al.* AZD2171, a pan-VEGF receptor tyrosine kinase inhibitor, normalizes tumor vasculature and alleviates edema in glioblastoma patients. *Cancer cell* 2007;11(1):83-95.
142. Carmeliet P, Jain RK. Angiogenesis in cancer and other diseases. *Nature* 2000;407(6801):249-57.

143. Shariat SF, Andrews B, Kattan MW, Kim J, Wheeler TM, Slawin KM. Plasma levels of interleukin-6 and its soluble receptor are associated with prostate cancer progression and metastasis. *Urology* 2001;58(6):1008-15.
144. Abraham Z, Rozenbaum M, Keren R. Skin ulcer at the blunt apex of a giant Warthin's tumor. *The Journal of dermatology* 2000;27(8):523-8.
145. Greenberg JI, Shields DJ, Barillas SG, *et al.* A role for VEGF as a negative regulator of pericyte function and vessel maturation. *Nature* 2008;456(7223):809-13.
146. Greenberg JI, Cheresch DA. VEGF as an inhibitor of tumor vessel maturation: implications for cancer therapy. *Expert Opinion on Biological Therapy* 2009;9(11):1347-56.
147. Samuel S, Fan F, Dang LH, Xia L, Gaur P, Ellis LM. Intracrine vascular endothelial growth factor signaling in survival and chemoresistance of human colorectal cancer cells. *Oncogene* 2010;30(10):1205-12.
148. Gerecht S, Sarkar K, Semenza GL. Physiological and Therapeutic Vascular Remodeling Mediated by Hypoxia-Inducible Factor 1. *Biophysical Regulation of Vascular Differentiation and Assembly*: Springer New York; 2011. p. 111-25.
149. Thurston G. Role of Angiopoietins and Tie receptor tyrosine kinases in angiogenesis and lymphangiogenesis. *Cell and tissue research* 2003;314(1):61-8.
150. Queen MM, Ryan RE, Holzer RG, Keller-Peck CR, Jorcyk CL. Breast cancer cells stimulate neutrophils to produce oncostatin M: potential implications for tumor progression. *Cancer Res* 2005;65(19):8896-904.
151. Fonseca JE SM, Canhão H, Choy E. Interleukin-6 as a key player in systemic inflammation and joint destruction. *Autoimmunity Reviews* 2009.
152. Kuroda K, Nakashima J, Kanao K, *et al.* Interleukin 6 is associated with cachexia in patients with prostate cancer. *Urology* 2007;69(1):113-7.
153. Iwase S, Murakami T, Saito Y, Nakagawa K. Steep elevation of blood interleukin-6 (IL-6) associated only with late stages of cachexia in cancer patients. *European cytokine network* 2004;15(4):312-6.
154. Roodman GD. Mechanisms of Bone Metastasis. *New England Journal of Medicine*; 2004. p. 1655-64.
155. Mancino AT, Klimberg VS, Yamamoto M, Manolagas SC, Abe E. Breast cancer increases osteoclastogenesis by secreting M-CSF and upregulating RANKL in stromal cells. *J Surg Res* 2001;100(1):18-24.

156. Nakagawa M, Kaneda T, Arakawa T, *et al.* Vascular endothelial growth factor (VEGF) directly enhances osteoclastic bone resorption and survival of mature osteoclasts. *FEBS Lett* 2000;473(2):161-4.
157. Hsieh TP, Sheu SY, Sun JS, Chen MH. Icarin inhibits osteoclast differentiation and bone resorption by suppression of MAPKs/NF-kappaB regulated HIF-1alpha and PGE(2) synthesis. *Phytomedicine* 2010;18(2-3):176-85.
158. Ariel IM, Kempner R. The treatment of hypercalcemia associated with metastases to bone from primary breast cancer. *Bulletin of the Hospital for Joint Diseases Orthopaedic Institute* 1988;48(1):82-7.
159. Kusama M, Kaise H, Nakayama S, *et al.* [Two cases of malignancy-associated hypercalcemia from bone metastases of breast cancer successfully treated with combination therapy using pamidronate and calcitonin]. *Gan to kagaku ryoho* 2000;27(5):763-6.
160. Warrell RP, Jr. Hypercalcemia and bone metastases in breast cancer. *Current opinion in oncology* 1990;2(6):1097-103.
161. Cook GJ, Houston S, Rubens R, Maisey MN, Fogelman I. Detection of bone metastases in breast cancer by 18FDG PET: differing metabolic activity in osteoblastic and osteolytic lesions. *J Clin Oncol* 1998;16(10):3375-9.
162. Cooksley T, Banerjee M, Younis N. Metastatic breast carcinoma presenting with profound hypocalcemia. *Southern medical journal* 2010;103(5):480-1.
163. Keller ET. The role of osteoclastic activity in prostate cancer skeletal metastases. *Drugs Today (Barc)* 2002;38(2):91-102.
164. Lin EH, Hassan M, Li Y, *et al.* Elevated circulating endothelial progenitor marker CD133 messenger RNA levels predict colon cancer recurrence. *Cancer* 2007;110(3):534-42.
165. Mehra N, Penning M, Maas J, *et al.* Progenitor marker CD133 mRNA is elevated in peripheral blood of cancer patients with bone metastases. *Clin Cancer Res* 2006;12(16):4859-66.
166. Roato I, Gorassini E, Brunetti G, *et al.* IL-7 modulates osteoclastogenesis in patients affected by solid tumors. *Ann N Y Acad Sci* 2007;1117:377-84.
167. Roato I, Grano M, Brunetti G, *et al.* Mechanisms of spontaneous osteoclastogenesis in cancer with bone involvement. *Faseb J* 2005;19(2):228-30.

168. Shiirevnyamba A, Takahashi T, Shan H, *et al.* Enhancement of osteoclastogenic activity in osteolytic prostate cancer cells by physical contact with osteoblasts. *British journal of cancer* 2011;104(3):505-13.
169. Abe M, Hiura K, Wilde J, *et al.* Osteoclasts enhance myeloma cell growth and survival via cell-cell contact: a vicious cycle between bone destruction and myeloma expansion. *Blood* 2004;104(8):2484-91.
170. Kumta SM, Huang L, Cheng YY, Chow LT, Lee KM, Zheng MH. Expression of VEGF and MMP-9 in giant cell tumor of bone and other osteolytic lesions. *Life Sci* 2003;73(11):1427-36.
171. Iguchi H, Yokota M, Fukutomi M, *et al.* A possible role of VEGF in osteolytic bone metastasis of hepatocellular carcinoma. *J Exp Clin Cancer Res* 2002;21(3):309-13.
172. Knowles H, Athanasou N. Hypoxia-inducible factor is expressed in giant cell tumour of bone and mediates paracrine effects of hypoxia on monocyte-osteoclast differentiation via induction of VEGF. *J Pathol* 2008.
173. Knowles HJ, Cleton-Jansen AM, Korsching E, Athanasou NA. Hypoxia-inducible factor regulates osteoclast-mediated bone resorption: role of angiopoietin-like 4. *Faseb J* 2010;24(12):4648-59.
174. Perez-Soler R. Individualized therapy in non-small-cell lung cancer: future versus current clinical practice. *Oncogene* 2009;28 Suppl 1:S38-45.
175. Chang DZ, Kumar V, Ma Y, Li K, Kopetz S. Individualized therapies in colorectal cancer: KRAS as a marker for response to EGFR-targeted therapy. *Journal of hematology & oncology* 2009;2:18.
176. Andreopoulou E, Hortobagyi GN. Prognostic factors in metastatic breast cancer: successes and challenges toward individualized therapy. *J Clin Oncol* 2008;26(22):3660-2.

APPENDIX A

Figures

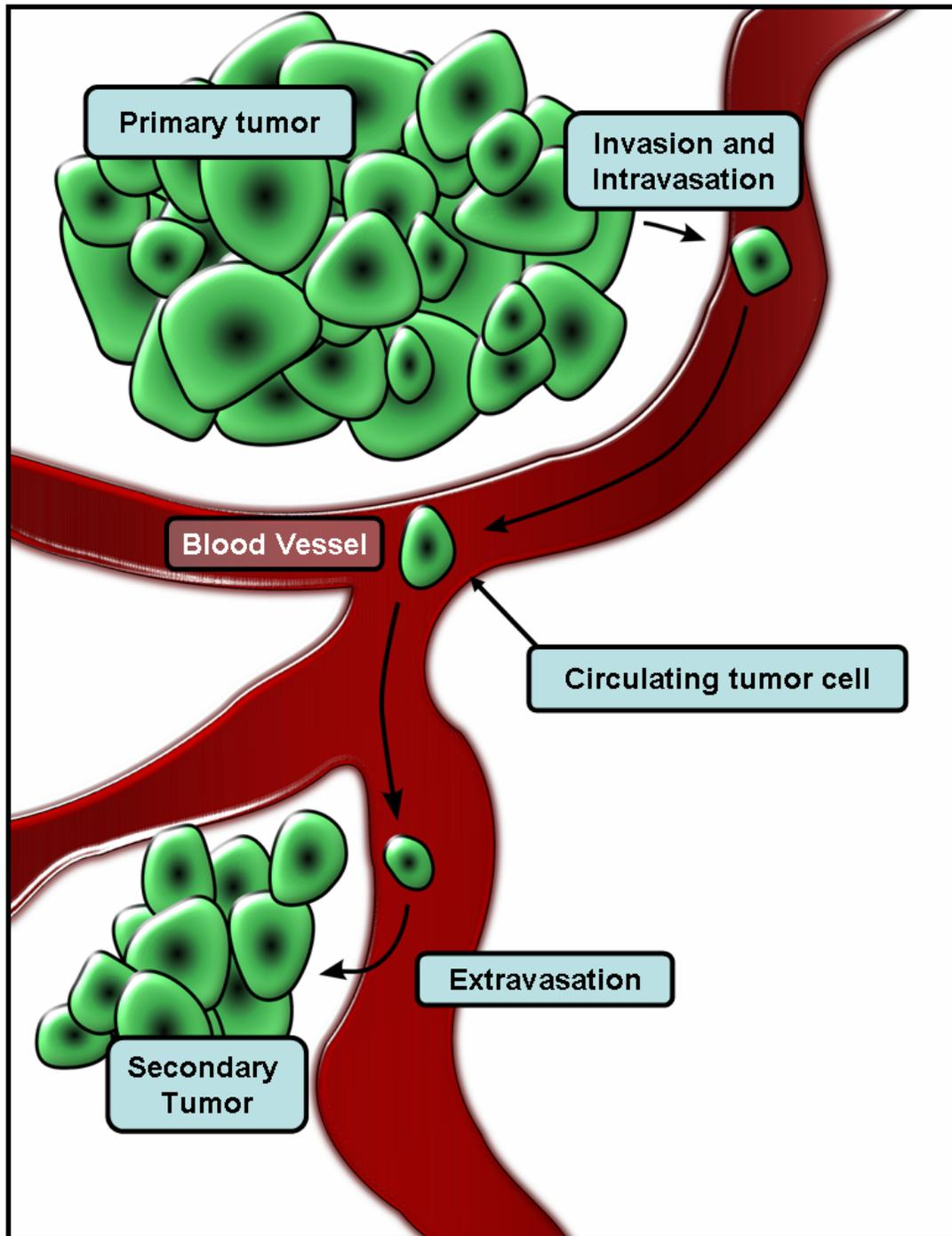


Figure A.1 Schematic Diagram of Generalized Metastatic Steps Necessary for Cancer Cells From Primary Tumors to Reach Secondary Sites

Figure A.1: *Schematic Diagram of Generalized Metastatic Steps Necessary for Cancer Cells From Primary Tumors to Reach Secondary Sites.* Primary tumor cells proliferate and start to invade the surrounding tissue. The tumor cells invade into the blood vessel in a process called intravasation and becomes a circulating tumor cell (CTC). The cell can then extravasate from the blood stream and implant itself into a secondary site where it metastasizes. The metastasized tumor cells proliferate to grow a secondary tumor at a distal site.

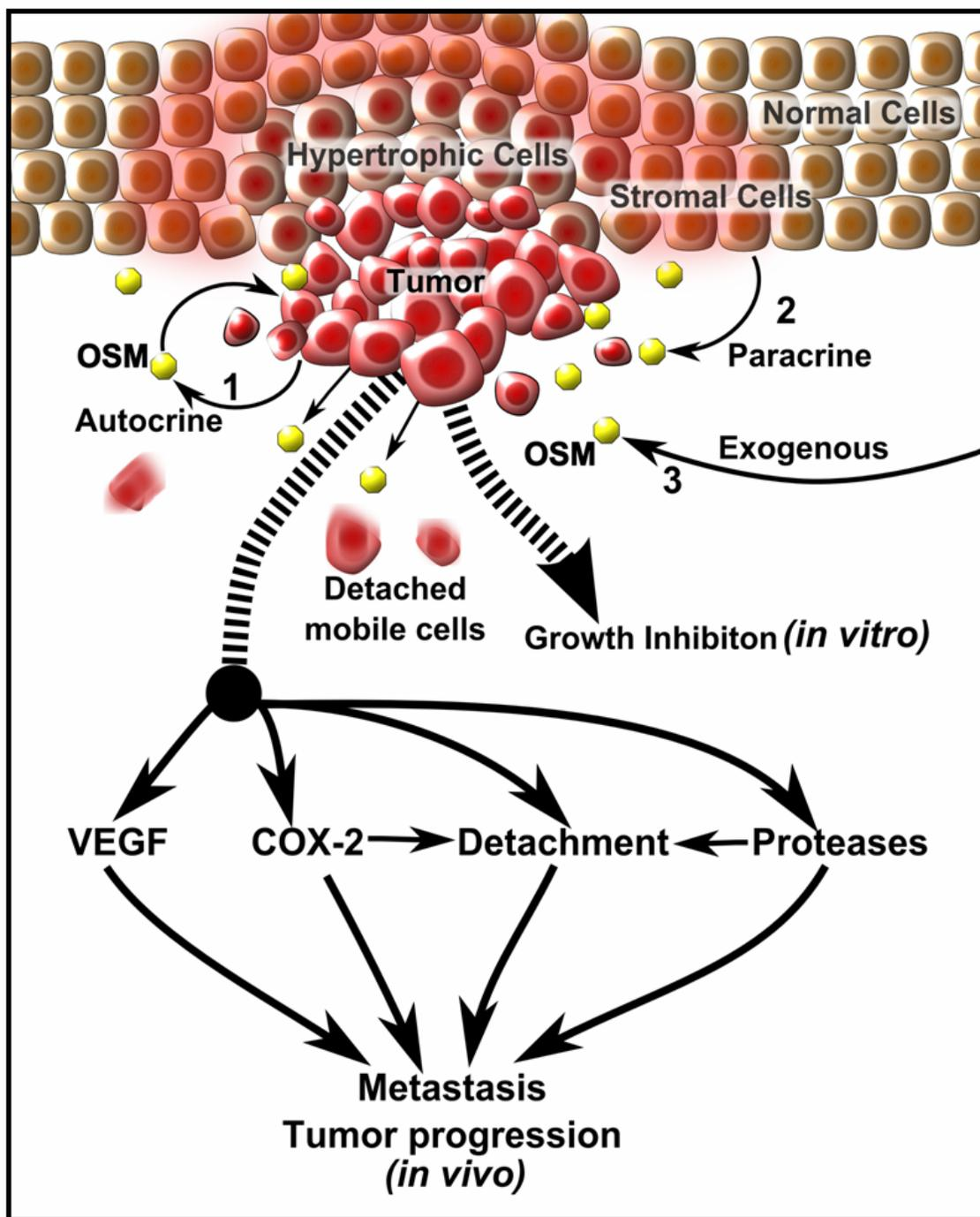


Figure A.2 OSM Induces Pro-Metastatic Effects in Mammary Cancer Cells

Figure A.2: *OSM Induces Pro-Metastatic Effects in Mammary Cancer Cells.* 1) OSM can signal in an autocrine manner as OSM produced by the tumor cells binds to its own receptors. 2) OSM can also be produced by stromal cells surrounding the tumor that can act on the cancer cells and other cells in the microenvironment. 3) Experimentally, we add recombinant OSM that acts exogenously. OSM can induce pro-metastatic factors such as VEGF, COX-2, and proteases that lead to tumor cell detachment, invasion, and increased metastatic potential.

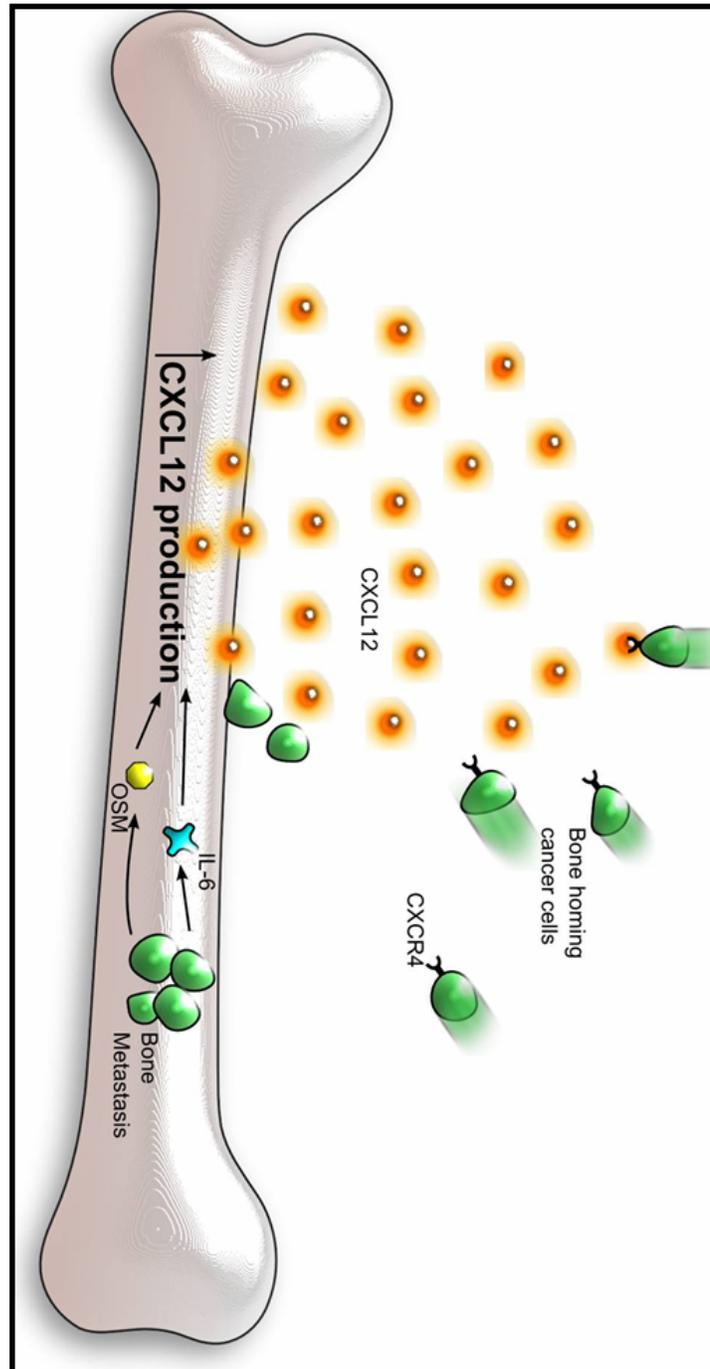


Figure A.3 CXCR4/CXCL12-Mediated Chemokine Attraction to the Bone

Figure A.3: *CXCR4/CXCL12-Mediated Chemokine Attraction to the Bone.* One of the known ways cancer cells can target the bone is by expressing CXCR4, which increases the cancer cell's propensity to move towards the CXCL12 concentration gradient. Injury to the bone as well as cancer metastasis to the bone increase inflammatory cytokines such as IL-6 and OSM. These cytokines are thought to contribute to CXCL12 production in the bone, leading to increased cancer cell migration to the bone.

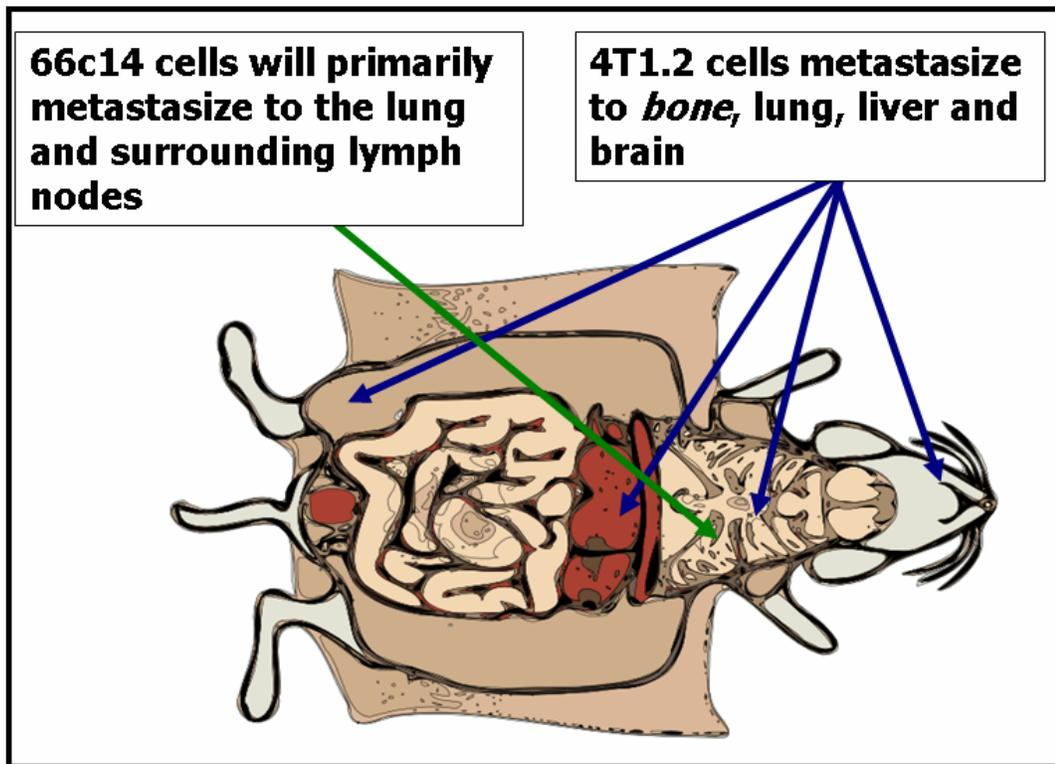


Figure A.4 66c14 and 4T1.2 Mouse Mammary Carcinoma Cells Metastasize to Different Organs When Injected Orthotopically into Balb/c Mouse

Figure A.4: *66c14 and 4T1.2 Mouse Mammary Carcinoma Cells Metastasize to Different Organs When Injected Orthotopically into Balb/c Mouse.* The metastatic profile of 4T1.2 cells are thought to resemble human breast cancer cells. 4T1.2 cells metastasize to the bone, lung, brain, and to the liver, while 66c14 cells metastasize only to the lung and the surrounding lymph nodes.

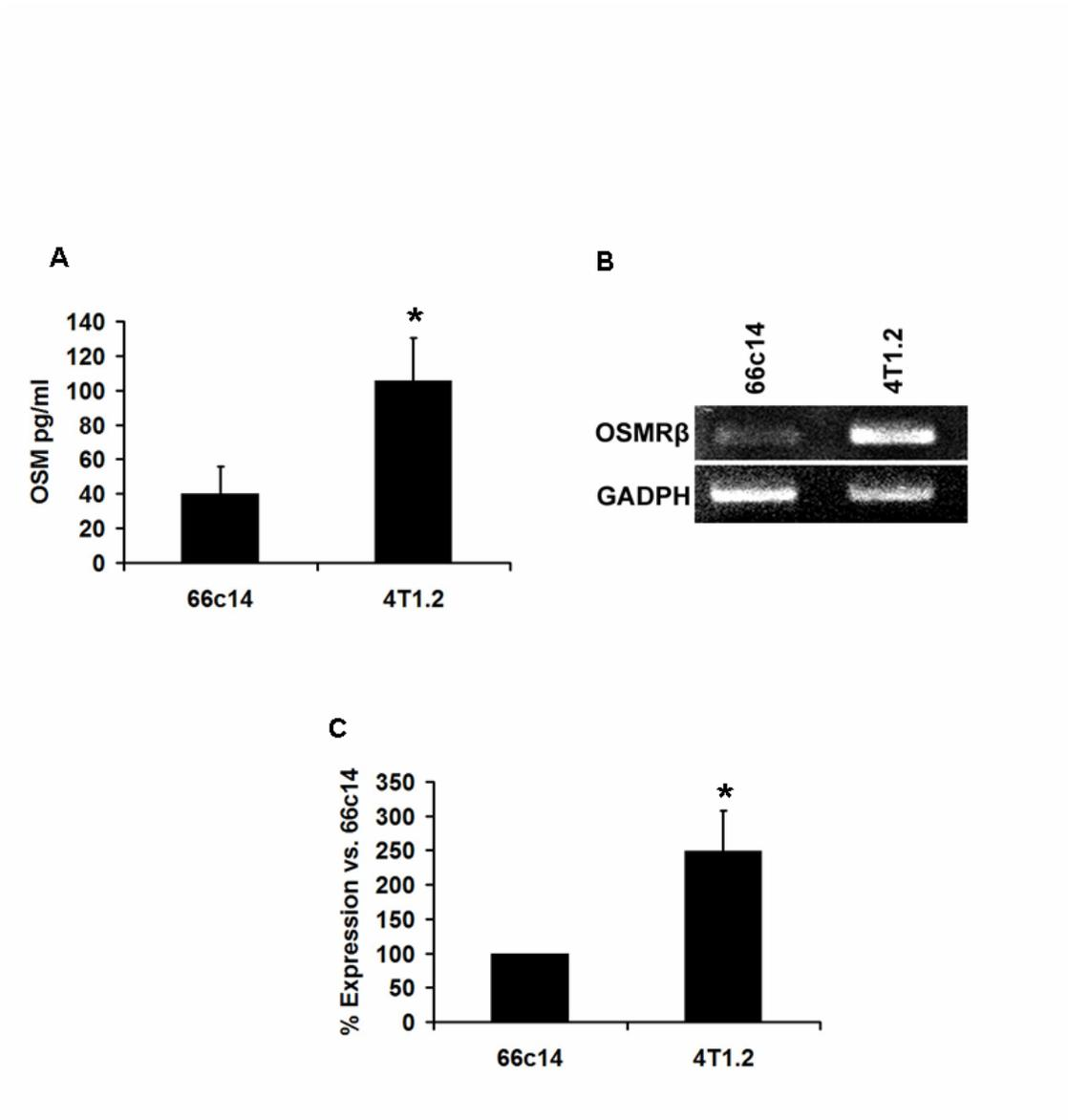


Figure A.5 The Metastatic 4T1.2 Cells Have More Intrinsic OSM Signaling

Figure A.5: *The Metastatic 4T1.2 Cells Have More Intrinsic OSM Signaling.* A, 4T1.2 cells produce over 2-fold more OSM by ELISA as compared to 66c14 cells. B, Representative image of a RT-PCR gel depicting higher OSMR β expression in 4T1.2 cells. C, 4T1.2 cells demonstrate 2.5-fold more OSMR β expression compared to 66c14 cells. Data represents an average of three separate experiments. Asterisks indicate significant differences ($p < 0.05$) vs -OSM control.

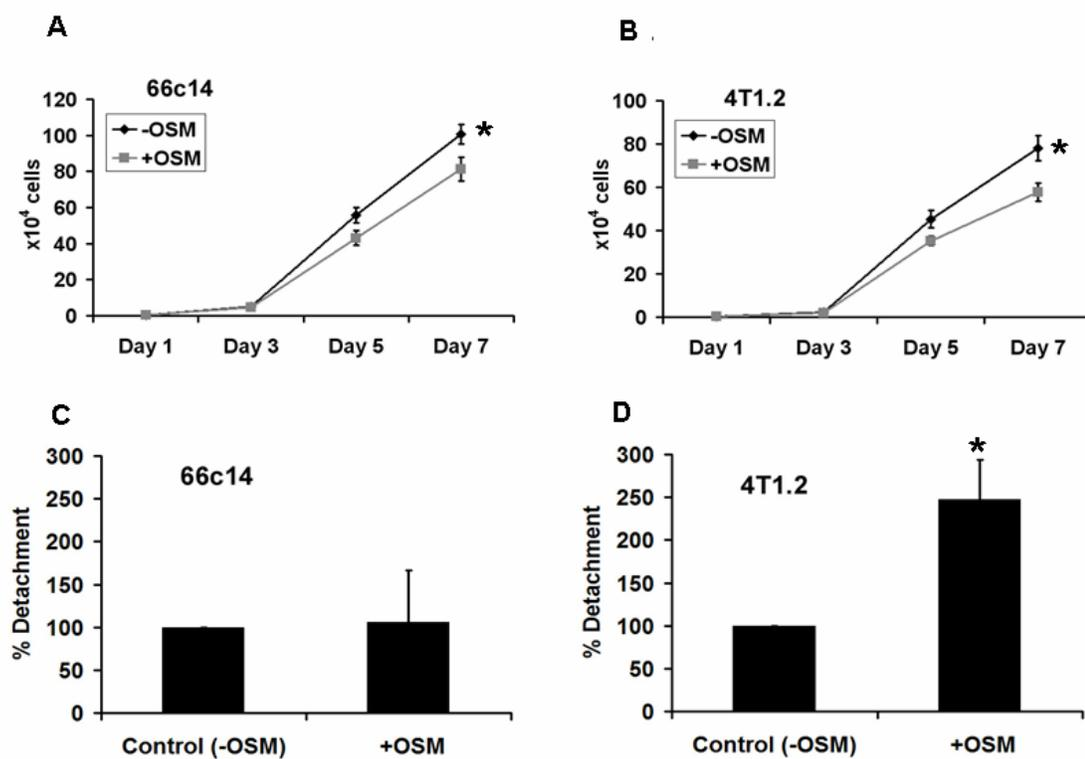


Figure A.6 OSM Inhibits Proliferation of 66c14 and 4T1.2 Cells but Only Induces Tumor Cell Detachment of 4T1.2 Cells

Figure A.6: *OSM Inhibits Proliferation of 66c14 and 4T1.2 Cells but Only Induces Tumor Cell Detachment of 4T1.2 Cells.* A, OSM decreases 66c14 cell proliferation by about 15% after 7 days in a cell proliferation assay. B, OSM decreases 4T1.2 cell proliferation by about 20% after 7 days in a cell proliferation assay. C, OSM does not induce detachment of 66c14 cells. D, OSM increases detachment 2.5-fold of 4T1.2 cells. Data represents an average of three separate experiments, each data point performed in duplicate. Asterisks indicate significant differences ($p < 0.05$) vs -OSM control.

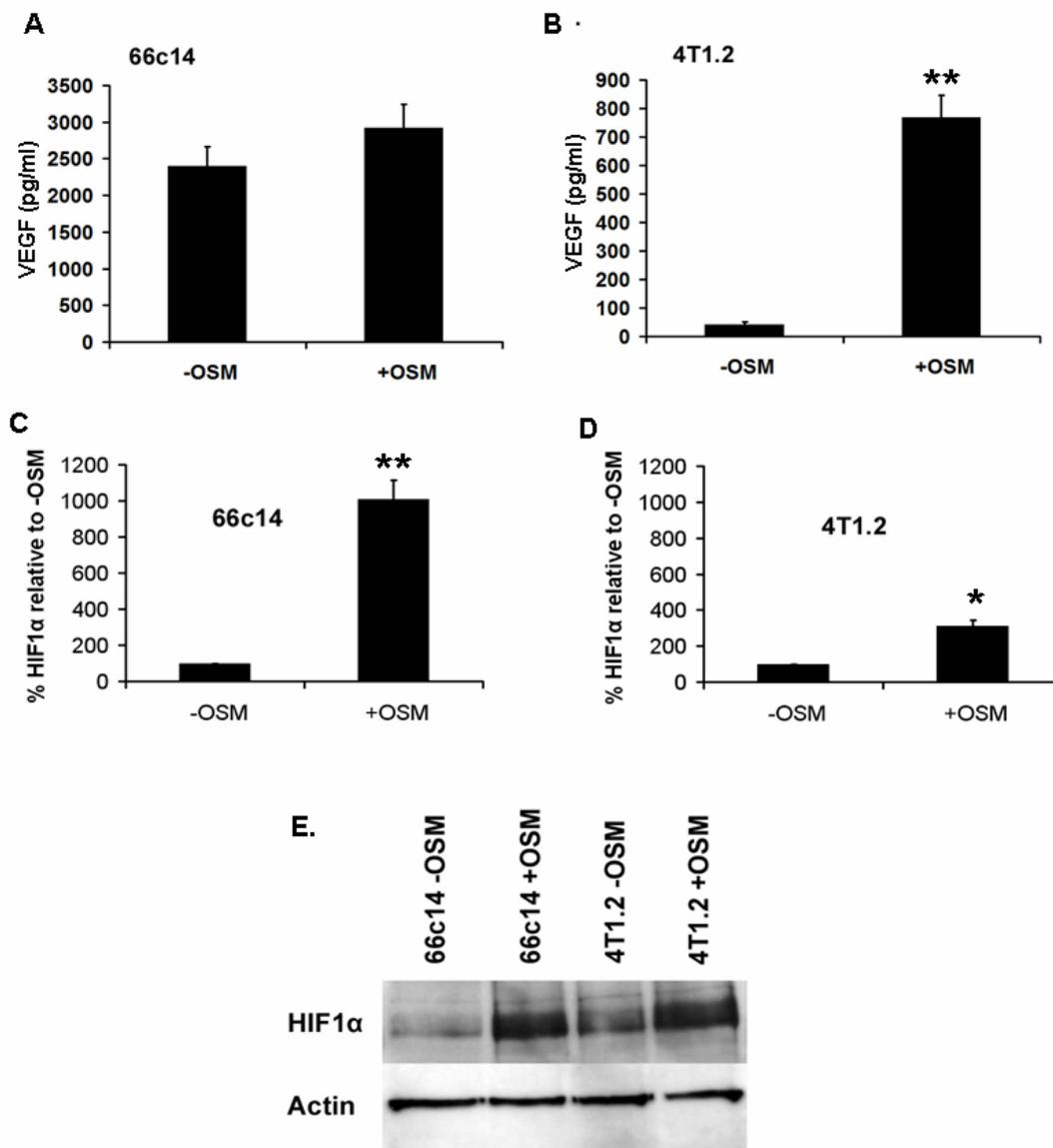


Figure A.7 OSM Increases VEGF Secretion by 4T1.2 but Not 66c14 cells, While HIF1 α Expression is Induced by OSM in Both 66c14 and 4T1.2 Cells

Figure A.7: *OSM Increases VEGF Secretion by 4T1.2 but Not 66c14 cells, While HIF1 α Expression is Induced by OSM in Both 66c14 and 4T1.2 Cells.* A, OSM does not significantly increase VEGF secretion in 66c14 cells. Note the high level of VEGF produced by untreated cells. B, OSM increases secreted VEGF levels in 4T1.2 cells by over 10-fold compared to non-treated cells. C, Quantification of Western blot analysis represented in E, shows that OSM increases HIF1 α expression approximately 10-fold compared to untreated 66c14 cells. D, Quantification of Western blot analysis represented in E, shows that OSM increases HIF1 α by about 3-fold compared to untreated 4T1.2 cells. E, Representative image of a HIF1 α Western blot depicting OSM-mediated upregulation of HIF1 α expression in 66c14 and 4T1.2 cells. Data represents an average of three separate experiments, each data point performed in duplicate. Double asterisks indicate significant differences ($p < 0.01$) vs -OSM control.

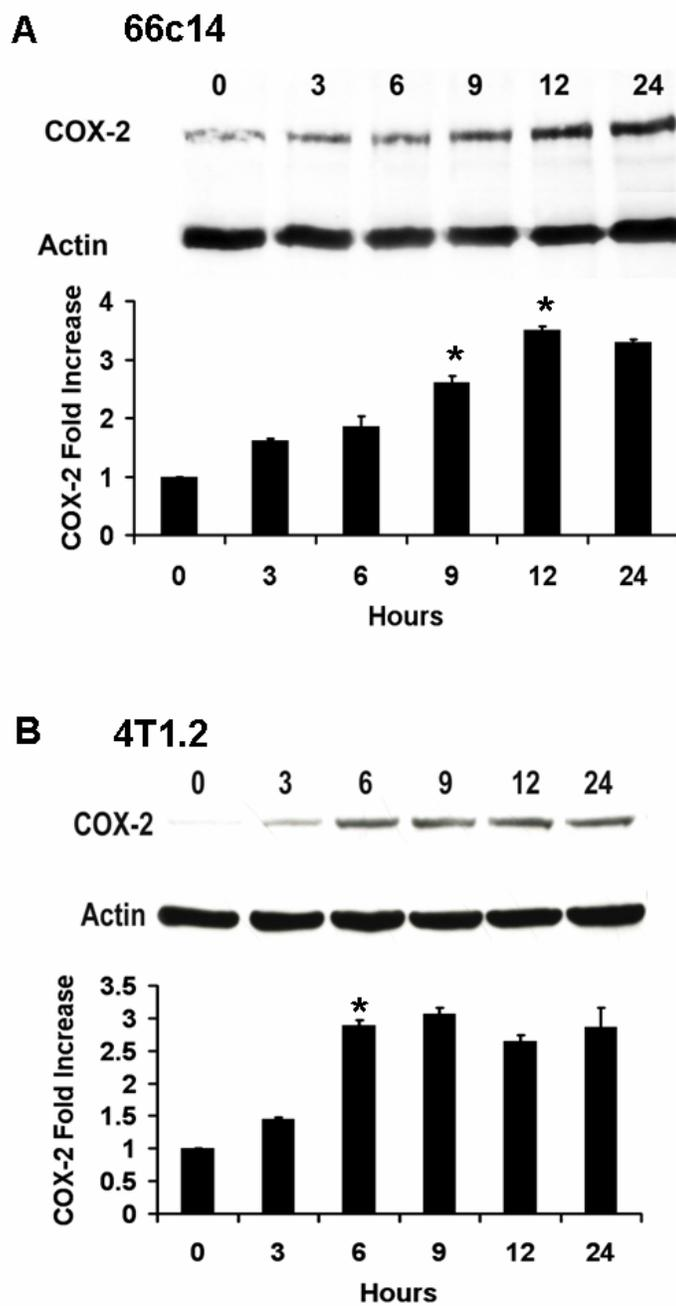


Figure A.8 OSM Increases COX-2 Expression in 66c14 and 4T1.2 Cells

Figure A.8: *OSM Increases COX-2 Expression in 66c14 and 4T1.2 Cells.* A, Maximal COX-2 expression in 66c14 cells stimulated by OSM peaks at 12 hours post-OSM treatment, leading to a 3.5-fold increase in COX-2 levels compared to time = 0. B, Maximal COX-2 expression in 4T1.2 cells stimulated by OSM peaks at 6 hours leading to a 3-fold increase compared to time = 0. Data represents an average of three separate experiments, each data point performed in duplicate. Asterisks indicate significant differences ($p < 0.05$) vs time = 0.

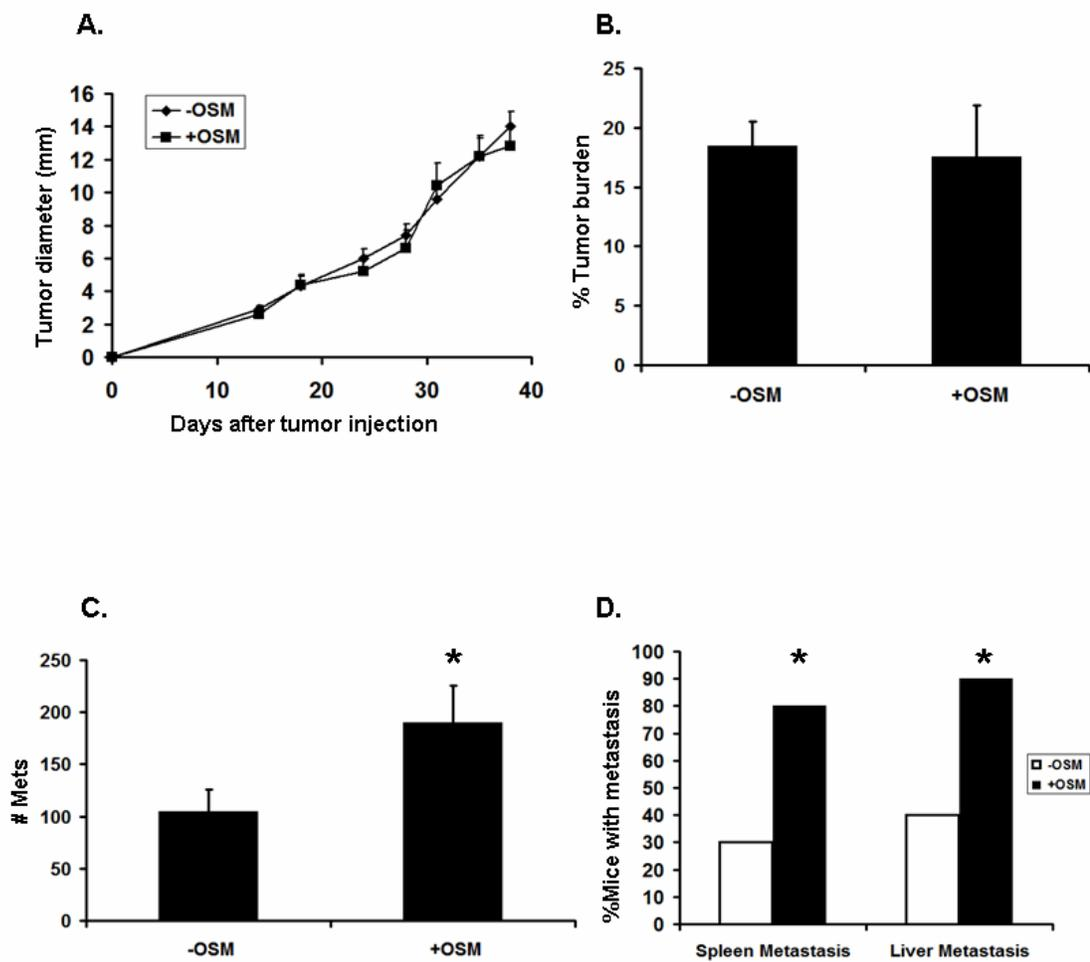


Figure A.9 Injection of Recombinant Mouse OSM (rmOSM) Increases Metastases but not Tumor Growth in vivo in an Orthotopic 4T1.2 Mouse Model

Figure A.9: *Injection of Recombinant Mouse OSM (rmOSM) Increases Metastases but not Tumor Growth in vivo in an Orthotopic 4T1.2 Mouse Model.* A, *In vivo*, OSM has no effect on tumor proliferation rates. B, rmOSM also has no effect on overall tumor burden (tumor weight/body weight). C, rmOSM increases total number of metastases to the lung by about 50%. D, About 80% of tumor-bearing mice that were treated with rmOSM have metastases to the spleen compared to only 30% of untreated mice. Ninety percent of tumor bearing mice that were treated with rmOSM have metastases to the liver, as compared to only 40% of untreated mice. Statistical analysis on section D was performed using the Fisher's exact test. Data represents an average of two separate experiments with five mice per group. Asterisks indicate significant differences ($p < 0.05$) vs untreated mice.

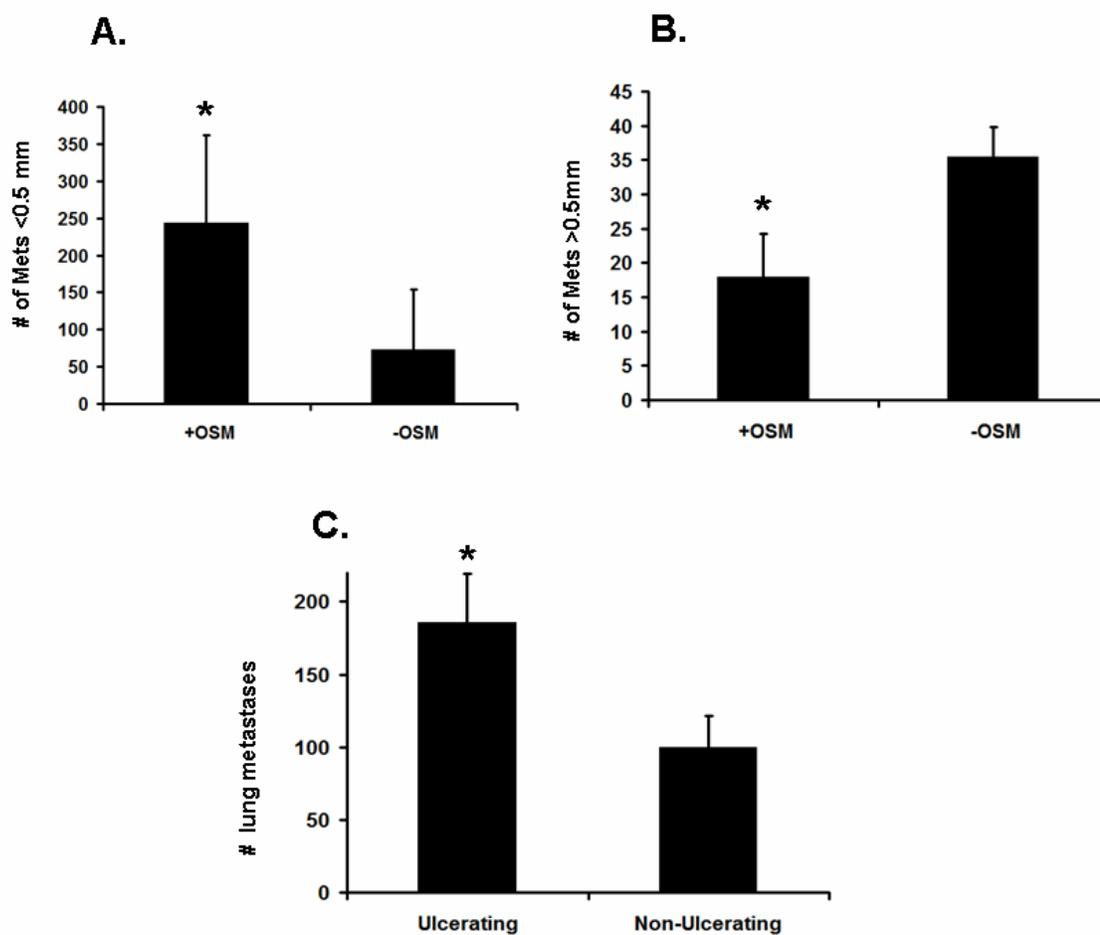


Figure A.10 In the 4T1.2 Mouse Models, the Size of Metastases Differs Depending on rmOSM Treatment, While the Number of Lung Metastases Changes with Tumor-Ulcerative Status

Figure A.10: *In the 4T1.2 Mouse Models, the Size of Metastases Differs Depending on rmOSM Treatment, While the Number of Lung Metastases Changes with Tumor-Ulcerative Status.* A, rmOSM-treated mice bearing 4T1.2 tumors exhibits nearly 4-times more small lung metastases (<0.5 mm) compared to untreated mice. B, rmOSM-treated mice bearing 4T1.2 tumors has 50% less large lung metastases (>0.5 mm) compared to untreated mice. C, Mice with ulcerated tumors have 80% more metastases to the lung compared to mice that did not have ulcerated tumors. Data represents an average of two separate experiments with five mice per group. Asterisks indicate significant differences ($P < 0.05$) vs untreated mice or non-ulcerated tumors.

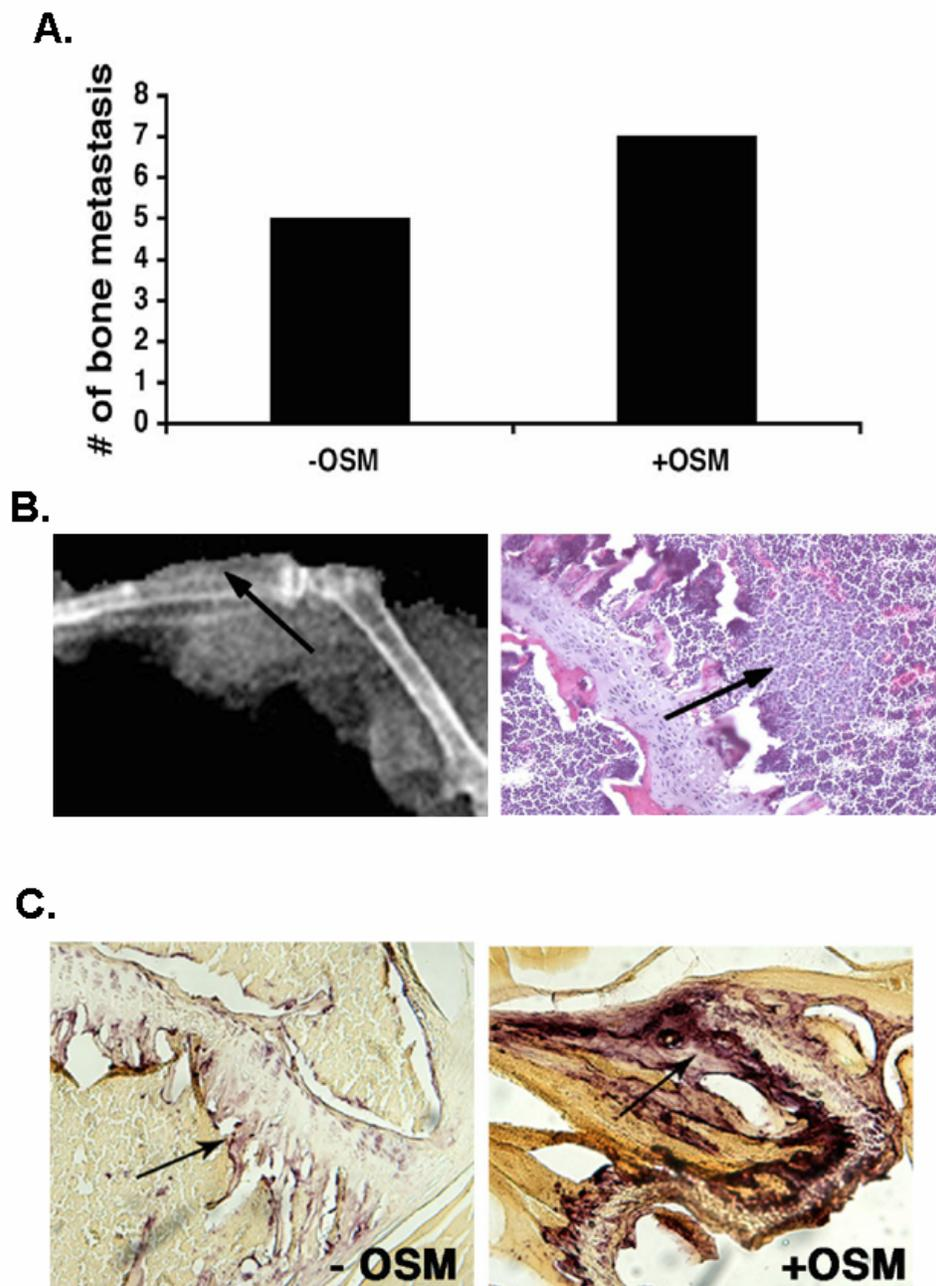


Figure A.11 OSM-Treated Mice Have More Bone Metastases and Potentially Reduced Bone Integrity

Figure A.11: *OSM-Treated Mice Have More Bone Metastases and Potentially Reduced Bone Integrity.* A, Mice that were treated with rmOSM have more bone metastases, but this data is not statistically significant (Fisher's exact test). B, The black arrows point to metastases depicted by shadows in the radiograph (left), and dense packed cells in the histological H&E section (right). C, Representative images of TRAP-stained bone sections. rmOSM treated mice (right panel) have darker TRAP staining in general compared to untreated mice (left panel), indicating increased osteoclast numbers and activity. Data represents an average of two separate experiments with five mice per group.

Plasmid Design

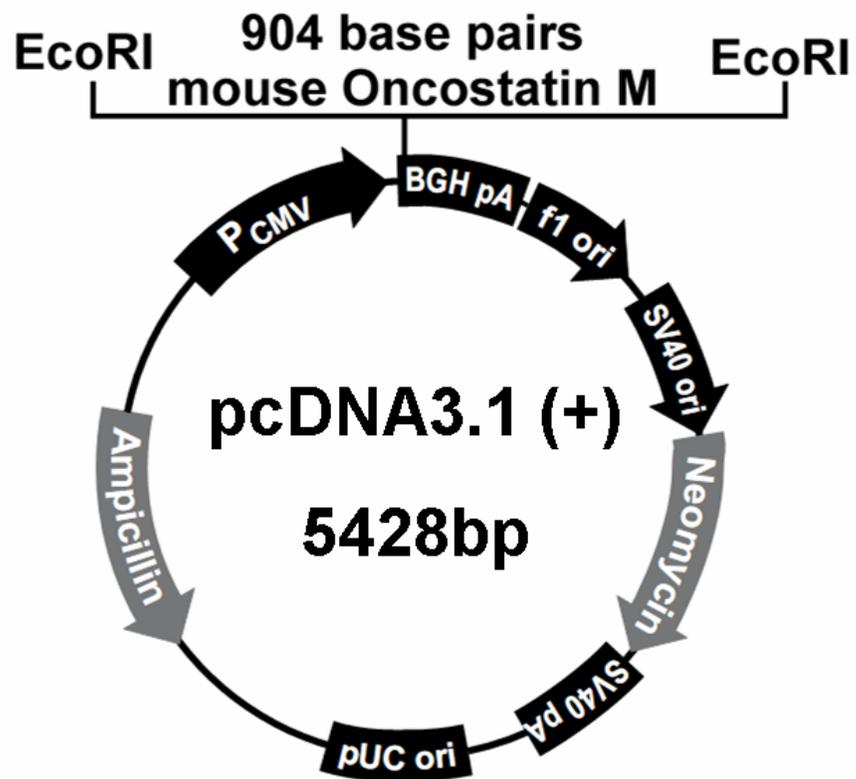


Figure A.12 Mouse OSM Expression Plasmid Design

Figure A.12: *Mouse OSM Expression Plasmid Design.* Mouse OSM cDNA was inserted into a mammalian expression vector (pcDNA3.1+) using the restriction enzyme EcoRI. The expression is controlled by the viral cytomegalovirus promoter which is designed to promote high levels of constitutive expression of the insert. This plasmid was used to transfect 66c14 and 4T1.2 cells to overexpress OSM endogenously.

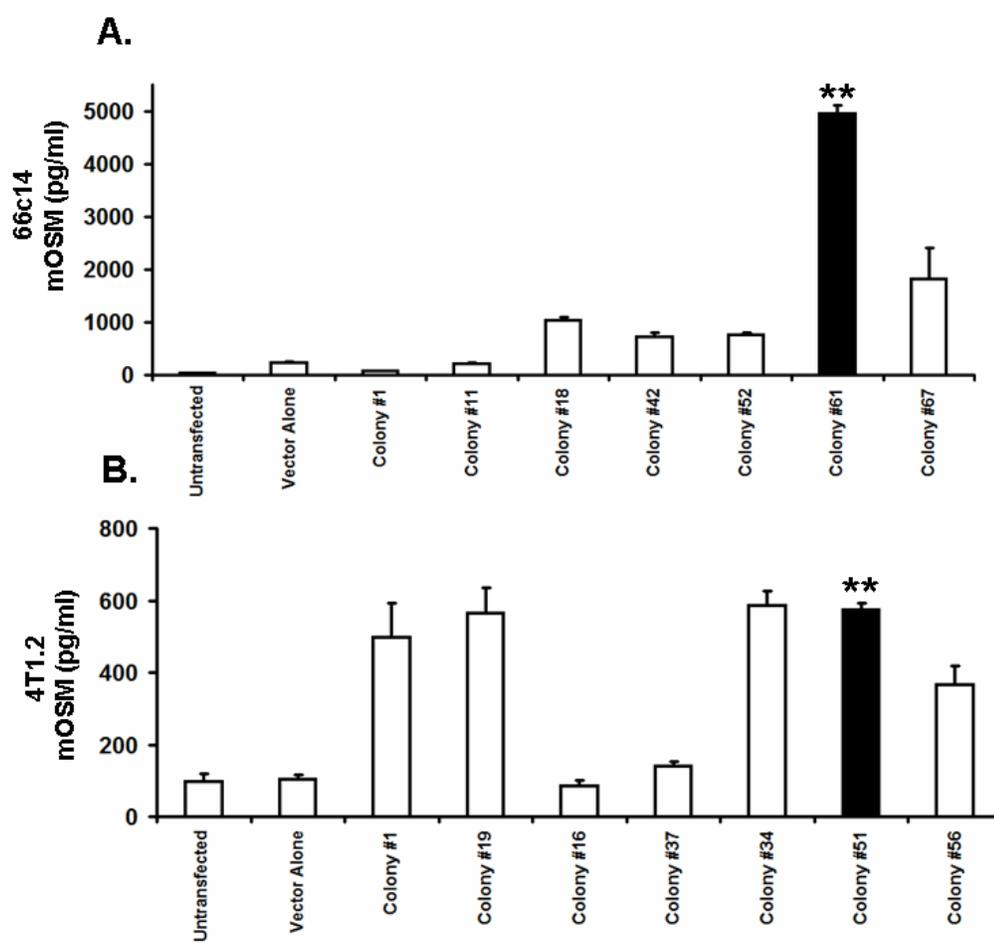


Figure A.13 Overexpression of OSM in 66c14 and 4T1.2 Cells Transfected With the pcDNA3.1+OSM Construct

Figure A.13: *Overexpression of OSM in 66c14 and 4T1.2 Cells Transfected With the pcDNA3.1+OSM Construct.* A, Colony #61 is the highest producing transfected 66c14 colony, secreting almost 5000 pg/ml of OSM as measured by ELISA which was nearly 60-fold higher than untransfected cells. B, Colony #51 is the highest producing transfected 4T1.2 colony, secreting almost 600pg/ml of OSM as measured by ELISA which was nearly 6-fold higher than untransfected cells. Data represents and average of two separate experiments and each data point performed in quadruplicate. Asterisks indicate significant differences ($P < 0.05$) vs vector control.

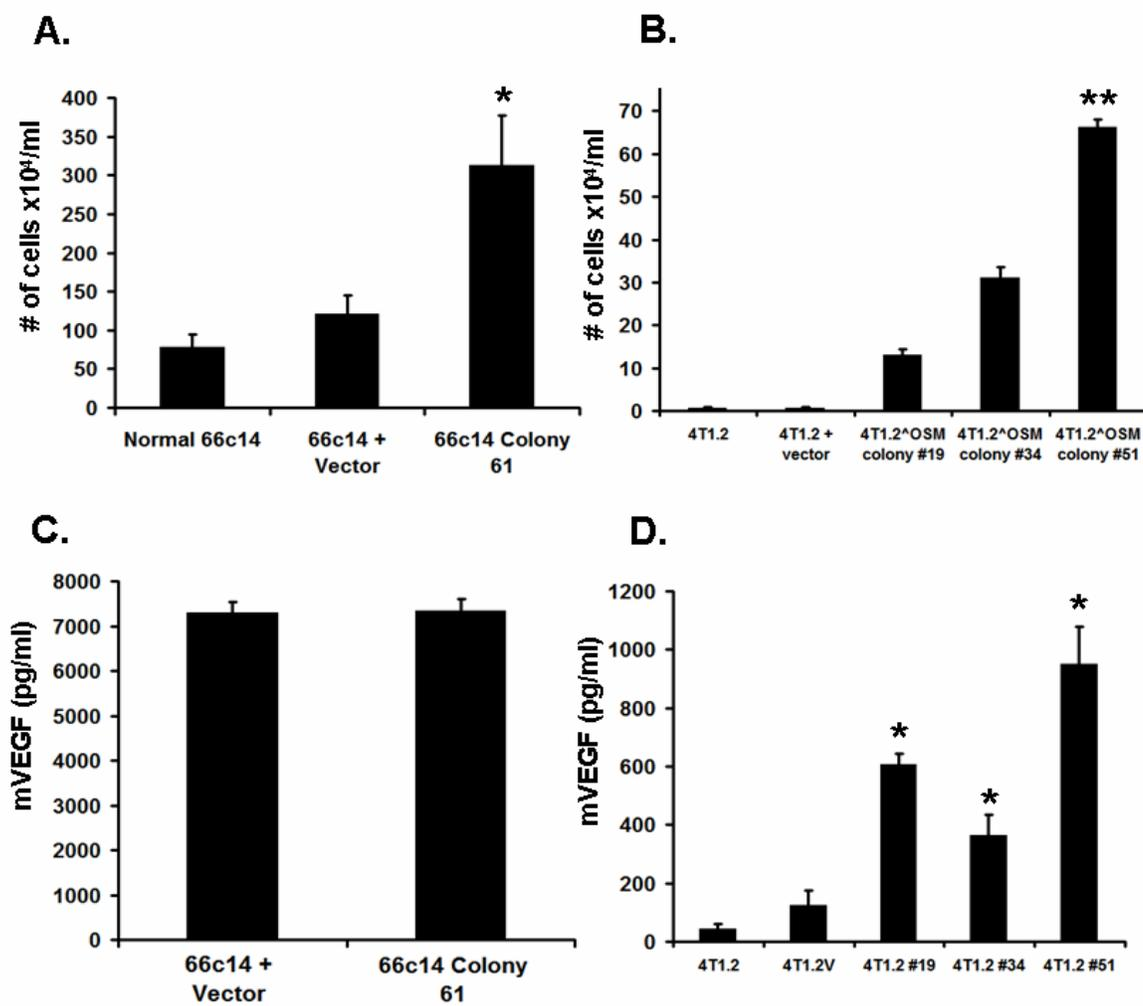


Figure A.14 OSM-Overexpressing 66c14 and 4T1.2 Cells Depict Similar Characteristics to Parental Cells Treated with rmOSM

Figure A.14: *OSM-Overexpressing 66c14 and 4T1.2 Cells Depict Similar*

Characteristics to Parental Cells Treated with rmOSM. A, OSM-overexpressing 66c14 or colony #61 has 3 times more detached cells compared to the vector control or untransfected cells. B, OSM-overexpressing 4T1.2 or colony #51 cells has 2 times more detached cells compared to other overexpressing colonies, and about 30-fold more detached cells compared to the vector control or the untransfected cells. C, There is no difference in secreted VEGF levels by ELISA between 66c14+vector cells and 66c14 OSM-overexpressing cells. D, OSM-overexpressing 4T1.2 or colony #51 has 10-fold more secreted VEGF levels as measured by ELISA compared to untransfected cells or the vector control. Data represents an average of three separate experiments and each data point performed in duplicate. Asterisks indicate significant differences (* P<0.05, ** P<0.01) vs vector control.

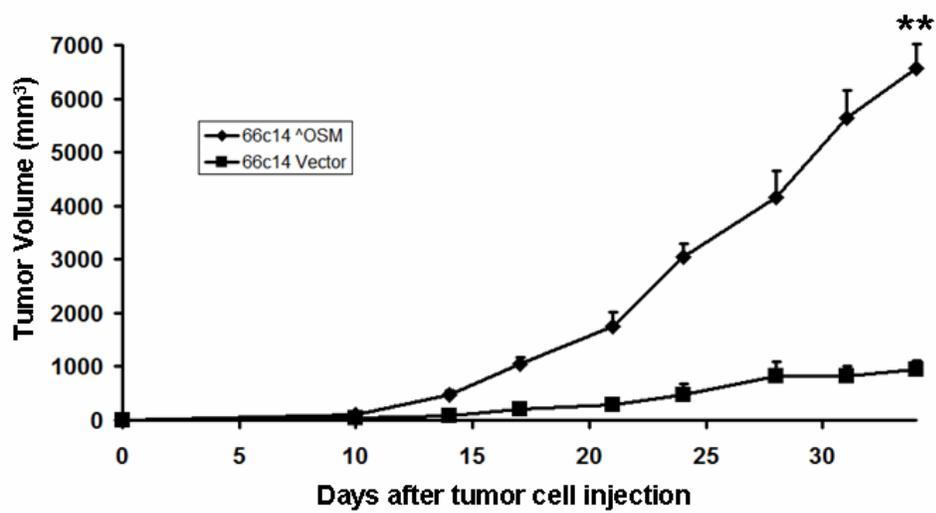


Figure A.15 OSM-Overexpressing 66c14 Cells Grow Much Faster Than Vector

Control Cells *in vivo* in an Orthotopic 66c14 Mouse Model

Figure A.15: *OSM-Overexpressing 66c14 Cells Grow Much Faster Than Vector Control Cells in vivo in an Orthotopic 66c14 Mouse Model.* By day 30, the size of the tumor is volumetrically about 7-fold larger on mice with 66c14^{OSM} tumor cells compared to 66c14+vector cells. The average tumor growth rate, as extrapolated by linear curve analysis, of the 66c14^{OSM} tumors is 209 mm³/day, while the growth rate of 66c14+vector tumors is 32 mm³/day. Overall, the growth rate of the tumor is 6.5 times faster in mice with 66c14^{OSM} tumors compared to 66c14+vector tumors. Data represents an average of one experiment with eleven mice per group. Double asterisks indicate significant differences (P<0.01) vs vector control cells.

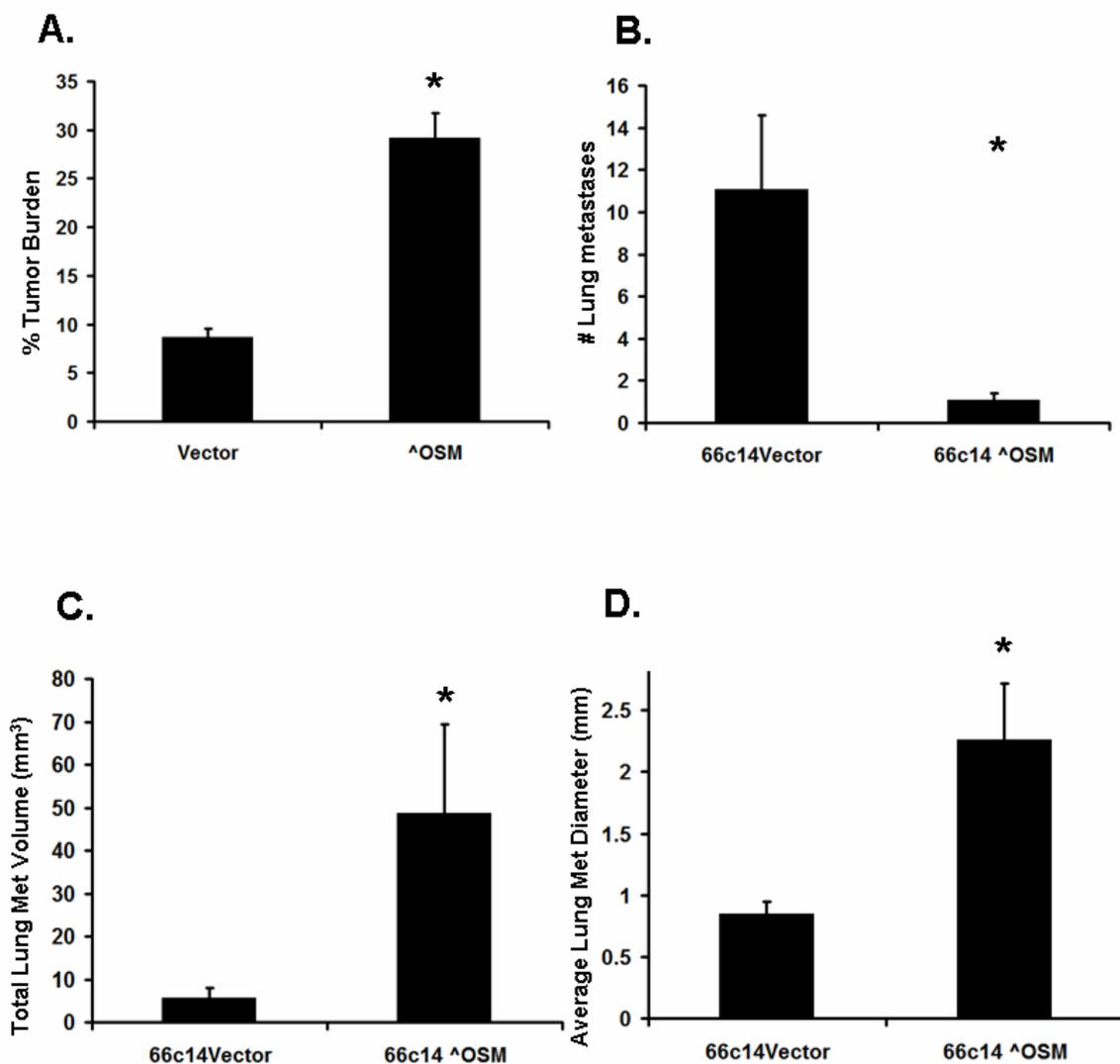


Figure A.16 OSM-Overexpressing 66c14 Cells Have Reduced Numbers of Metastases, but Larger Total Metastatic Volume Compared to 66c14+Vector Cells *in vivo* in an Orthotopic 66c14 Mouse Model

Figure A.16: *OSM-Overexpressing 66c14 Cells Have Reduced Numbers of Metastases, but Larger Total Metastatic Volume Compared to 66c14+Vector Cells in vivo in an Orthotopic 66c14 Mouse Model.* A, Tumor burden is 3-fold higher in 66c14^{OSM} injected mice compared to mice injected with 66c14+vector cells. B, Total number of metastases to the lung are 11 times higher in 66c14+vector tumor cell-injected mice compared to 66c14^{OSM} tumor cell-injected mice. C, Total volume of lung metastases are 6 times higher in 66c14^{OSM} tumor cell-injected mice compared to mice injected with 66c14+vector cells. D, The average size of the lung metastases is larger in mice bearing 66c14^{OSM} tumors by about 2.5-fold compared to mice bearing 66c14+vector tumors. Data represents an average of one experiment with eleven mice per group. Asterisks indicate significant differences ($P < 0.05$) vs vector control cells.

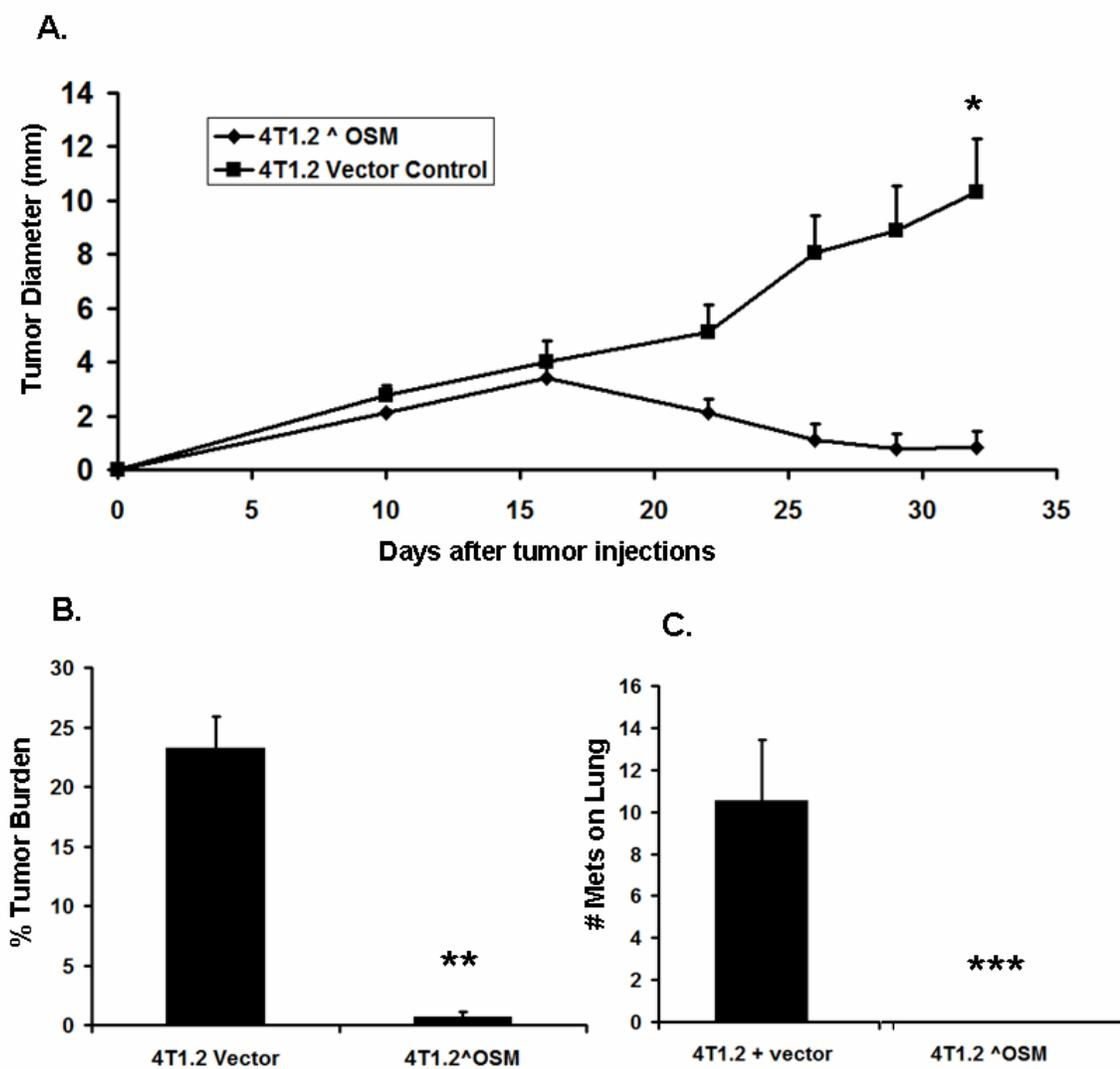
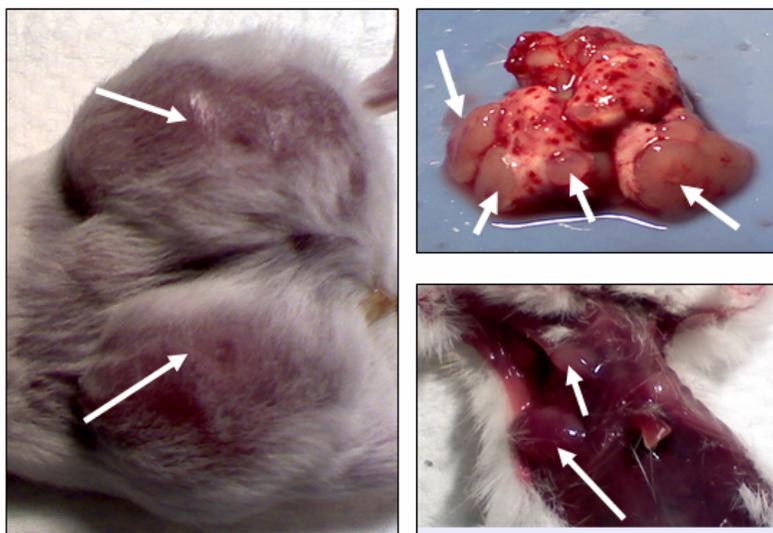


Figure A.17 OSM-Overexpressing 4T1.2 Cells fail to Grow and Metastasize *in vivo* in an Orthotopic 4T1.2 Mouse Model

Figure A.17: *OSM-Overexpressing 4T1.2 Cells fail to Grow and Metastasize in vivo in an Orthotopic 4T1.2 Mouse Model.* A, 4T1.2^{OSM} cells injected into mice, grew tumors up to day 16, which subsequently shrank in size while the tumors from 4T1.2+vector cell-injected mice continued to grow. B, 4T1.2^{OSM} injected mice have an average tumor burden of 1%, while 4T1.2+vector injected mice have an average tumor burden of 24%. C, 4T1.2^{OSM}-injected mice have no lung metastases, while 4T1.2+Vector mice average about 10 metastases to the lung. Data represents an average of one experiment with ten mice per group. Asterisks indicate significant differences (*P<0.05, **P<0.01, ***P<0.001) vs vector control cells.

A.



B.

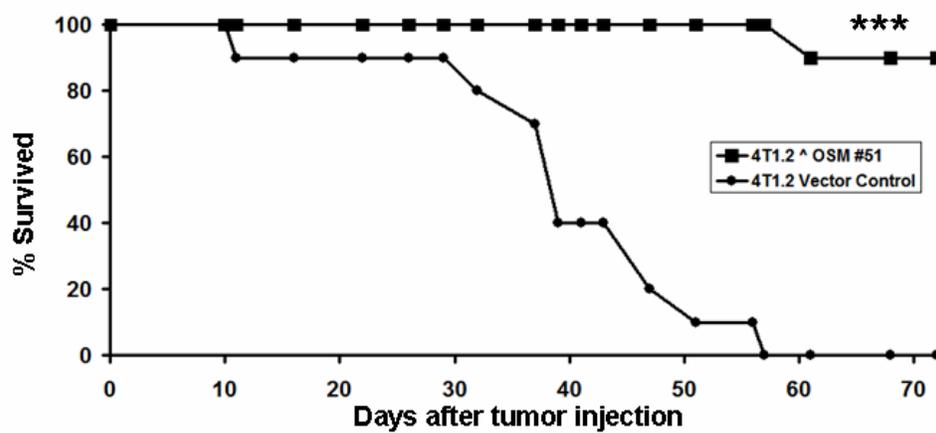


Figure A.18 4T1.2[^]OSM-Injected Mice Have a Much Higher Survival Rate

Figure A.18: *4T1.2^{OSM}-Injected Mice Have a Much Higher Survival Rate.* A, The photographs depict endpoint criteria for the survival experiment showing a 20mm in diameter tumor (left), 10% weight loss, or high levels of metastases causing cachexia (right panels). B, 4T1.2^{OSM} cell-injected mice survived longer than controls, with 90% of the mice still alive at the end of the experiment (day 72) and no sign of metastatic disease. All of the 4T1.2+Vector cell-injected mice died by day 57. Statistical analysis on section B was done with the Log-Rank test. Data represents an average of one experiment with ten mice per group. Triple asterisks indicate significant differences ($P < 0.001$) vs vector control cells.

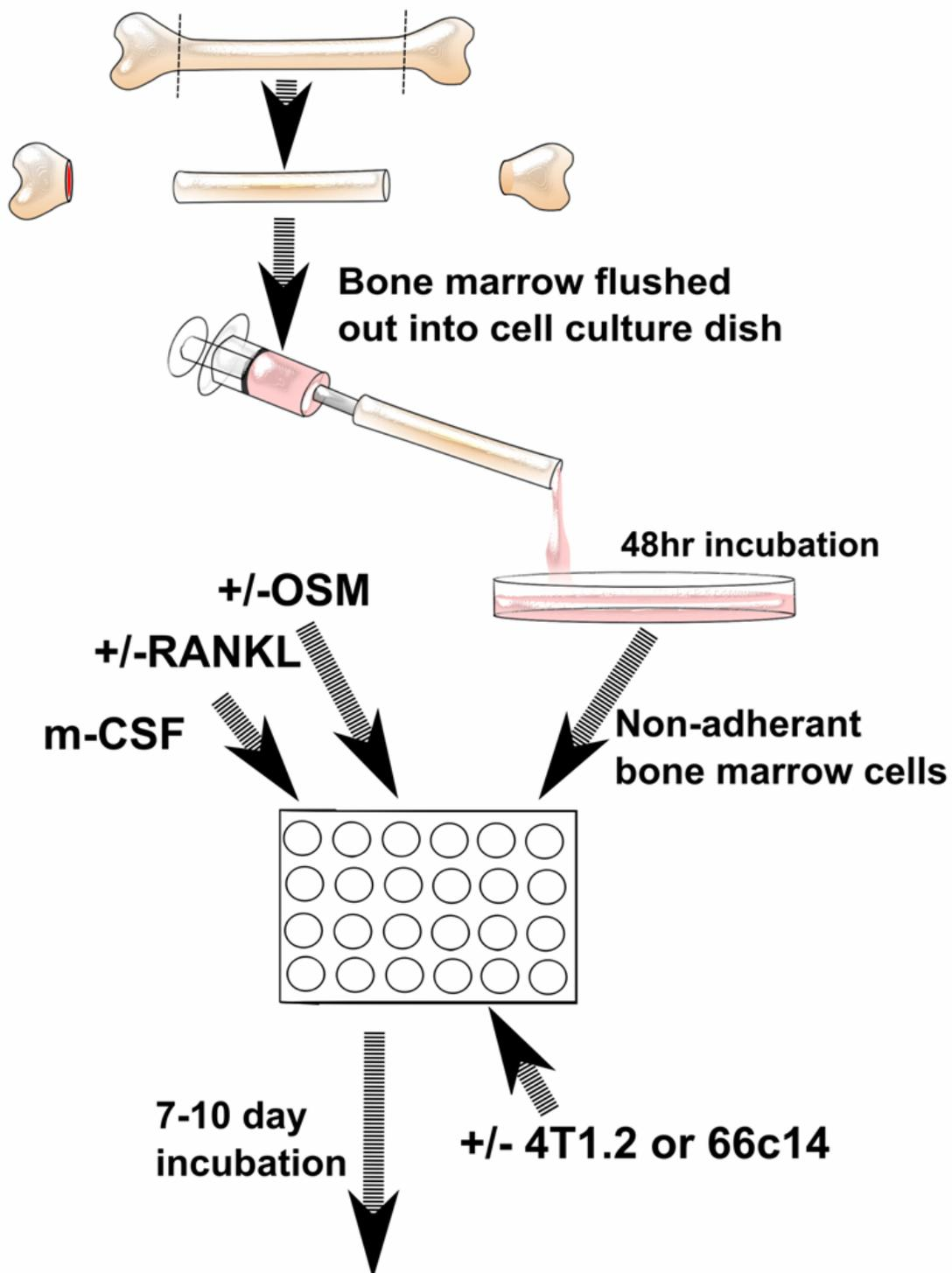


Figure A.19 Schematic Demonstrating Preparation of Pre-Osteoclasts for Osteoclastogenesis Experiment

Figure A.19: *Schematic Demonstrating Preparation of Pre-Osteoclasts for Osteoclastogenesis Experiment.* Femurs and tibias are extracted from Balb/c mice and their bone marrow is flushed out into a culture dish. After a 48 hour incubation at 37°C, non-adherent bone marrow cells are collected for co-cultures. The collected bone marrow cells are co-cultured with 4T1.2 or 66c14 cells and treated with 5 ng/ml m-CSF, 10 ng/ml +/- RANKL, +/- 25 ng/ml OSM. After a 7-10 day incubation at 37°C, osteoclasts are stained via a TRAP+ stain.

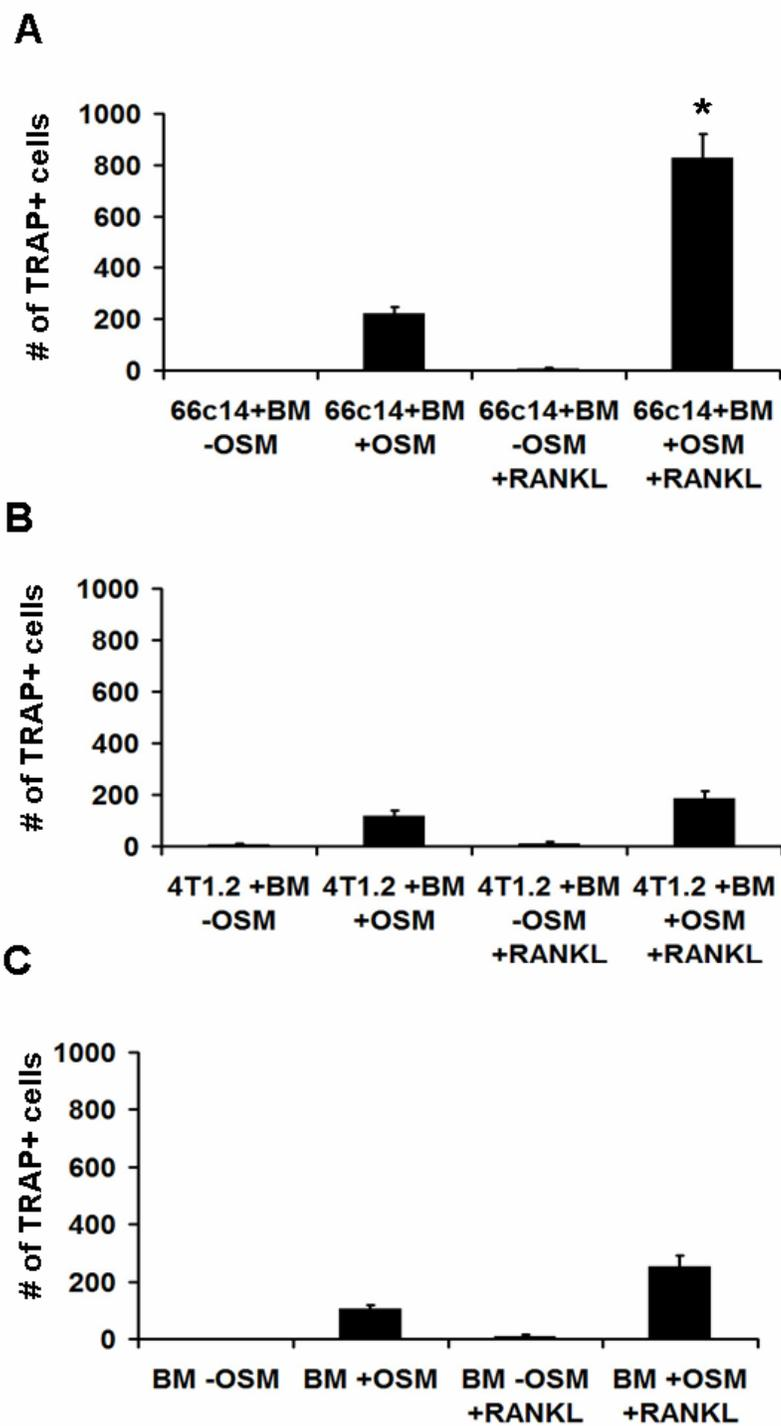


Figure A.20 66c14 Mouse Breast Cancer Cells and OSM Synergistically Increase Osteoclastogenesis with Non-Adherent Bone Marrow (BM) Cells

Figure A.20: *66c14 Mouse Breast Cancer Cells and OSM Synergistically Increase Osteoclastogenesis with Non-Adherent Bone Marrow (BM) Cells.* In the absence of OSM, there is little to no TRAP+ cells in any of the cultures. A, Without RANKL, 66c14 +BM+OSM cultures generated about 200 TRAP+ cells, while in the presence of RANKL, the number of TRAP+ cells increases to about 800. B, Without RANKL, 4T1.2+BM+OSM cultures generate about 150 TRAP+ cells, while in the presence of RANKL, the number of TRAP+ cells increase to about 200. This increase was non-significant. C, Without RANKL, BM+OSM cultures generate about 150 TRAP+ cells, while in the presence of RANKL, the number of TRAP+ cells increases to about 250. Data represents an average of six separate experiments and each data point performed in duplicate. Asterisks indicate significant differences ($P < 0.05$) vs BM only cultures.

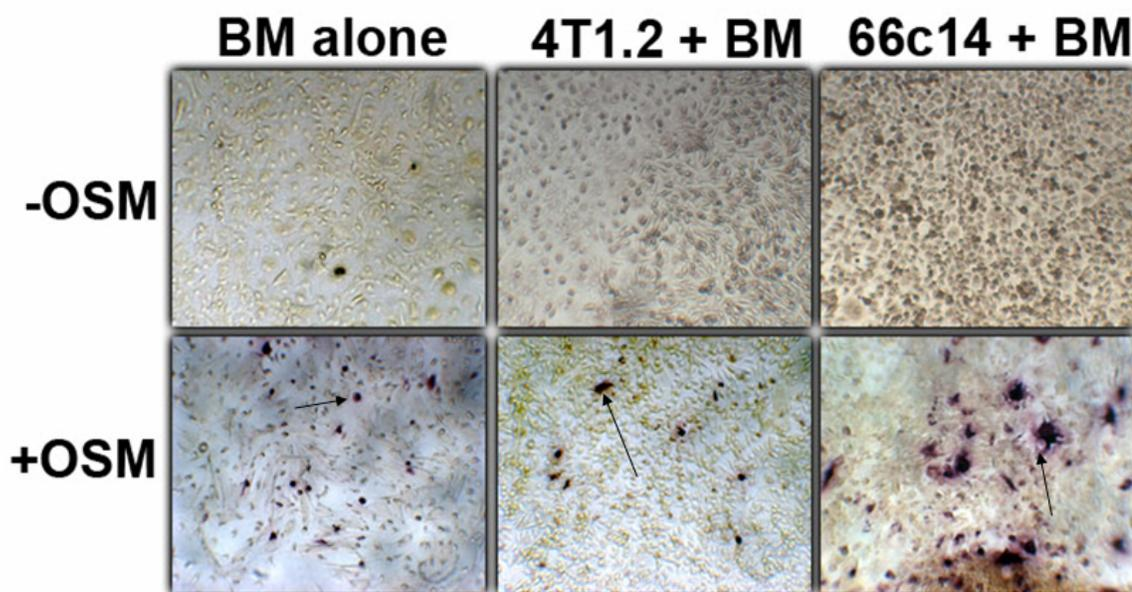


Figure A.21 Representative Images of TRAP+ Cells Detected in
Osteoclastogenesis Assays

Figure A.21: *Representative Images of TRAP+ Cells Detected in Osteoclastogenesis Assays.* Black arrows indicate TRAP+ stained cells (dark purple). Largest osteoclasts are seen in co-cultures containing 66c14 cells +OSM.

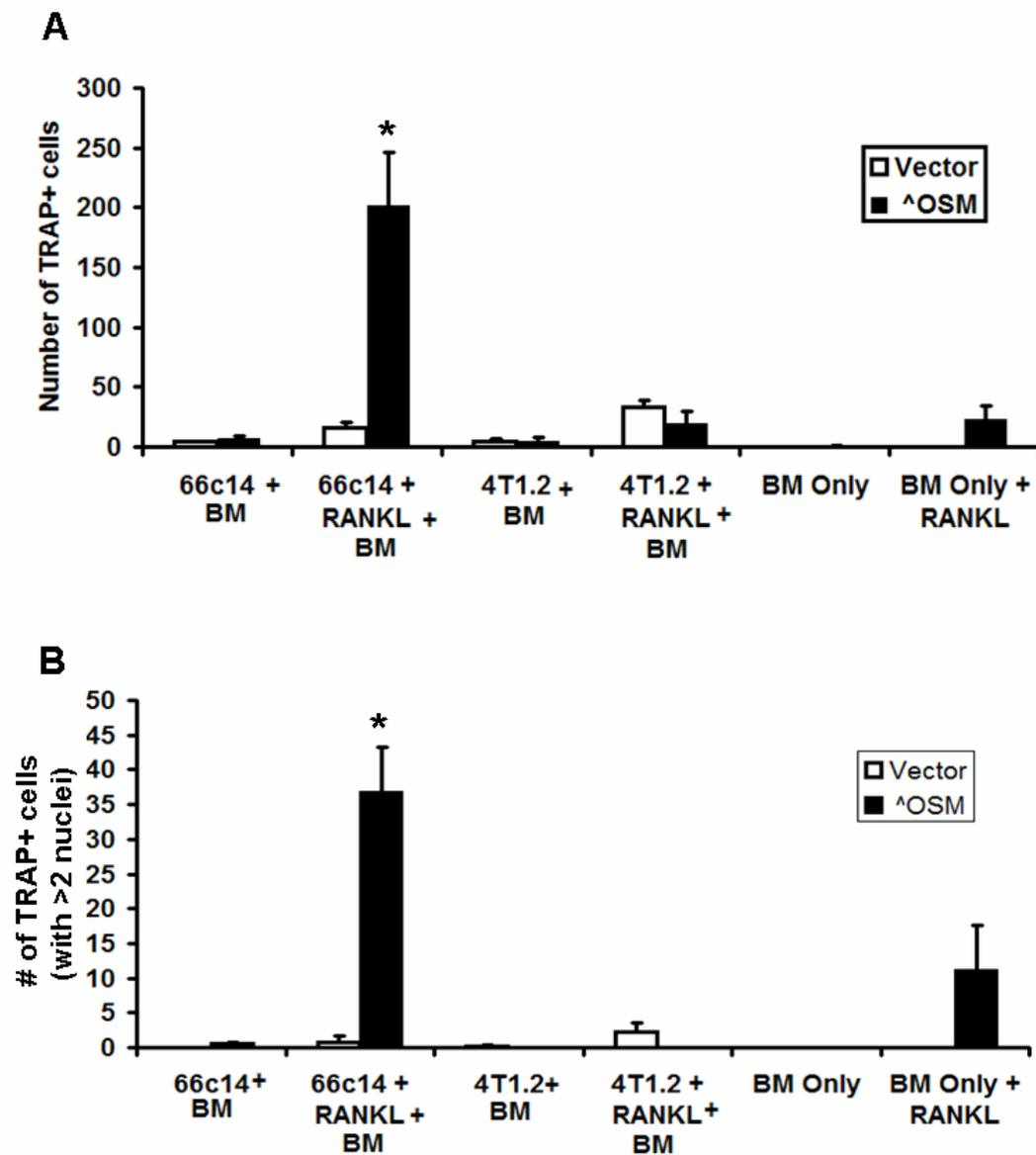


Figure A.22 As with the Addition of Recombinant OSM, 66c14^hOSM Cells Increase Osteoclast Differentiation of BM cells in the Presence of RANKL

Figure A.22: *As with the Addition of Recombinant OSM, 66c14^{OSM} Cells Increase Osteoclast Differentiation of BM cells in the Presence of RANKL.* A, 66c14^{OSM} cells increase osteoclast differentiation by 8-fold compared to 66c14 cells transfected with an empty vector. Co-cultures containing 4T1.2 OSM-overexpressing cells do not increase the number of TRAP⁺ cells. B, TRAP⁺ multinucleated cells are seen predominantly in cultures containing OSM-overexpressing 66c14^{OSM} cells. There is a 15-fold increase in TRAP⁺ cells in co-cultures containing 66c14^{OSM} cells compared to co-cultures containing 66c14+vector control cells. Data represents an average of two separate experiments, and each data point performed in quadruplicate. Asterisks indicate significant differences ($P < 0.05$) vs BM only cultures.

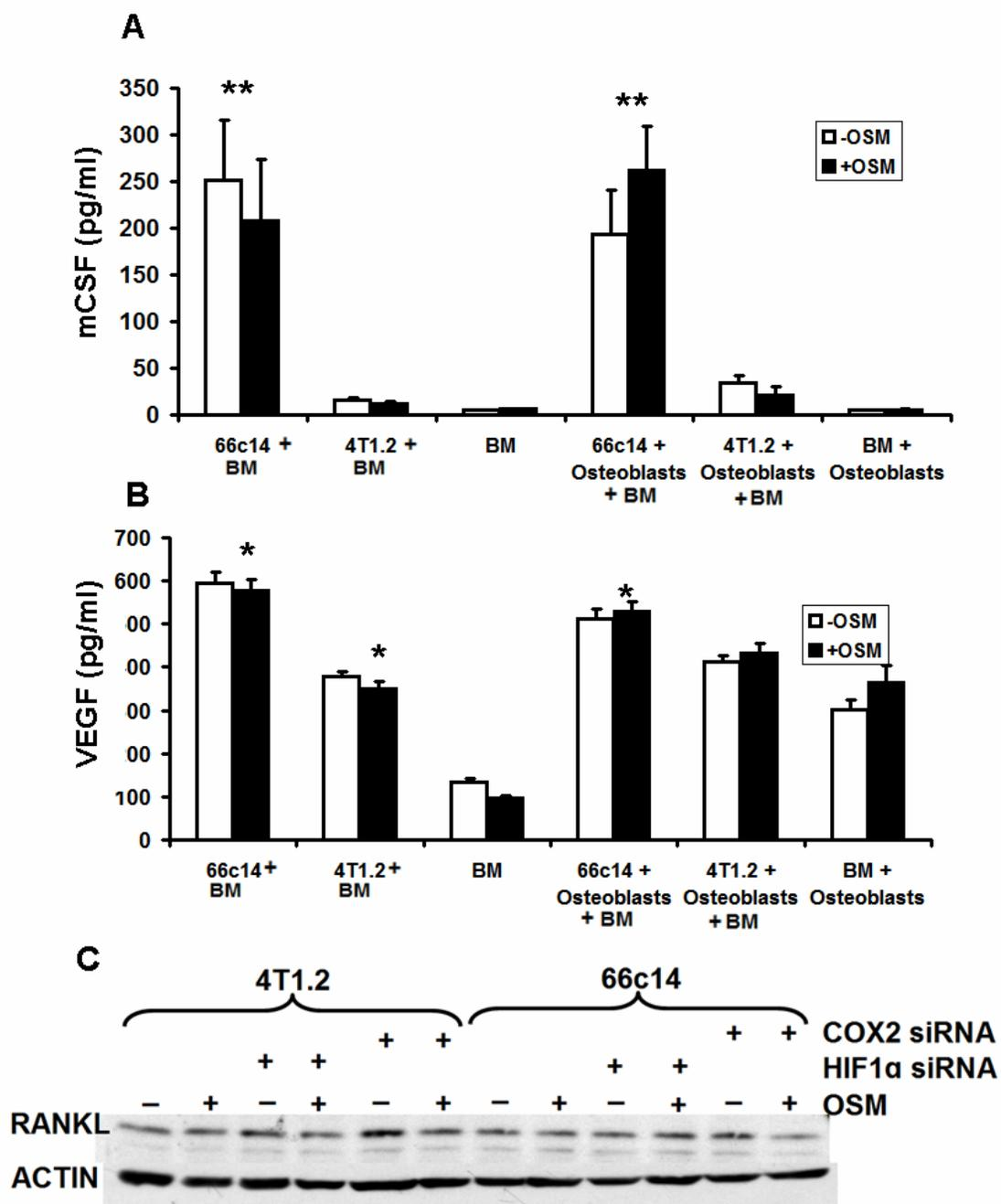


Figure A.23 66c14 Cells Express Pro-Osteoclastic Markers Analyzed via ELISA on Osteoclastogenesis Culture Supernatants, While Expression of RANKL is Unchanged as Analyzed by Western Blot

Figure A.23: *66c14 Cells Express Pro-Osteoclastic Markers Analyzed via ELISA on Osteoclastogenesis Culture Supernatants, While Expression of RANKL is Unchanged as Analyzed by Western Blot.* A, 66c14 express 9-fold higher levels of m-CSF compared to the other cells, while 4T1.2 cells or BM cells alone do not express a significant amount. The additions of OSM or osteoblasts in the culture have no effect of m-CSF expression levels. B, 66c14 cells have the highest expression of VEGF, having 2-fold more VEGF secretion compared to 4T1.2 cells and 4-fold more VEGF compared to BM cells alone. Again, OSM has minimal effect on these VEGF levels. Addition of osteoblasts in the co-culture system increased the VEGF level in 4T1.2 and BM alone cultures by about 20-50%. C. Both 4T1.2 cells and 66c14 cells produce RANKL however, RANKL expression is not significantly affected by OSM. Except for section C, data represents an average of six separate experiments and each data point performed in duplicate. Asterisks indicate significant differences (*P<0.05, **P<0.01) vs BM only cultures. Data for section C is a representative image of 2 separate experiments.

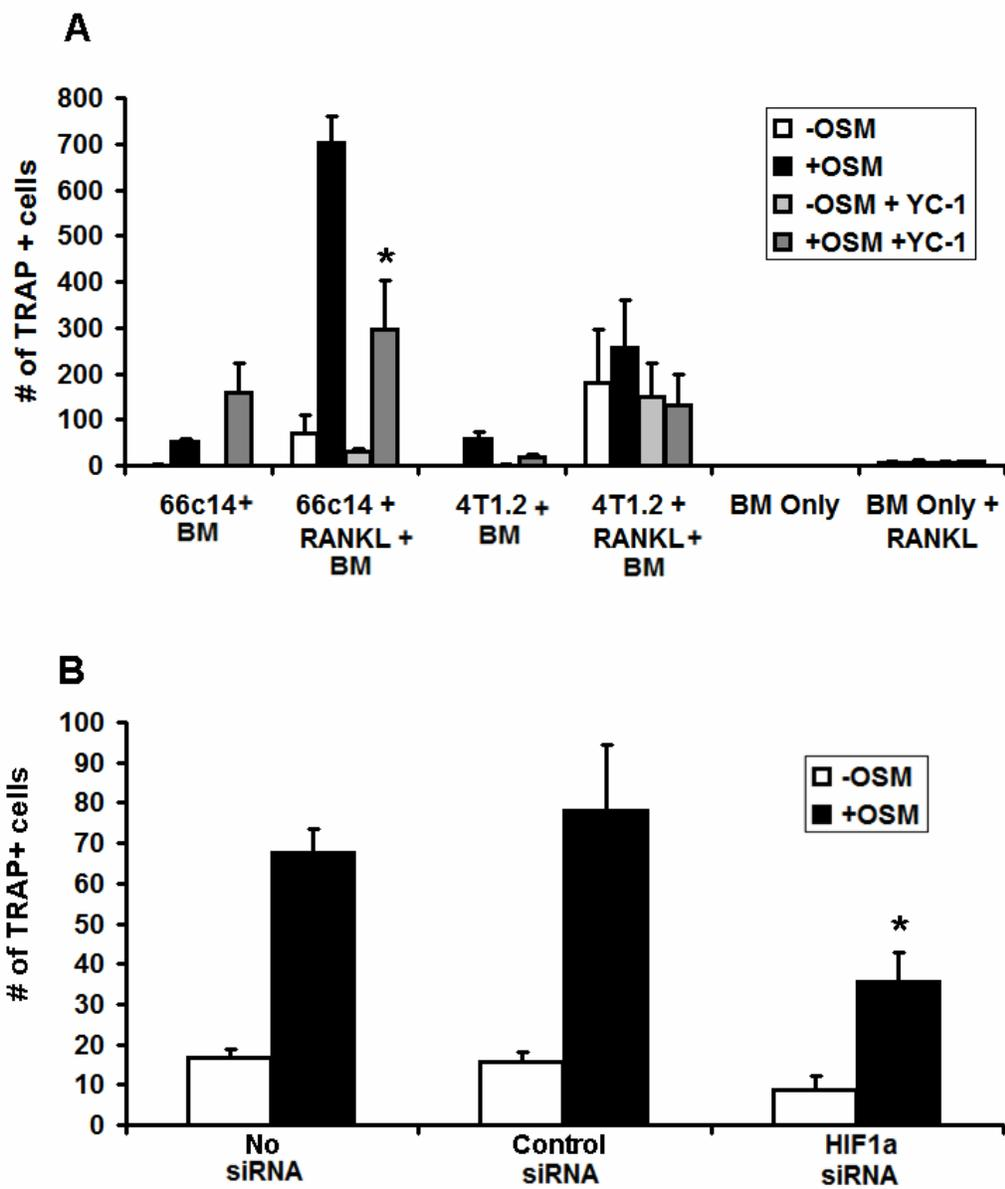
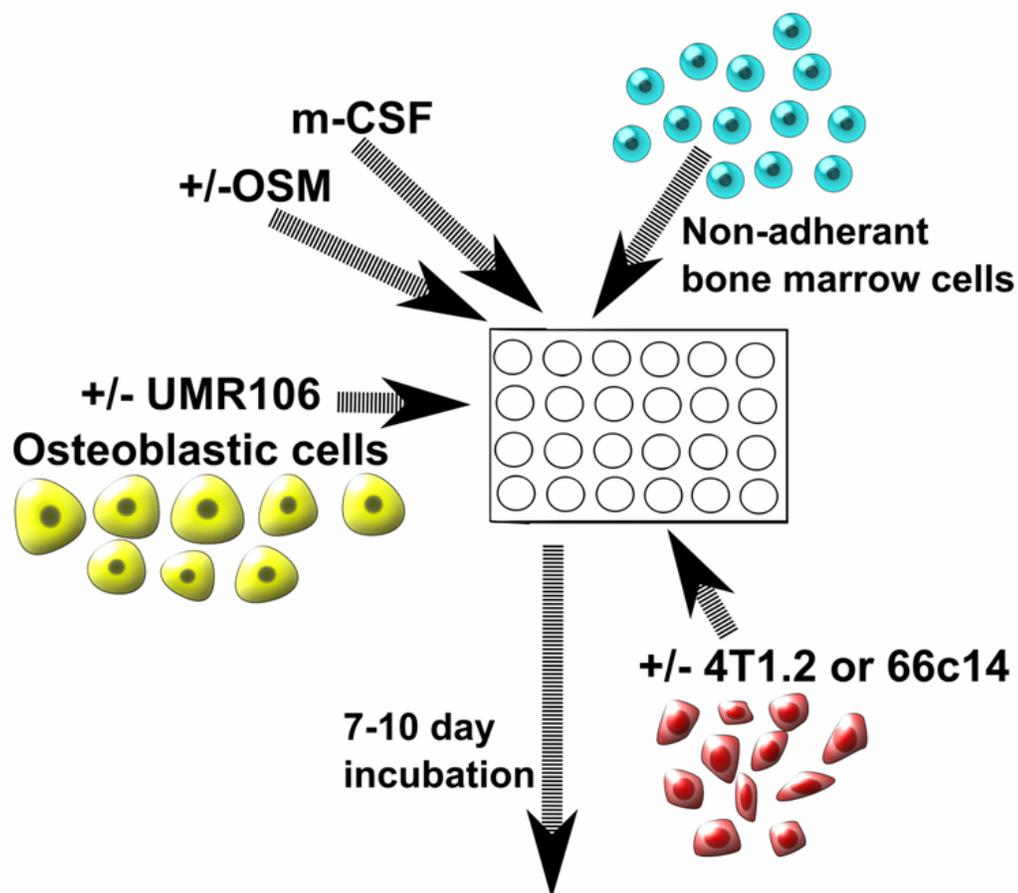


Figure A.24 Suppression of HIF1 α by the HIF1 α Inhibitor YC-1 Inhibits 66c14+OSM-Mediated Osteoclast Differentiation of BM Cells

Figure A.24: *Suppression of HIF1 α by the HIF1 α Inhibitor YC-1 Inhibits 66c14+OSM-Mediated Osteoclast Differentiation of BM Cells.* A, OSM increases osteoclastogenesis in RANKL-treated 66c14 cell co-cultures by 7-fold. YC-1 a chemical inhibitor to HIF1 α decreases osteoclast differentiation in co-cultures containing 66c14 and RANKL by about 60%. YC-1 has no effect on cultures containing 4T1.2 cells or BM cells alone. B, Conditioned media from 66c14 cells treated with +/- OSM and +/- HIF1 α siRNA was applied to bone marrow cell osteoclastogenesis experiments. OSM increases osteoclastogenesis by 3.5-fold while HIF1 α siRNA reduces osteoclast differentiation by 50%. Data represents an average of two separate experiments, and each data point performed in quadruplicate. Asterisks indicate significant differences (*P<0.05) vs 66c14 + OSM cultures without HIF1 α inhibition



**Figure A.25 Schematic Diagram of Osteoclastogenesis Co-Culture Experiments
with Osteoblasts**

Figure A.25: *Schematic Diagram of Osteoclastogenesis Co-Culture Experiments with Osteoblasts.* The non-adherent bone marrow cells were prepared as before, and co-cultured with 4T1.2 or 66c14 cells +/-OSM, and m-CSF for 7-10 days. UMR106 osteoblastic cells are added to the co-cultures as a source of RANKL.

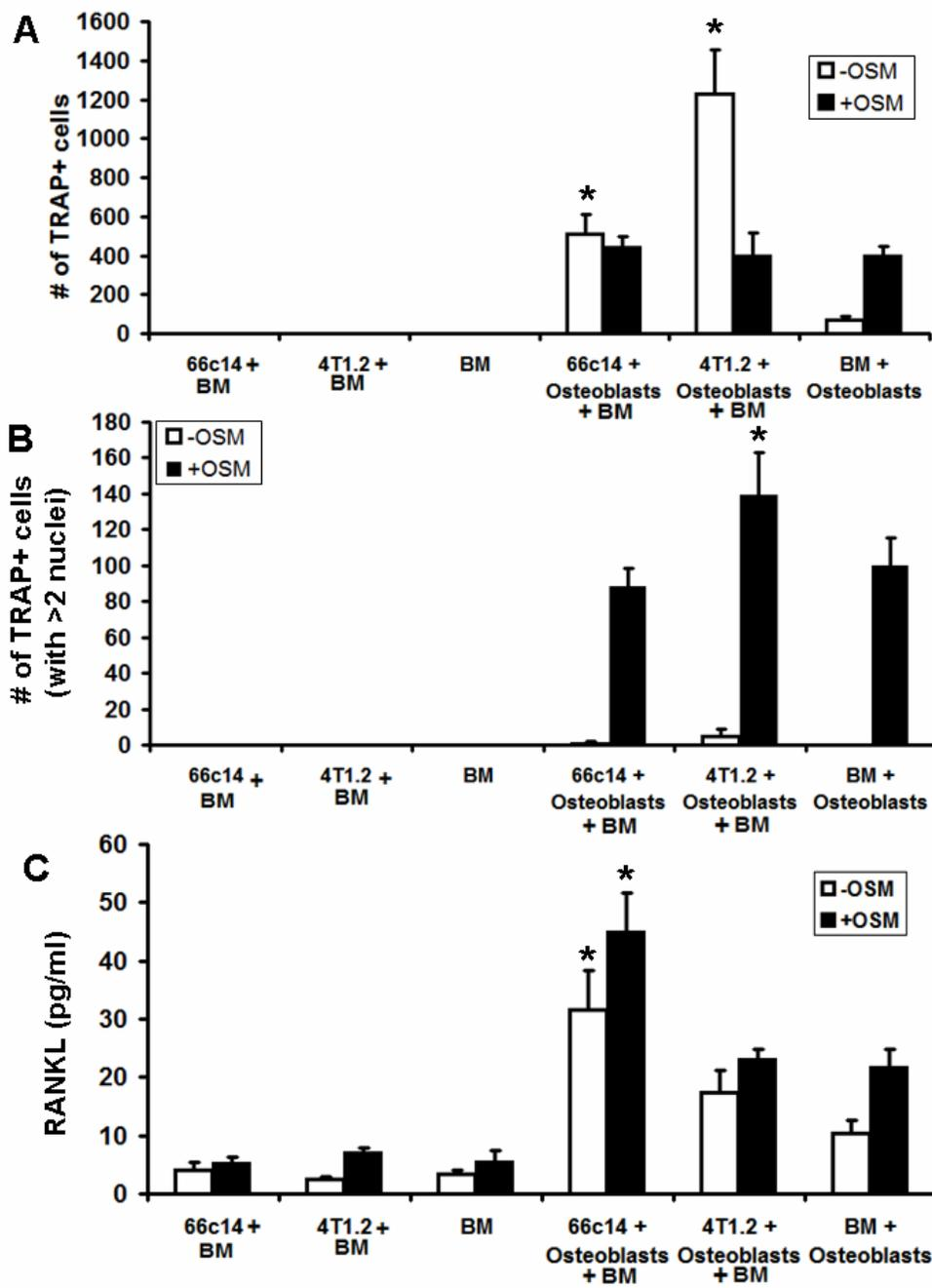


Figure A.26 Osteoblasts, in Conjunction with OSM, Increase the Number of Multi-Nucleated TRAP+ Cells in Osteoclastogenesis Experiments

Figure A.26: *Osteoblasts, in Conjunction with OSM, Increase the Number of Multi-Nucleated TRAP+ Cells in Osteoclastogenesis Experiments.* Co-cultures were grown for 7-10 days +m-CSF (5ng/ml) and +/-OSM (25 ng/ml) but no RANKL. A, Without the presence of osteoblasts, neither OSM nor cancer cells induces the differentiation of osteoclasts in bone marrow cells. The addition of osteoblasts causes an increase in osteoclastogenesis. 4T1.2-OSM+osteoblast cultures produces 2.5-fold higher number of TRAP+ cells compared to +OSM treated culture, while in cultures containing 66c14 cells there is no difference between +/- OSM treatments. The addition of OSM to cultures containing BM+osteoblast co-cultures increase TRAP+ cells by 3-fold. B, Multinucleated TRAP+ cells were seen only in osteoclastogenesis cultures with osteoblasts in the presence of OSM. Cultures containing 4T1.2 cells have about 20-30% higher number of multinucleated cells than BM+osteoblast co-cultures. C, RANKL ELISA performed on these osteoclastogenesis co-culture experiments reveal that the addition of osteoblasts to the cultures increases the level of secreted RANKL. The highest levels of RANKL is seen in co-cultures containing 66c14 cells and shows a 2-fold increase in RANKL levels compared to other cell co-cultures conditions. There is also a trend where OSM increases RANKL secretion levels but this trend is not statistically significant. Data represents an average of two separate experiments, and each data point performed in quadruplicate. Asterisks indicate significant differences (*P<0.05) vs BM + osteoblast cultures.

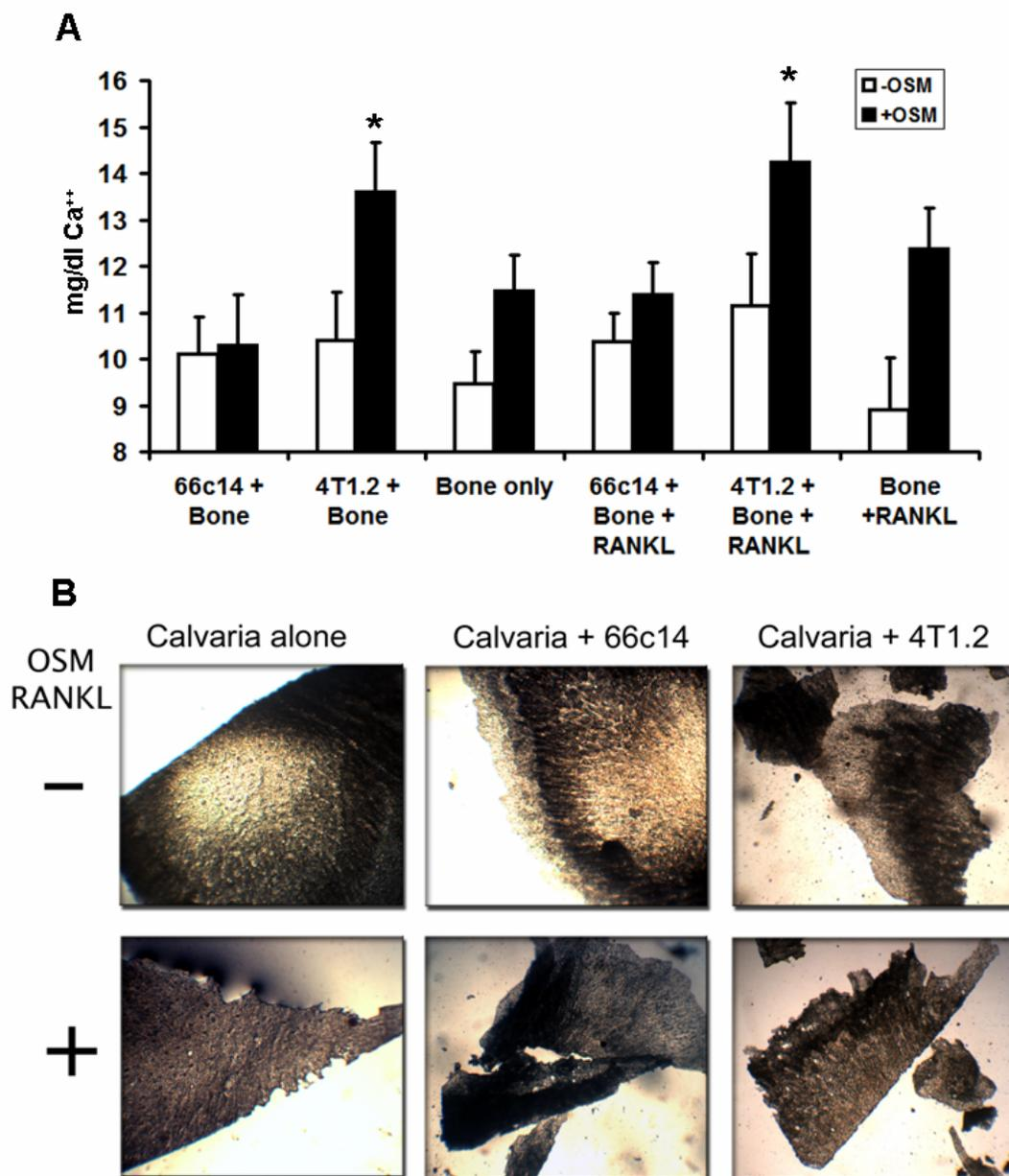


Figure A.27 Osteoclast Activity is Higher in Cultures Containing 4T1.2 Cells

Figure A.27: *Osteoclast Activity is Higher in Cultures Containing 4T1.2 Cells.*

Osteoclast activity is measured in a bone resorption assay of cancer cells, BM cells, and live mouse calvaria for 10 days for release of calcium from the bone to the medium. A, OSM has no effect on cultures containing 66c14 cells, while OSM causes an increase in free calcium in cultures containing only bone by about 10-20%. 4T1.2 cells + OSM has 30% higher amounts of free calcium compared to -OSM controls. The addition of RANKL increases free calcium levels in all conditions by about 10%. B, Representative images of calvaria seen in bone resorption cultures. Straight edges indicate little to no resorption, while jagged edges and fragmentation of bone indicate a higher level of bone resorption. Data represents an average of five separate experiments. Asterisks indicate significant differences (* $P < 0.05$) vs BM + osteoblast cultures.

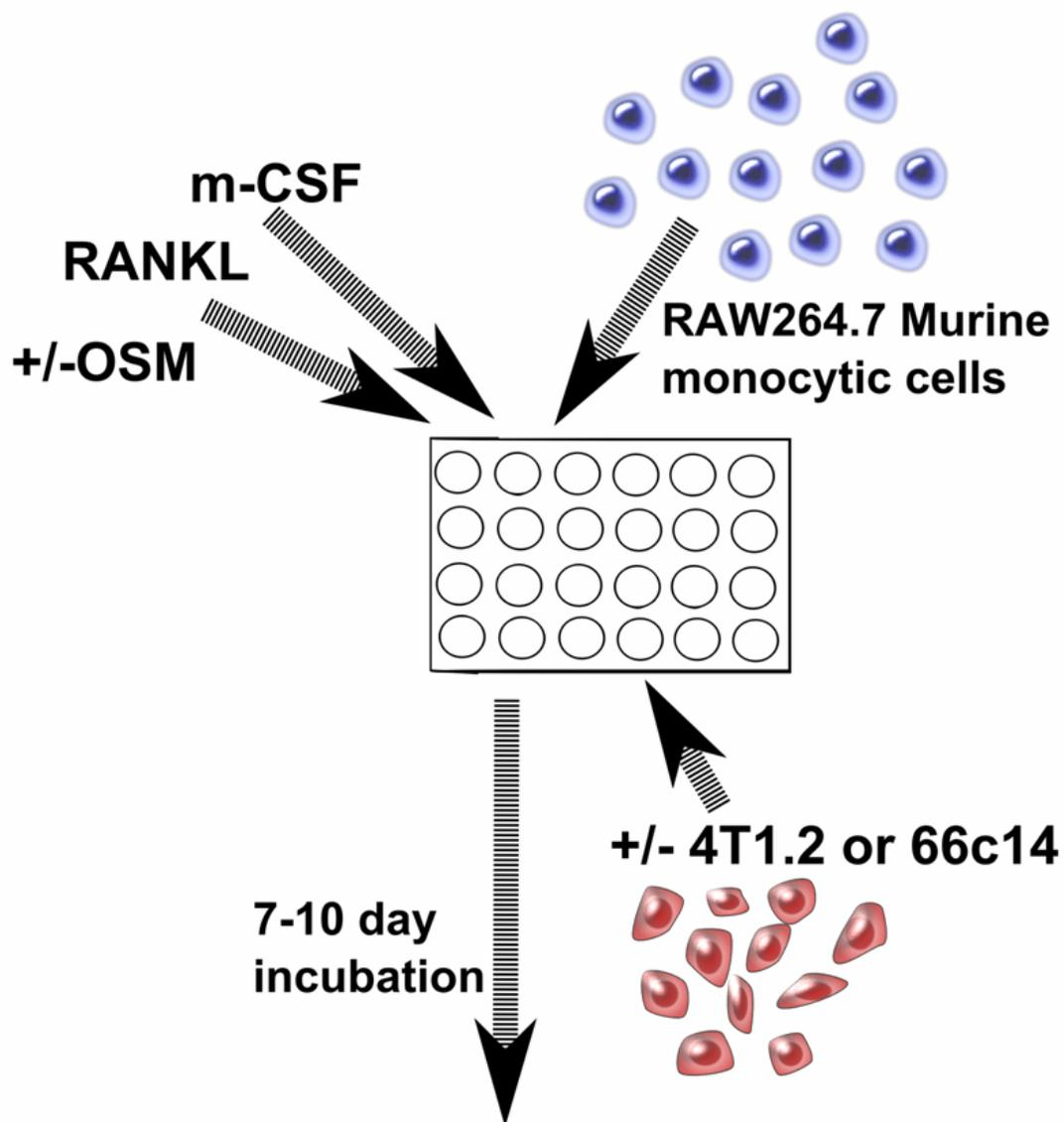


Figure A.28 Schematic of Osteoclastogenesis Co-Culture Experiments Including RAW264.7 Cells

Figure A.28: *Schematic of Osteoclastogenesis Co-Culture Experiments Including RAW264.7 Cells.* RAW264.7 monocytic cells have been shown to differentiate into osteoclasts and are used in the osteoclastogenesis co-cultures to replace bone marrow cells. As before, 4T1.2 or 66c14 cells are added to the co-culture along with 5ng/ml of m-CSF +/- 25 ng/ml OSM, 10 ng/ml, +/- RANKL. After 7-10 day incubation, osteoclasts are stained via a TRAP+ stain.

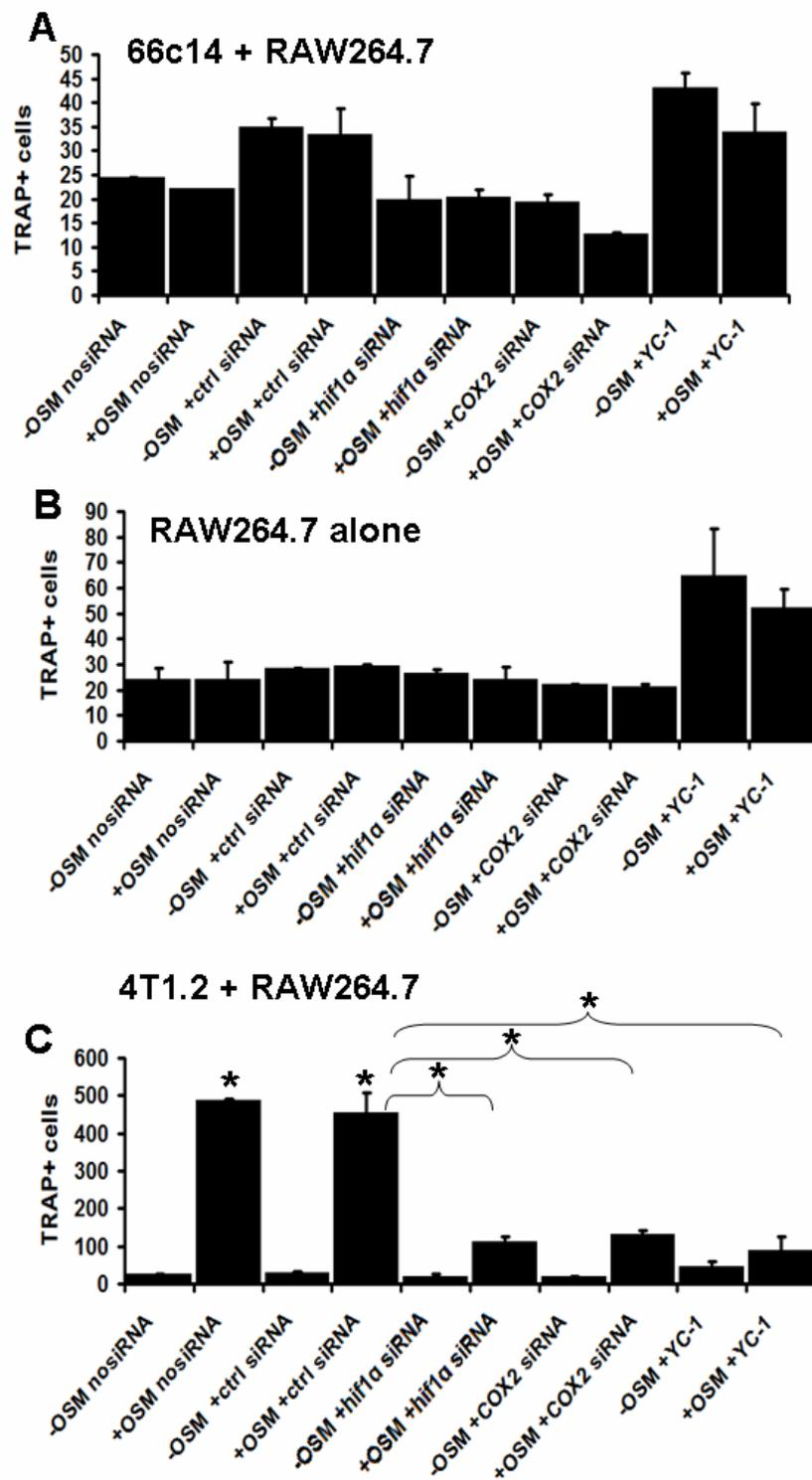


Figure A.29 RAW264.7 Monocytic Cell Lines Undergo Osteoclastogenesis in Response to OSM-Stimulated 4T1.2 Cells but Not 66c14 Cells

Figure A.29: *RAW264.7 Monocytic Cell Lines Undergo Osteoclastogenesis in Response to OSM-Stimulated 4T1.2 Cells but Not 66c14 Cells.* Unlike with BM cells, there is no significant difference of osteoclastogenesis with OSM treatments of co-cultures containing A) 66c14 cells or B) RAW264.7 cells alone. The total number of TRAP+ cells is around 20-35. The YC-1 HIF1 α chemical inhibitor increases osteoclast differentiation in these cultures by about 50%. C, OSM significantly increases RAW264.7 osteoclastogenesis in cultures containing 4T1.2 cells by approximately 10-fold compared to -OSM controls. HIF1 α siRNA, COX2 siRNA, and YC-1 decrease OSM-induced osteoclastogenesis by about 70%. Data represents an average of two separate experiments, and each data point performed in quadruplicate. Asterisks indicate significant differences (*P<0.01) vs – OSM controls unless otherwise depicted.

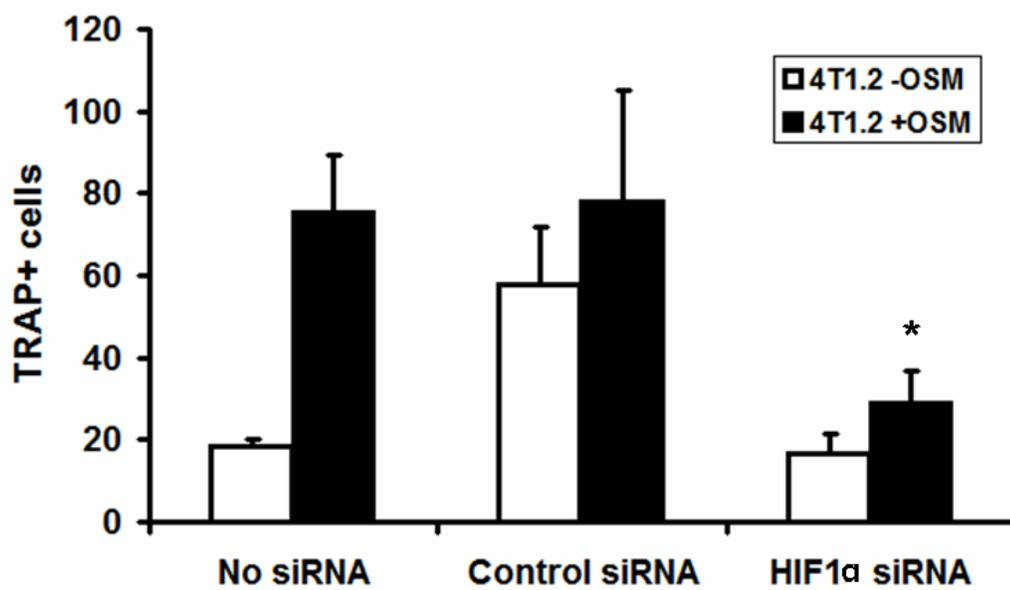


Figure A.30 Conditioned Media From OSM-Treated Cancer Cells Increases Osteoclastogenesis of RAW264.7 Cells and Is Mediated by HIF1 α

Figure A.30: *Conditioned Media From OSM-Treated Cancer Cells Increases Osteoclastogenesis of RAW264.7 Cells and Is Mediated by HIF1 α .* Conditioned media from 4T1.2 cells treated with +/- OSM and +/- HIF1 α siRNA is applied to RAW264.7 cell osteoclastogenesis co-culture experiments. OSM increases osteoclast differentiation by 4-fold while the HIF1 α siRNA attenuated OSM-mediated osteoclastogenesis by 60%. Data represents an average of two separate experiments, and each data point performed in quadruplicate. Asterisks indicate significant differences (*P<0.05) vs control siRNA treatments.

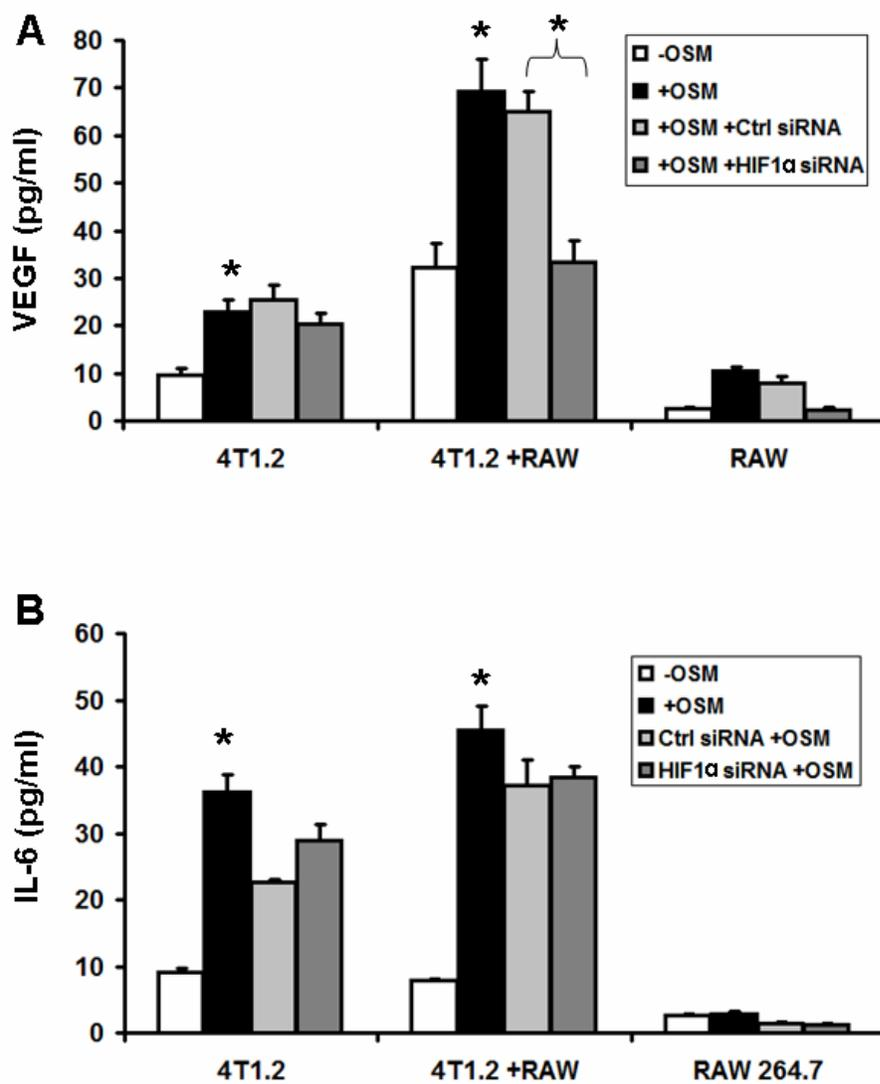


Figure A.31 4T1.2 Cells Produce VEGF and IL-6 in Response to OSM

Figure A.31: *4T1.2 Cells Produce VEGF and IL-6 in Response to OSM.* A, OSM-treated 4T1.2 cells produce a 2-fold increase in VEGF secretion by ELISA, but this production is not inhibited by HIF1 α siRNA. When 4T1.2 cells are co-cultured with RAW264.7 cells, the amount of secreted VEGF increases by 3-fold overall, while the addition of OSM increases the level of VEGF by another 2-fold in the co-culture. HIF1 α siRNA was able to reduce OSM-mediated VEGF induction in the co-cultures to the level of controls (-OSM treatment). B, Secreted IL-6 levels increases in response to OSM 4-fold in 4T1.2 cells. IL-6 levels are not affected by co-culturing with RAW264.7 cells or by HIF1 α siRNA. RAW264.7 cells by themselves produce little VEGF or IL-6 on their own. Data represents an average of two separate experiments, and each data point performed in quadruplicate. Asterisks indicate significant differences (*P<0.05) vs – OSM controls unless otherwise depicted.

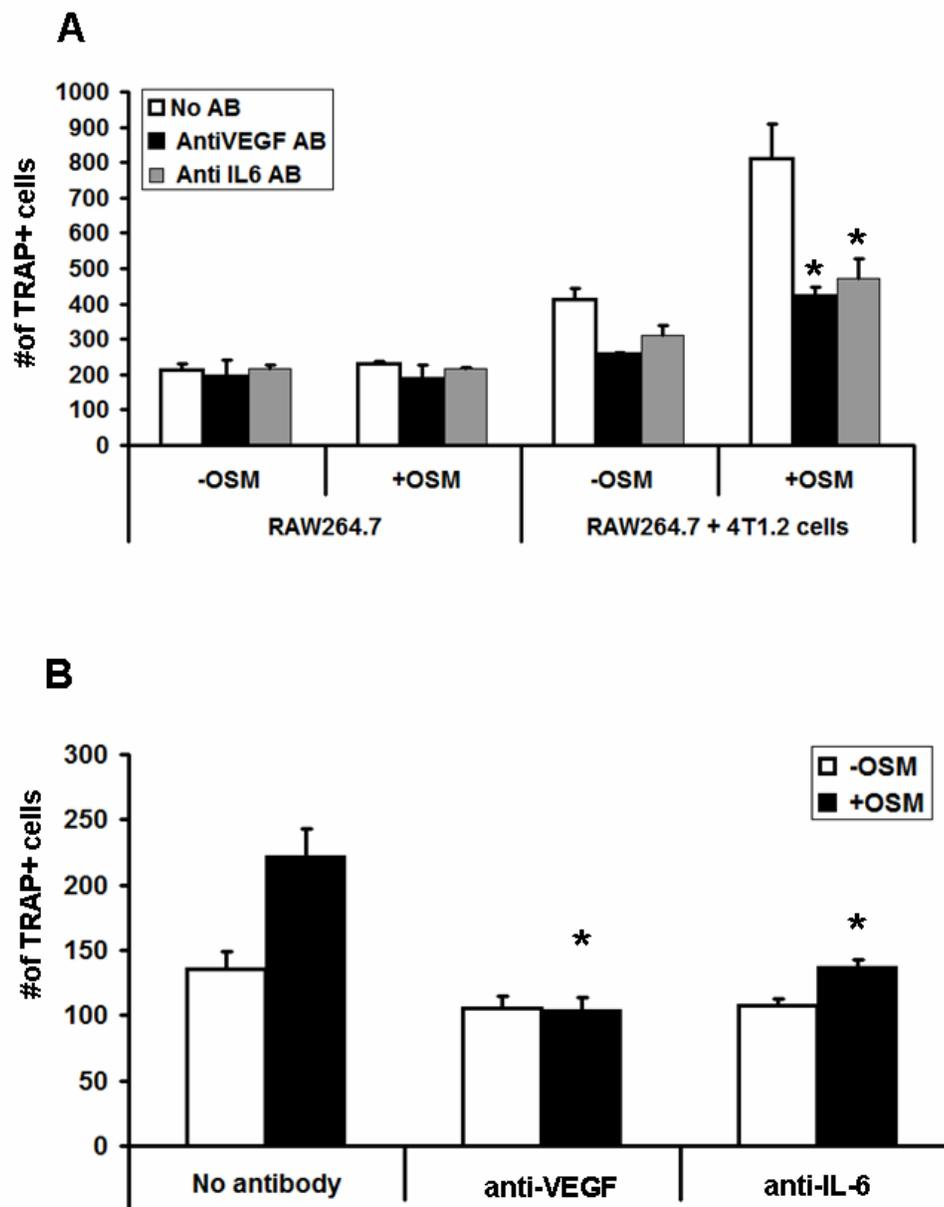


Figure A.32 Neutralizing Antibodies to VEGF and IL-6 Inhibit Osteoclastogenesis in RAW264.7 Cells

Figure A.32: *Neutralizing Antibodies to VEGF and IL-6 Inhibit Osteoclastogenesis in RAW264.7 Cells.* A, Treatment with OSM, increases osteoclast differentiation in the 4T1.2+RAW264.7 co-cultures by about 3-fold. Addition of VEGF or IL-6 neutralizing antibodies inhibits OSM-mediated stimulation of osteoclast differentiation in co-cultures containing 4T1.2 and RAW264.7 cells by about 50%. B, Conditioned media from 4T1.2 cells treated with +/- OSM, +/- anti VEGF neutralizing antibody, and +/- anti-IL-6 neutralizing antibody were added to RAW264.7 cultures. Conditioned media from 4T1.2 cells treated with anti-VEGF or anti-IL-6 neutralizing antibodies attenuated OSM-mediated increase in osteoclastogenesis to control levels (-OSM). Data represents an average of two separate experiments, and each data point performed in quadruplicate. Asterisks indicate significant differences (*P<0.05) vs cultures untreated with antibodies.

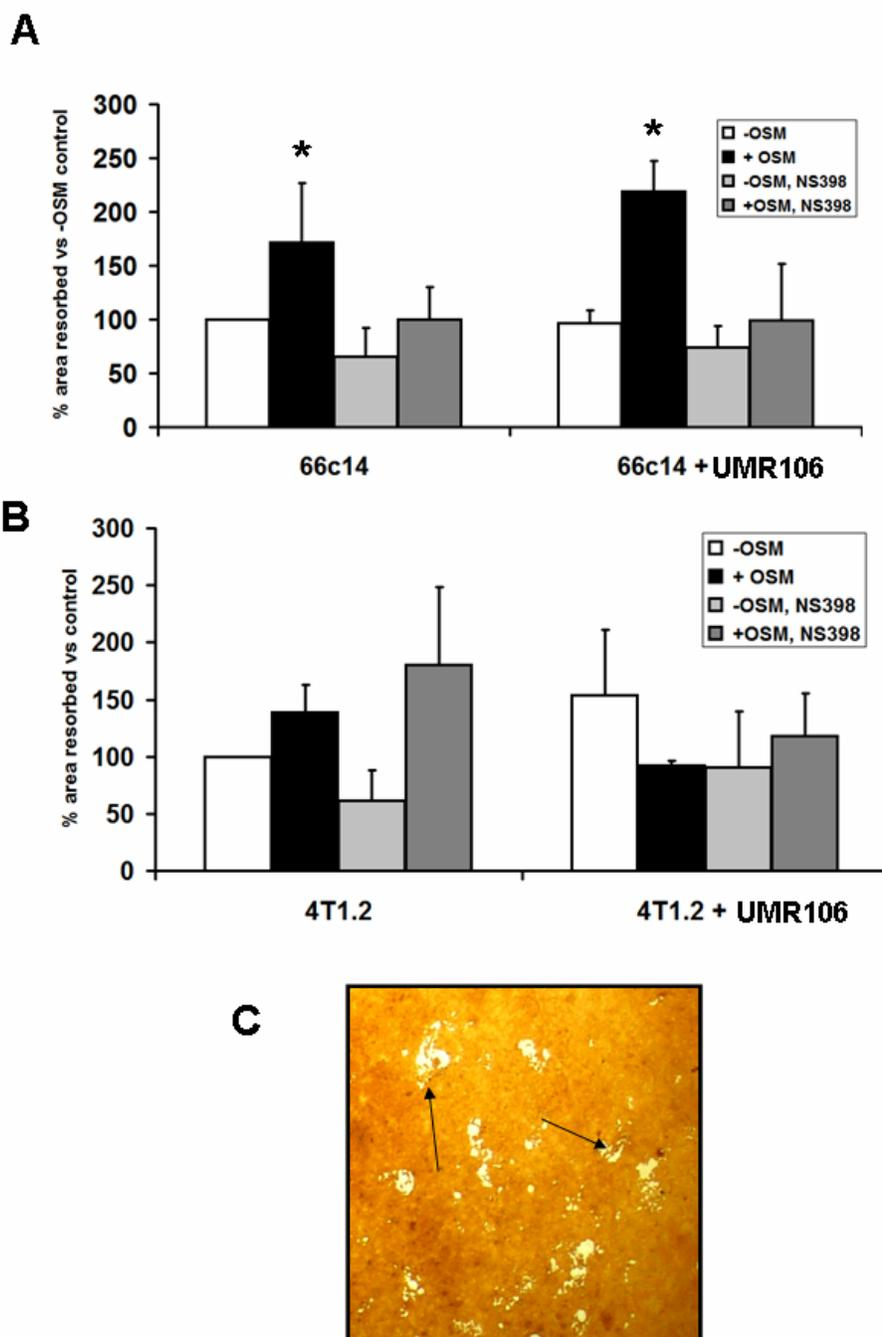


Figure A.33 Conditioned Media From 66c14 but Not 4T1.2 cells Treated with OSM Significantly Increases RAW264.7 Cell-Derived Osteoclast Activity

Figure 33: *Conditioned Media From 66c14 but Not 4T1.2 cells Treated with OSM Significantly Increases RAW264.7 Cell-Derived Osteoclast Activity.* Osteoclasts are derived from differentiating RAW264.7 cells in osteoclast differentiation media containing 100 ng/ml of RANKL and 25 ng/ml m-CSF in α -MEM. Differentiated osteoclasts are plated on osteologic multi-test plates. Conditioned media from 66c14 and 4T1.2 cells treated with +/- OSM and +/- UMR106 osteoblastic cells were added to the multi test plates. The cells were also treated with +/- NS398, a COX-2 inhibitor. A, Conditioned media from 66c14 cells treated with OSM increases osteoclast activity by 2-fold, while NS398 inhibits osteoclast activity down to control levels (-OSM). The conditioned media from 66c14 cultures containing UMR106 cells, slightly but not significantly, increases osteoclast activity. B, Conditioned media from 4T1.2 cells treated with OSM, slightly but not significantly, increases osteoclast activity and NS398 fails to inhibit osteoclast activity. The presence of UMR106 cells in 4T1.2 cell conditioned media attenuated any effect of OSM mediated increase of osteoclast activity. C, representative images of osteoclast activity in osteologic plates. White areas represent areas resorbed by osteoclasts. Data represents an average of three separate experiments. Asterisks indicate significant differences (*P<0.05) vs -OSM controls.

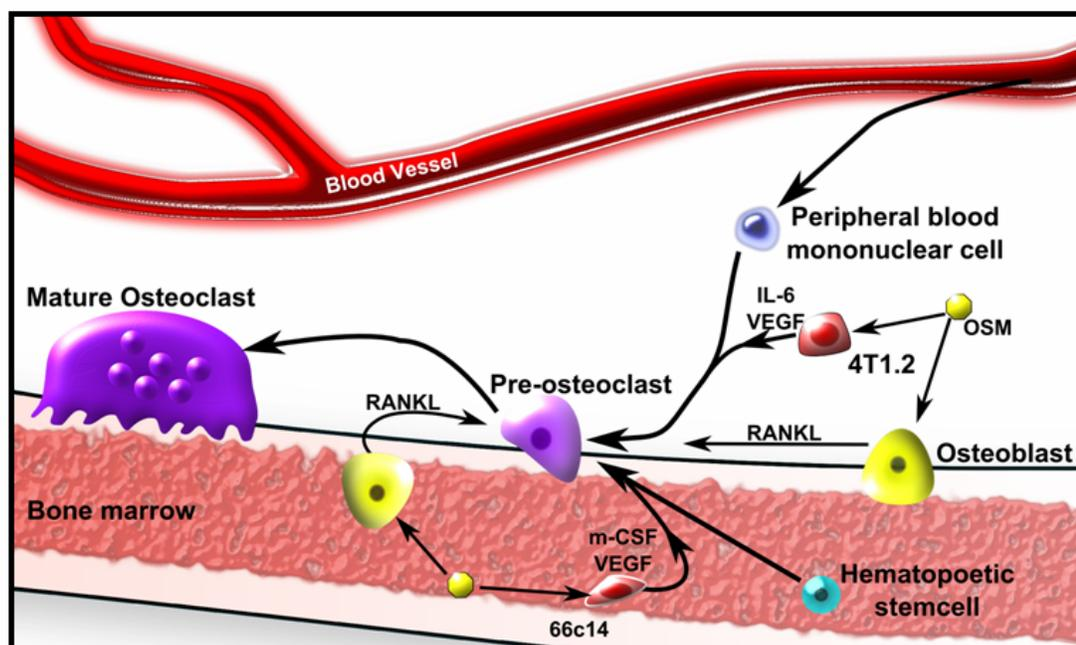


Figure A.34 Model of Osteoclastogenesis

Figure A.34: *Model of Osteoclastogenesis.* 4T1.2 cells and 66c14 cells stimulate different pro-osteoclastic lineages. While all osteoclasts are of haematopoietic lineage, osteoclasts that reside in the bone are derived from either the haematopoietic cells in the bone marrow or the peripheral blood mononuclear cells circulating in the blood. RANKL derived from osteoblasts or other cells in the bone stimulate osteoclast differentiation of both PBMCs and BM cells. 4T1.2 cells stimulate osteoclastogenesis in PBMC's while 66c14 cells stimulate osteoclastogenesis in bone marrow derived haematopoietic stem cells. 66c14 cells produce m-CSF, an early stimulator of osteoclastogenic pathway, while 4T1.2 cells do not. It is thought that PBMCs are more differentiated than bone marrow haematopoietic stem cells and do not need m-CSF. Additionally, IL-6 secreted by 4T1.2 cells treated with OSM may stimulate osteoclast differentiation with the PBMCs rather than the BM cells.

APPENDIX B

Interleukin-6 Review Manuscript

CLINICAL SIGNIFICANCE OF INTERLEUKIN-6 (IL-6) IN CANCER METASTASIS
TO BONE: POTENTIAL OF ANTI-IL-6 THERAPIES

By
Ken Tawara, Julia T. Oxford, and Cheryl L. Jorcyk

A manuscript accepted
for publication at the journal,
Cancer Management and Research

April 2011

TABLE OF CONTENTS

ABSTRACT	3
INTRODUCTION	4
Frequency, Consequences, and Mechanisms of Cancer Cell Metastases to Bone	6
Interleukin-6, Other Cytokines, and Growth Factors in the Bone Microenvironment	8
IL-6 Production by Cancer Cells and Stromal Cells in the Bone Microenvironment Facilitates Invasion and Metastasis	11
IL-6 and Its Soluble Receptor as a Prognostic Factor for Cancers that Metastasize to Bone	13
Serum IL-6 Levels May Predict Response to Cancer Therapy	16
IL-6 Promotes Chemotherapy Resistance	16
IL-6 as a Target for Therapy	17
Conclusion	21
Conflicts of Interest	22
REFERENCES	23
FIGURE LEGENDS	35
FIGURES	38
TABLES	42

ABSTRACT

Metastatic events to the bone occur frequently in numerous cancer types such as breast, prostate, lung and renal carcinomas, melanoma, neuroblastoma, and multiple myeloma. Accumulating evidence suggests that the inflammatory cytokine interleukin-6 (IL-6) is frequently upregulated and is implicated in the ability of cancer cells to metastasize to bone. IL-6 is able to activate various cell signaling cascades that include the signal transducers and activator of transcription (STAT) pathway, the phosphatidylinositol-3 kinase (PI3K) pathway, and the mitogen-activated protein kinase (MAPK) pathway. Activation of these pathways may explain the ability of IL-6 to mediate various aspects of normal and pathogenic bone remodeling, inflammation, cell survival, proliferation, and pro-tumorigenic effects. This review article will discuss the role of IL-6: i) in bone metabolism, ii) in cancer metastasis to bone, iii) in cancer prognosis, and iv) as potential therapies for metastatic bone cancer.

INTRODUCTION

Bone homeostasis is maintained by a variety of cell types that control remodeling of the bone matrix. Two important cell types that mediate bone homeostasis are osteoblasts and osteoclasts. Osteoblasts contribute to the bone matrix by production of type I collagen, deposition of hydroxyapatite crystals into the collagen matrix, and regulation of osteoclast activity (1, 2). Osteoblasts are of mesenchymal origin and differentiate from pre-osteoblasts. This process occurs via bone morphogenic proteins (BMPs) that induce runt-related transcription factor 2 (Runx2), leading to increased alkaline phosphatase activity (1). Conversely, osteoclasts resorb bone matrix (3) and differentiate from the hematopoietic cell lineage upon stimulation in a differentiation process called osteoclastogenesis. Osteoclastogenesis is mediated by cytokines such as receptor activator of NF- κ B ligand (RANKL) and macrophage-colony stimulating factor (m-CSF) (Fig. 1A) (3, 4). RANKL, a membrane-bound ligand, and m-CSF a secreted factor, are primarily produced by osteoblasts (5). Osteoclastogenesis is regulated primarily via RANKL and osteoblast-produced osteoprotegerin (OPG) expression, a decoy receptor to RANKL that suppresses RANKL activity (6). Osteoblasts that express RANKL have cell-to-cell contact with osteoclasts via ligand-receptor binding between RANKL and RANK (receptor activator of NF- κ B) expressed on osteoclasts (7). RANKL functions to promote osteoclast differentiation and activity through stimulation of various pathways including the phosphatidylinositol-

3 kinase (PI3K) pathway and the mitogen activated protein kinase (MAPK) pathway. The MAPK pathway leads to the activation of c-fos, nuclear factor of activated T-cells-2 (NFAT2), and other transcription factors.(8, 9) Cleavage of RANKL from the cell membrane by proteinases such as matrix metalloproteinase-7 (MMP7) yields the soluble form of RANKL (sRANKL), which has a physiological function that is still disputed, although both anti- and pro-osteoclastogenic effects have been reported (5, 10-12).

As osteoclasts differentiate in response to pro-osteoclastic factors, these cells create a segregated zone, a sealed area between the osteoclast and the bone matrix (9). Osteoclasts then release hydrogen ions into the segregated zone, solubilizing the hydroxyapatite crystals and promoting acid-activated proteinases such as cathepsin K to degrade the collagen matrix (9, 13). Osteoblasts generate new matrix to fill the vacant area. The rate at which osteoclasts differentiate and resorb bone is carefully regulated by osteoblast-produced RANKL and OPG. Other cells in the bone matrix such as osteocytes, terminally-differentiated osteoblasts, are able to regulate the generation and resorption of bone matrix by affecting osteoblast and osteoclast activity (14). When osteocytes are mechanically stimulated by shock to bone resulting in dynamic fluid movement, they promote alkaline phosphatase activity in osteoblasts by cell-to-cell contact through the RANK/RANKL complex, increasing bone mineralization and turnover (15-17). In this manner, damaged sections of the bone are removed and are replaced with new bone matrix by osteoblasts.

In normal bone, homeostasis is constantly maintained and bone integrity is preserved by a continuous cycle of bone renewal. However, when cancer cells

metastasize to the bone, the balanced and complex interplay of the cells is disrupted, leading to a pathologic condition that compromises bone integrity. One of the many characteristics that bone-homing cancer cells have in common is that most of them release copious levels of interleukin (IL-6), which helps in facilitating bone invasion and growth of metastatic lesions (18-20). In this mini-review article, the role of IL-6 in facilitating bone metastasis and approaches to measure serum IL-6 to predict progression of metastatic disease will be discussed. Additionally, new therapies targeting IL-6 and their potential efficacy in preventing bone metastasis will be reviewed.

Frequency, Consequences, and Mechanisms of Cancer Cell Metastases to Bone

Various types of cancers metastasize to the bone, including breast, prostate, lung, thyroid, kidney, multiple myeloma, melanoma, and neuroblastoma (21-25). Usually the bone is only compromised at the site of metastasis, and not all types of bone metastases affect the bone in the same way. For example, breast cancer predominantly causes osteolytic lesions, resulting in an upregulation of osteoclast activity and subsequent decreased bone density and integrity that may lead to fractures (22, 26). Conversely, prostate cancer results in primarily osteoblastic lesions that are caused by cytokine-induced upregulation of osteoblast activity and subsequent increased bone density (26). This type of bone metastases causes thickening of the bone, resulting in the possibility of nerve compression, vertebral fusion, and spinal cord compression depending on the location of the metastases. In contrast to what is found in normal bone where collagen fibers are highly organized and tightly packed, bone created by osteoblastic lesions

contains disorganized and fragile collagen fibrils (27). This leads to a high degree of bone brittleness, increase in potential fractures, and pain as the normal bone is replaced by abnormal bone created by the osteoblastic lesions. A subset of prostate cancers may also cause osteolytic lesions due to the expression of different cytokines that promote osteoclast activity rather than osteoblast activity (28). Multiple myeloma causes only osteolytic lesions. Other cancers, including lung, kidney and thyroid carcinomas, result in primarily osteolytic lesions, but osteoblastic lesions occur occasionally (26, 29).

Metastasis of the primary tumor to the bone occurs in about 60-75% of patients with breast cancer, prostate cancer, neuroblastoma, or multiple myeloma (21-23, 30).

Metastases to the bone from other cancers such as lung, kidney, and thyroid only occur in 30-50% of patients (24).

The molecular mechanisms that determine when a cancer cell will metastasize to bone are not completely understood. Recent evidence shows that the CXC chemokine receptor 4/chemokine (C-X-C motif) ligand 12 CXCR4/CXCL12 axis may play a role in this metastatic process. Studies have demonstrated that cancer cells are attracted to the bone marrow due to the relatively high levels of CXCL12 expressed by osteoblasts, which acts as an attractant for the CXCR4 ligand-positive cancer cells (31). Numerous studies have demonstrated that bone metastatic cancer cells from the breast, prostate, and myeloma overexpress the CXCR4 ligand, which promotes homing and metastasis to the bone and other organs (32-35). Inflammatory cytokines, such as IL-6, increase CXCR4 expression in breast cancer cells, specifically in a STAT3, and c-Jun dependent manner (36). Given these findings, therapeutics designed to block the CXCR4/CXCL12 axis are being evaluated in the prevention of bone metastases (37).

Once cancer cells colonize in the bone, they have to adapt to the challenges of cell survival and growth in a foreign tissue environment. The bone is a reservoir of a complex mixture of growth factors (38) that are released as the bone is degraded by metastatic lesions. The mixture of these growth factors include TGF-beta, insulin like growth factor 1 (IGF-1), insulin like growth factor 2 (IGF-2), platelet derived growth factor, bone morphogenic proteins, fibroblast growth factors, and other factors that significantly improve tumor cell survival and growth (39). These factors can promote the expression of pro-survival signals such as B-cell lymphoma 2 (Bcl-2), and AKT which inhibit apoptosis in the cancer cells. In addition, these factors can also support further osteoclast differentiation and activity, leading to a vicious positive feedback loop (the viscous tumor-bone cycle) where additional growth factors are released, stimulating increased cancer cell growth and accelerated bone destruction. This accelerated bone destruction can lead to rapid loss of bone integrity in cancer patients causing fractures, pain, and loss of mobility.

Interleukin-6, other Cytokines, and Growth Factors in the Bone

Microenvironment

IL-6 is a major pleiotropic, pro-inflammatory cytokine which plays a role in immune response, hematopoiesis, cell differentiation, wound repair, and bone remodeling (40, 41). Inflammation in the bone caused by injury or disease increases expression of IL-6 by reactive stromal cells of the bone and infiltrating monocytes and macrophages, promoting bone remodeling evidenced by higher osteoclast activity (42). The reactive stromal cells for bone metastases are generally the mesenchymal stem cells

in the bone marrow as well as the fibroblasts, osteoblasts, and osteocytes in the region. IL-6 production is directly stimulated by prostaglandin E2 (PGE2) and transforming growth factor-beta (TGF β), while interleukin-1 beta (IL-1 β), and lipopolysaccharides indirectly stimulate IL-6 production via NF- κ B activation (Fig. 2) (43-48). IL-6 binds to its heterotrimeric receptor, consisting of two gp130 subunits and an IL-6 receptor subunit, on target cells and activates the signal transducers and activators of transcription (STAT), mitogen-activated protein kinase (MAPK), and phosphatidylinositol-3 kinase (PI3K).(49-52) IL-6 signaling through the Jak/STAT3 pathways lead to expression of RANKL from osteoblast/stromal cells, causing direct stimulation of osteoclast differentiation and activity and resulting in bone destruction (Fig 3) (53, 54). Studies using IL-6 knockout mice have demonstrated that IL-6 is necessary for upregulating osteoclast activity and bone resorption *in vivo*. IL-6 knockout mice were shown to be protected from increased osteoclast activity and subsequent bone degradation when their bones were injected with the arthritis-inducing antigen heat-killed Mycobacterium tuberculosis (55). IL-6 knockout bones that received antigen injections had less RANKL and interleukin-17 (IL-17) expression as well as reduced osteolysis and cartilage destruction near the site of injection compared to wild-type mice. IL-17 is a pro-inflammatory and pro-osteoclastogenic cytokine implicated in arthritis and tumorigenesis that is produced in CD4⁺ helper and tumor infiltrating T-cells when activated by IL-6 (56, 57). Additional mouse studies have demonstrated that inhibition of IL-6 activity, with an IL-6 receptor (IL-6R) antagonist that inhibits downstream receptor signaling, reduces bone resorption (58). These

results suggest that IL-6 plays a major role in the upregulation of additional pro-osteoclastic factors essential for osteoclast activity.

Deregulation of IL-6 expression is implicated in disorders of bone homeostasis such as osteoporosis and osteopetrosis. Sex hormones such as 17- β -estradiol and testosterone have been implicated for regulating IL-6 levels in the bone microenvironment. 17- β -estradiol is known for its bone-preserving effects, which is supported by the fact that post-menopausal women experience a decrease in bone mineralization and density that may lead to osteoporosis (59). A recent study shows that 17- β -estradiol reduces both IL-6 and IL-8 production by monocytes and multiple myeloma cells through a mechanism that is not yet fully understood (60, 61). The chemokine interleukin-8 (IL-8) is also a pro-inflammatory molecule, which like IL-6, can increase inflammation in the bone and cause excessive bone resorption by upregulating the transcription factor NF- κ B (62, 63). In turn, increased NF- κ B activity stimulates IL-6 expression and secretion into the extracellular matrix (64). Studies have shown that the binding of 17- β -estradiol to the estrogen receptor inhibits NF- κ B transcriptional activity by preventing inhibitor of nuclear factor κ B alpha (I κ B α) degradation, leading to decreased IL-6 expression (60, 65). I κ B α is normally constitutively expressed and bound to NF- κ B, thus preventing the translocation of the transcription factor into the nucleus and initiation of the transcription of NF- κ B-related genes (66). 17- β -estradiol has also been shown to suppress IL-6 activity by inhibiting STAT3 through upregulation of protein inhibitor of activated STAT3 (PIAS3) (67). In addition, testosterone decreases IL-6 expression by inhibiting NF- κ B activity in osteoblasts via the hypothalamic-pituitary-adrenal axis, normally a potent stimulator of

IL-6 production. Both of these result in testosterone-mediated bone-preserving effects (68-70). Therapies that involve suppression of testosterone and 17- β -estradiol are effective against androgen-dependent prostate and breast cancer respectively, however bone density decreases significantly with these therapies leading to an increased chance of developing osteoporosis (71).

IL-6 Production by Cancer Cells and Stromal Cells in the Bone Microenvironment Facilitates Invasion and Metastasis

IL-6 produced by cancer cells initiates a variety of downstream signaling cascades that can lead to bone destruction (Fig. 1B). Many cancer cell types that metastasize to the bone endogenously produce and secrete high levels of IL-6. On the other hand, other cancer cell types stimulate the surrounding stromal cells to release copious amounts of this cytokine. Some cancer cell types such as IL-6-dependent multiple myeloma cells do not express IL-6 and rely on the bone microenvironment's reactive stromal cells to produce IL-6 in response to the presence of the tumor cells (72). This stroma-dependent increase of IL-6 in the extracellular matrix may be specific to the microenvironment of the metastasis. For example, injection of Walker (W256) mouse mammary cancer cells and MatLyLu (MLL) mouse prostate cancer-like cells into mice has been shown to differentially express IL-6 depending on the location (73). Specifically, local injection of W256 and MLL cells into the bone caused upregulation of IL-6, macrophage colony stimulating factor (M-CSF), RANKL, and Dickkopf-related protein 1 (DKK1) in the bone stromal cells. DKK1 is a member of the dickkopf family of factors that has been shown to be elevated in the bone marrow of patients with

breast cancer bone metastases (74). However, when these cells metastasized to non-osseous organs, there was little to no expression of IL-6, M-CSF, RANKL or DKK1, indicating that some cancer cells stimulate surrounding cells to release pro-osteoclastic factors only in the bone microenvironment (73, 75).

It has been proposed that cancer cells induce an inflammatory response in osteoblasts which may lead to the stimulation of osteoclast differentiation and activity (76, 77). The inflammatory response of osteoblasts in response to cancer cell-conditioned medium *in vitro* has been shown to cause an upregulation of PGE2, which induces IL-6 and activates osteoclasts via RANKL and PTHrP production (18, 74, 75). This effect was seen in breast cancer cells, oral squamous carcinoma cell lines, and in neuroblastoma cells (18, 75, 76). The induction of the inflammatory response to the cancer cell-conditioned medium may be due to NF κ B activation via an IL-6-independent mechanism within the osteoblasts (77). Suppression of NF κ B activity with methylseleninic acid reduced cytokine production by osteoblasts in response to cancer cell-conditioned medium, which may translate to reduced bone destruction *in vivo*.

IL-6 has been demonstrated to increase RANKL expression from osteoblasts and thus stimulate osteoclastogenesis. However inhibitors of RANKL fail to suppress IL-6-mediated osteoclastogenesis and bone resorption (78, 79). This suggests that IL-6 has potential redundant pathways that upregulate bone destruction and could interfere with the efficacy of targeted therapies against RANKL such as denosumab, an monoclonal humanized antibody against RANKL (80). RANKL-independent pathways could mediate IL-6 induced osteoclastogenesis. For instance, cancer induced inflammation leads to the stimulation of NF- κ B activity, which initiates IL-6 production

(Fig 2). NF- κ B activity is also able to stimulate cyclooxygenase-2 (COX2) activity, which would result in the production of PGE2, stimulating more IL-6 release (81). High levels of PGE2 have been shown to promote potent, pro-osteoclastic factors (82). IL-6 may also be inducing other pro-osteoclastic factors that functions independently from RANKL such as IL-1 beta (83). IL-1 beta has also been shown to increase NF- κ B activity (84) that could result in a feedback loop that further increases IL-6.

IL-6 and Its Soluble Receptor as a Prognostic Factor for Cancers that Metastasize to Bone

Predicting disease outcomes in cancer patients with metastasis to bone is difficult due to the inherent high level of tumor cell heterogeneity within a specific type of cancer. Current attempts at general prognostics are based mostly on tumor grading, staging, and invasive characteristics derived from histological and other types of physical analysis of biopsies (85). Specific, factor-based categorization of cancer is limited to a handful of well-characterized receptor and antigenic tests. For example, prostate specific antigen (PSA) has long been used as a prognostic factor to estimate progression of prostate cancer (86). Immuno-assays are performed to detect receptors for estrogen (ER), progesterone (PR), and human epidermal growth factor receptor 2 (Her2/neu) to aid in directing treatment strategies for breast cancer (87). Improving prediction accuracy by using more prognostic factors can hasten the detection of any changes in the progression of the disease.

Recently, interest in using serum IL-6 as a specific prognostic factor for prostate cancer and breast cancer has risen (88-90). Current research demonstrates that serum

IL-6 levels are significantly increased in many cancer patients with invasive prostate cancer compared to benign prostatic hyperplasia (BPH) (91). It has been shown that higher levels of serum IL-6 in patients with castration-resistant prostate cancer correlates to shortened survival times (92). Serum IL-6 is also elevated in prostate and breast cancer patients with distal metastases compared to patients without metastases,(92, 93) and higher serum IL-6 levels have been associated with lower patient survival rates in metastatic breast and prostate cancer (94). The spread of breast cancer cells into the local lymphatic system is also significantly correlated with increased IL-6 levels (93). Other studies have supported these findings and have shown that IL-6 correlates with the extent and size of prostate cancer bone metastases; specifically, the larger and more compromised the bone was, the higher the level of serum IL-6 (95, 96). Furthermore, significant elevation of IL-6 levels in the serum have been seen in prostate cancer patients who have experienced a relapse, where IL-6 levels positively correlate with cachexia (90, 97). Additionally, IL-6 levels have been shown to correlate with measures of morbidity and poor patient health (98). In one case study, a sharp increase in serum IL-6 was detected in terminally ill cancer patients who were experiencing extreme cachexia (99).

A comprehensive study involving patients with metastatic gastric cancer, which can also metastasize to the bone,(100, 101) demonstrated a significant correlation between serum IL-6 levels and the extent of gastric cancer progression (102). Specifically, IL-6 levels correlated with tumor grade and the extent of invasion into the gastric organ as well lymphatic and hepatic systems. Long-term survival rates were much higher with patients that had low levels of serum IL-6, and post-surgical

probability of metastasis was higher in patients with high serum IL-6 (102). The use of serum IL-6 levels for prognosis in a clinical setting is limited by gaps in the current understanding of mechanisms by which IL-6 specifically mediates the progression of metastatic disease as well as a lack of large clinical trials to assess baseline and range of fluctuation of serum IL-6 levels.

In addition to serum IL-6 levels, the concentration of soluble receptor to IL-6 (sIL-6R) in the serum may also help predict the aggressiveness of cancer metastasis and the level of bone destruction. Even in the absence of cancer, high levels of serum concentration of sIL-6R can predict the rate and level of osteolysis in patients with hyperparathyroidism (103). High levels of sIL-6R in the serum have also been associated with increased generalized inflammation, rheumatoid arthritis, inflammatory bowel disease, asthma, and inflammation associated colorectal cancer (104). sIL-6R enables a process called IL-6 trans-signaling, where cells that do not possess IL-6 receptor or have low levels of it can respond to IL-6 (Fig 3). This occurs through an unclear mechanism by incorporating the sIL-6 receptor into the gp130 receptor dimer on the cells, forming a IL-6 receptor heterotrimer and enabling the cells to respond to IL-6 (105). Interest in IL-6 trans-signaling has increased in the past several years as new research show that sIL-6R is produced by various cancer cells and the serum concentration is associated with decreased survival and increased aggressiveness of metastases in breast, prostate, and colorectal cancers (95, 106, 107). Some data suggest that IL-6 trans-signaling causes various effects that promote cancer metastases including, increased detachment, proliferation, and migration through a pathway that is independent of STAT1, STAT3, or MAPK (108). This suggests that IL-6 trans-

signaling is distinct from the canonical IL-6 signaling pathway and could be due to the lack of the membrane signaling domain on the sIL-6 receptor subunit (Fig 3). However, IL-6 trans-signaling does cause increased RANKL expression in synovial fibroblasts through a STAT3 dependant manner,(53) which suggest that trans-signaling may use some of the canonical IL-6 pathway to exert its effects. Although there is a convincing amount of evidence to suggest that higher serum sIL-6R levels may be associated with a worse cancer prognosis, little is known about the specifics of the IL-6 trans-signaling pathway, and more studies need to be done before assessing if sIL-6R is a therapeutic target.

Serum IL-6 Levels May Predict Response to Cancer Therapy

It is critical to determine throughout a patient's treatment whether the current therapy plan should be maintained or if new therapies needs to be initiated. Changes in serum IL-6 levels in patients undergoing chemotherapies or targeted therapeutics may act as a biomarker that can predict whether a patient is responding or not. In one clinical study, combination therapy using docetaxel and zoledronic acid, a bisphosphonate that inhibits osteoclastic activity, was administered to prostate cancer patients with bone metastases (109). Patients that responded to the therapy had a 35% decrease in overall serum IL-6 levels, while patients that did not respond had a 76% increase in serum IL-6 levels (109). A confounding variable in this finding is that some of the increase in serum IL-6 may be due to a stress response to the chemotherapeutic agents themselves, and the high levels of IL-6 may actually confer drug resistance (110). However, IL-6 has also been correlated to C-reactive protein (CRP) levels in the serum,

and reduction in CRP levels alone may indicate positive biologic effects of chemotherapeutics indicated by a reduction in serum IL-6 (111, 112). Although there is a dearth of clinical studies using IL-6 as a predictive biomarker of therapeutic response, initial studies support the concept that changes in serum cytokine levels such as IL-6 are worthy of more investigation.

IL-6 Promotes Chemotherapy Resistance

Chemotherapeutics traditionally have been and are currently, a mainstay in therapies against metastatic disease. However, resistance to chemotherapeutics is common and the mechanisms mediating resistance have been difficult to determine. Recent experimental results suggest that chemotherapy resistance is mediated through a relatively heterogeneous set of mechanisms, including down regulation of apoptotic signals, increased drug clearing and deactivation from cancer cells, multidrug resistance gene mutations, and stimulation of cell survival pathways via gene amplification (113-115).

A substantial amount of chemotherapy resistance research presently focuses on upstream mediators of cell survival. In the bone microenvironment, high concentrations of IL-6 have recently been shown to confer resistance to apoptosis in breast and prostate cancer cells as well as neuroblastoma cells (18, 116, 117). Specifically, prostate cancer cell activity of NF- κ B has been shown to cause high IL-6 production, which promotes docetaxel resistance in prostate tumors and associated bone metastases by upregulating the pro-survival AKT pathway in an IL-6 dependant manner (Fig 3) (49). Additionally, resistance to paclitaxel is observed in breast cancer patients whose metastatic lesions

show high levels of IL-6 (115). This high IL-6 production could itself be a function of the cancer cell's response to chemotherapeutics. One particular study presented evidence that paclitaxel induced expression of IL-6 in cervical cancer cells via the c-Jun N-terminal kinase (JNK) signaling pathway (110). More studies need to be conducted to assess the full role of IL-6 in conferring chemotherapeutic resistance, but these preliminary studies may support a rationale for using combination therapy of IL-6 inhibitors along with classical chemotherapeutic agents.

IL-6 as a Target for Therapy

Currently, the only kinds of therapies that can treat bone metastases are supportive therapies using i) bisphosphonates to reduce osteolytic burden, ii) radiotherapy and analgesics to alleviate pain, and iii) surgical intervention to reinforce weak bones (24, 118, 119). The humanized monoclonal antibody to the IL-6 receptor, tocilizumab (Actemra[®]) was approved by the FDA on January 11th, 2010 and was previously approved in Japan and the European Medicines Agency (EMA) in 2008 (Table 1) (120). Although tocilizumab is approved only for rheumatoid arthritis (RA) in the United States and Europe as well as Castleman's disease in Japan, recent studies have shown that tocilizumab is also effective as an antitumor agent against U87MG glioma cells. Tocilizumab exerts an inhibitory effect on the JAK/STAT3 pathway by preventing IL-6 from binding to its receptor, thereby inhibiting IL-6 signaling (121). Similar antitumor effects were seen with S6B45 multiple myeloma cells where a modified version of tocilizumab significantly inhibited the proliferation of these cells *in vitro* (122). Tocilizumab has also been effective in blocking cartilage and bone

destruction in IL-6-mediated autoimmune diseases such as synovitis and RA, where the mechanism of bone destruction is similar to that of bone metastases and high, local IL-6 levels were reported (123). Thus, tocilizumab may be effective as part of a combination therapy with bisphosphonates to control cancer cell-mediated destruction of the bone. However, there is no public data that exists for the efficacy of tocilizumab in inhibiting the progression of bone metastases. Other inhibitors to IL-6 activity for the treatment of various autoimmune diseases such as lupus, RA, Crohn's disease, and Castleman's disease are being developed or undergoing FDA approval.

Another anti-IL-6 drug that is being developed for bone metastatic prostate and renal carcinomas and multiple myeloma is (Centocor's) CNTO-328 (Siltuximab) (124). This chimeric, monoclonal antibody to IL-6 (120, 125) recently completed initial clinical trials for prostate cancer, kidney cancer, and renal cell carcinoma with mixed results. Some preliminary results from the completed trials indicate minimal side effects with the inhibitor however, there was a general lack of correlation with IL-6 inhibition and reduction in tumor growth (125, 126). The lack of tumor inhibition may be due to the nature of the trial that attempted to ascertain the safety profile of the drug, thereby leading to the use of a lower dose than may be effective. New clinical trials with dose escalation; however, are planned. On the other hand, clinical trials on relapsed and refractory multiple myeloma is still ongoing. Preliminary results from a Phase 2 trial on these patients demonstrate positive results with manageable side effects and good safety profile (127). This is supported by a study showing that siltuximab can inhibit prostate cancer cell growth *in vitro* and to improve survival by reducing the level of cachexia in an animal model of prostate cancer (128). In addition, siltuximab has

been shown in mice to inhibit the conversion of androgen-dependent prostate cancer into a more aggressive, bone metastatic, and difficult to treat androgen-independent prostate cancer (129). Treatment with siltuximab also decreased serum CRP levels, which correlated to improved outcome in treatment-resistant prostate cancer (112). Other recent data indicate that STAT3 and MAPK activity is suppressed in patients taking siltuximab, which may inhibit IL-6 mediated drug resistance (130). However, in a separate Phase 2 clinical trial involving castration-resistant prostate cancer where the disease had progressed beyond docetaxel therapy, siltuximab had a minimal clinical effect, despite positive biological IL-6 inhibition (131). New clinical trials using a combination of siltuximab and chemotherapeutics such as docetaxel are underway (131).

The use of antibodies for therapeutically inhibiting cytokines such as IL-6 may soon be replaced by utilizing small protein, non-antibody-based inhibitors called avimers. Avimers may surpass monoclonal antibodies in efficacy and potency, while reducing cost. Because these proteins lack immunoglobulin domains, they are much less immunoreactive, and their smaller size (~4 kDa) allows tighter interactions between the avimer and their target cytokine or receptor (132, 133). In addition, due to their reduced immunoreactive nature, they should theoretically reduce occurrences of serious side effects such as acute allergic reactions, which currently is a common problem with antibody therapeutics. Because of the promising features of this type of biological therapeutic, many pharmaceutical companies are pursuing the development of drugs based on non-antibody protein compounds, but the majority of these compounds are still in preclinical or Phase 1 trials.

Avida recently developed an avimer against IL-6 called C326 or AMG-220 (134). Their studies show that this avimer has superior stability and drug longevity compared to antibody-based inhibitors,(73) resulting in an increase in both the half-life and the shelf-life of the drug. Avida published results demonstrating that their avimer against IL-6 has an IC_{50} in the picomolar range leading to much smaller doses, and as it can be produced in *E. coli*, the cost is reduced (133). AMG-220 is also being developed for Castleman's disease, an autoimmune disorder that is characterized by high levels of serum IL-6 which is thought to cause the hyper-proliferation of B-cells, leading to high fevers, joint pain, weight loss and anemia (135). Currently, a Phase 1 trial for Crohn's disease is also in progress and is recruiting volunteers with stable disease and generally good health (133, 136, 137).

Although not all IL-6 inhibitors currently being developed or on the market are designed for cancer, IL-6 inhibitors, in principle, should work similarly for all diseases where IL-6 is deregulated. Therefore, IL-6 inhibitors should effectively inhibit IL-6-dependant cancers by reducing metastases to the bone and bone destruction. Availability of IL-6 inhibitors for the treatment of various cancers and bone metastases should improve as new uses of the inhibitors are approved by the FDA.

Conclusion

Recent research and publications have demonstrated that IL-6 is one of the many major factors upregulating and modulating cancer-mediated bone destruction. The information presented in this review illustrates the potential of IL-6 as a prognostic factor. In addition, fluctuations in serum IL-6 levels could help direct additional

treatment strategies in the future but clinical studies are needed to assess that potential. There is also evidence from *in vitro*, *in vivo*, and preliminary clinical trials to suggest that specific anti-IL-6 therapies may improve cancer survival rates and reduce metastatic burden in patients some types of cancers. However, additional studies and appropriate clinical trials need to be done to fully ascertain the effectiveness of anti-IL-6 therapies in cancer patients.

Conflicts of Interest

We declare that we have no conflict of interest.

REFERENCES

1. Jensen ED, Gopalakrishnan R, Westendorf JJ. Regulation of gene expression in osteoblasts. *Biofactors* 2010;36(1):25-32.
2. Orimo H. The mechanism of mineralization and the role of alkaline phosphatase in health and disease. *J Nippon Med Sch* 2010;77(1):4-12.
3. Teitelbaum SL. Bone resorption by osteoclasts. *Science* 2000;289(5484):1504-8.
4. Ducy P, Schinke T, Karsenty G. The osteoblast: a sophisticated fibroblast under central surveillance. *Science* 2000;289(5484):1501-4.
5. Nakashima T, Kobayashi Y, Yamasaki S, *et al.* Protein expression and functional difference of membrane-bound and soluble receptor activator of NF-kappaB ligand: modulation of the expression by osteotropic factors and cytokines. *Biochem Biophys Res Commun* 2000;275(3):768-75.
6. Kearns AE, Khosla S, Kostenuik PJ. Receptor activator of nuclear factor kappaB ligand and osteoprotegerin regulation of bone remodeling in health and disease. *Endocr Rev* 2008;29(2):155-92.
7. Martin TJ, Ng KW. Mechanisms by which cells of the osteoblast lineage control osteoclast formation and activity. *J Cell Biochem* 1994;56(3):357-66.
8. Takayanagi H, Kim S, Koga T, *et al.* Induction and Activation of the Transcription Factor NFATc1 (NFAT2) Integrate RANKL Signaling in Terminal Differentiation of Osteoclasts. *Developmental Cell* 2002;3(6):889-901.
9. Boyle WJ, Simonet WS, Lacey DL. Osteoclast differentiation and activation. *Nature* 2003;423(6937):337-42.
10. Hikita A, Yana I, Wakeyama H, *et al.* Negative Regulation of Osteoclastogenesis by Ectodomain Shedding of Receptor Activator of NF- κ B Ligand. *J Biol Chem* 2006;281(48):36846-55.
11. Lynch CC, Hikosaka A, Acuff HB, *et al.* MMP-7 promotes prostate cancer-induced osteolysis via the solubilization of RANKL. *Cancer Cell* 2005;7(5):485-96.

12. Sasano T, Suzuki O, Kanzaki H, *et al.* Is RANKL shedding involved in immune cell-mediated osteoclastogenesis? *Interface Oral Health Science 2009*: Springer Japan; 2009. p. 403-5.
13. Vaes G. Cellular biology and biochemical mechanism of bone resorption. A review of recent developments on the formation, activation, and mode of action of osteoclasts. *Clin Orthop Relat Res* 1988(231):239-71.
14. Teti A, Zallone A. Do osteocytes contribute to bone mineral homeostasis? Osteocytic osteolysis revisited. *Bone* 2009;44(1):11-6.
15. Heino TJ, Hentunen TA, Vaananen HK. Osteocytes inhibit osteoclastic bone resorption through transforming growth factor-beta: enhancement by estrogen. *J Cell Biochem* 2002;85(1):185-97.
16. Taylor AF, Saunders MM, Shingle DL, Cimbala JM, Zhou Z, Donahue HJ. Mechanically stimulated osteocytes regulate osteoblastic activity via gap junctions. *Am J Physiol Cell Physiol* 2007;292(1):C545-52.
17. Chan M, Lu X, Huo B, *et al.* A Trabecular Bone Explant Model of Osteocyte–Osteoblast Co-Culture for Bone Mechanobiology. *Cellular and Molecular Bioengineering* 2009;2(3):405-15.
18. Ara T, Song L, Shimada H, *et al.* Interleukin-6 in the bone marrow microenvironment promotes the growth and survival of neuroblastoma cells. *Cancer Res* 2009;69(1):329-37.
19. Paule B, Clerc D, Rudant C, *et al.* Enhanced expression of interleukin-6 in bone and serum of metastatic renal cell carcinoma. *Hum Pathol* 1998;29(4):421-4.
20. Thomas RJ, Guise TA, Yin JJ, *et al.* Breast cancer cells interact with osteoblasts to support osteoclast formation. *Endocrinology* 1999;140(10):4451-8.
21. Coleman RE. Clinical Features of Metastatic Bone Disease and Risk of Skeletal Morbidity. *Clin Cancer Res* 2006;12(20):6243s-9s.
22. Coleman RE, Rubens RD. The clinical course of bone metastases from breast cancer. *British journal of cancer* 1987;55(1):61-6.
23. DuBois SG, Kalika Y, Lukens JN, *et al.* Metastatic Sites in Stage IV and IVS Neuroblastoma Correlate With Age, Tumor Biology, and Survival. *Journal of Pediatric Hematology/Oncology* 1999;21(3):181-9.
24. Ricciardi S, de Marinis F. Treatment of bone metastases in lung cancer: the actual role of zoledronic acid. *Rev Recent Clin Trials* 2009;4(3):205-11.

25. Yang M, Jiang P, An Z, *et al.* Genetically Fluorescent Melanoma Bone and Organ Metastasis Models. *Clin Cancer Res* 1999;5(11):3549-59.
26. Guise TA, Mohammad KS, Clines G, *et al.* Basic mechanisms responsible for osteolytic and osteoblastic bone metastases. *Clin Cancer Res* 2006;12(20 Pt 2):6213s-6s.
27. Eric AGB, Kristiann MD, Kenneth JP, Charles CC, Thomas JR, Laurie KM. Skeletal metastasis of prostate adenocarcinoma in rats: Morphometric analysis and role of parathyroid hormone-related protein. *The Prostate* 1999;39(3):187-97.
28. Keller ET, Brown J. Prostate cancer bone metastases promote both osteolytic and osteoblastic activity. *J Cell Biochem* 2004;91(4):718-29.
29. Roodman GD. Mechanisms of bone metastasis. *N Engl J Med* 2004;350(16):1655-64.
30. Coleman RE. Metastatic bone disease: clinical features, pathophysiology and treatment strategies. *Cancer Treat Rev* 2001;27(3):165-76.
31. Taichman RS, Cooper C, Keller ET, Pienta KJ, Taichman NS, McCauley LK. Use of the Stromal Cell-derived Factor-1/CXCR4 Pathway in Prostate Cancer Metastasis to Bone. 2002. p. 1832-7.
32. Chinni SR, Yamamoto H, Dong Z, Sabbota A, Bonfil RD, Cher ML. CXCL12/CXCR4 transactivates HER2 in lipid rafts of prostate cancer cells and promotes growth of metastatic deposits in bone. *Mol Cancer Res* 2008;6(3):446-57.
33. Hinton CV, Avraham S, Avraham HK. Role of the CXCR4/CXCL12 signaling axis in breast cancer metastasis to the brain. *Clinical & experimental metastasis* 2010;27(2):97-105.
34. Luker KE, Luker GD. Functions of CXCL12 and CXCR4 in breast cancer. *Cancer letters* 2006;238(1):30-41.
35. Ooi LL, Dunstan CR. CXCL12/CXCR4 axis in tissue targeting and bone destruction in cancer and multiple myeloma. *J Bone Miner Res* 2009;24(7):1147-9.
36. Helbig G, Christopherson KW, 2nd, Bhat-Nakshatri P, *et al.* NF-kappaB promotes breast cancer cell migration and metastasis by inducing the expression of the chemokine receptor CXCR4. *J Biol Chem* 2003;278(24):21631-8.
37. Hirbe AC, Morgan EA, Weilbaecher KN. The CXCR4/SDF-1 chemokine axis: a potential therapeutic target for bone metastases? *Current pharmaceutical design* 2010;16(11):1284-90.

38. Hauschka PV, Mavrakos AE, Iafrati MD, Doleman SE, Klagsbrun M. Growth factors in bone matrix. Isolation of multiple types by affinity chromatography on heparin-Sepharose. *J Biol Chem* 1986;261(27):12665-74.
39. Khan SN, Bostrom MP, Lane JM. Bone growth factors. *The Orthopedic clinics of North America* 2000;31(3):375-88.
40. Naugler WE, Karin M. The wolf in sheep's clothing: the role of interleukin-6 in immunity, inflammation and cancer. *Trends in molecular medicine* 2008;14(3):109-19.
41. Naka T, Nishimoto N, Kishimoto T. The paradigm of IL-6: from basic science to medicine. *Arthritis Res* 2002;4 Suppl 3:S233-42.
42. Athanasou NA. Pathology of bone injury. *Diagnostic Histopathology* 2009;15(9):437-43.
43. Tosato G, Jones KD. Interleukin-1 induces interleukin-6 production in peripheral blood monocytes. *Blood* 1990;75(6):1305-10.
44. Holt I, Davie MW, Braidman IP, Marshall MJ. Prostaglandin E2 stimulates the production of interleukin-6 by neonatal mouse parietal bones. *Bone Miner* 1994;25(1):47-57.
45. Eickelberg O, Pansky A, Mussmann R, *et al.* Transforming Growth Factor- β 1 Induces Interleukin-6 Expression via Activating Protein-1 Consisting of JunD Homodimers in Primary Human Lung Fibroblasts. *J Biol Chem* 1999;274(18):12933-8.
46. Zhang Y, Broser M, Rom W. Activation of the interleukin 6 gene by Mycobacterium tuberculosis or lipopolysaccharide is mediated by nuclear factors NF IL 6 and NF-kappa B. *Proc Natl Acad Sci U S A* 1995;92(8):3632.
47. Libermann TA, Baltimore D. Activation of interleukin-6 gene expression through the NF-kappa B transcription factor. *Molecular and cellular biology* 1990;10(5):2327-34.
48. Fitzgerald DC, Meade KG, McEvoy AN, *et al.* Tumour necrosis factor-alpha (TNF-alpha) increases nuclear factor kappaB (NFkappaB) activity in and interleukin-8 (IL-8) release from bovine mammary epithelial cells. *Veterinary immunology and immunopathology* 2007;116(1-2):59-68.
49. Domingo-Domenech J, Oliva C, Rovira A, *et al.* Interleukin 6, a nuclear factor-kappaB target, predicts resistance to docetaxel in hormone-independent prostate cancer and nuclear factor-kappaB inhibition by PS-1145 enhances docetaxel antitumor activity. *Clin Cancer Res* 2006;12(18):5578-86.

50. Heinrich PC, Behrmann I, Muller-Newen G, Schaper F, Graeve L. Interleukin-6-type cytokine signalling through the gp130/Jak/STAT pathway. *Biochem J* 1998;334 (Pt 2):297-314.
51. Murakami M, Hibi M, Nakagawa N, *et al.* IL-6-induced homodimerization of gp130 and associated activation of a tyrosine kinase. *Science* 1993;260(5115):1808-10.
52. Wegiel B, Bjartell A, Culig Z, Persson JL. Interleukin-6 activates PI3K/Akt pathway and regulates cyclin A1 to promote prostate cancer cell survival. *Int J Cancer* 2008;122(7):1521-9.
53. Hashizume M, Hayakawa N, Mihara M. IL-6 trans-signalling directly induces RANKL on fibroblast-like synovial cells and is involved in RANKL induction by TNF-alpha and IL-17. *Rheumatology (Oxford)* 2008;47(11):1635-40.
54. O'Brien CA, Gubrij I, Lin SC, Saylor RL, Manolagas SC. STAT3 activation in stromal/osteoblastic cells is required for induction of the receptor activator of NF-kappaB ligand and stimulation of osteoclastogenesis by gp130-utilizing cytokines or interleukin-1 but not 1,25-dihydroxyvitamin D3 or parathyroid hormone. *J Biol Chem* 1999;274(27):19301-8.
55. Wong PK, Quinn JM, Sims NA, van Nieuwenhuijze A, Campbell IK, Wicks IP. Interleukin-6 modulates production of T lymphocyte-derived cytokines in antigen-induced arthritis and drives inflammation-induced osteoclastogenesis. *Arthritis Rheum* 2006;54(1):158-68.
56. McGeachy MJ, Bak-Jensen KS, Chen Y, *et al.* TGF-beta and IL-6 drive the production of IL-17 and IL-10 by T cells and restrain T(H)-17 cell-mediated pathology. *Nat Immunol* 2007;8(12):1390-7.
57. Wang L, Yi T, Kortylewski M, Pardoll DM, Zeng D, Yu H. IL-17 can promote tumor growth through an IL-6-Stat3 signaling pathway. *J Exp Med* 2009;206(7):1457-64.
58. Moonga BS, Adebajo OA, Wang HJ, *et al.* Differential effects of interleukin-6 receptor activation on intracellular signaling and bone resorption by isolated rat osteoclasts. *J Endocrinol* 2002;173(3):395-405.
59. Gambacciani M, Vacca F. Postmenopausal osteoporosis and hormone replacement therapy. *Minerva Med* 2004;95(6):507-20.
60. Kanda N, Watanabe S. 17beta-estradiol, progesterone, and dihydrotestosterone suppress the growth of human melanoma by inhibiting interleukin-8 production. *J Invest Dermatol* 2001;117(2):274-83.

61. Kramer PR, Kramer SF, Guan G. 17 beta-estradiol regulates cytokine release through modulation of CD16 expression in monocytes and monocyte-derived macrophages. *Arthritis Rheum* 2004;50(6):1967-75.
62. Bendre MS, Montague DC, Peery T, Akel NS, Gaddy D, Suva LJ. Interleukin-8 stimulation of osteoclastogenesis and bone resorption is a mechanism for the increased osteolysis of metastatic bone disease. *Bone* 2003;33(1):28-37.
63. Manna SK, Ramesh GT. Interleukin-8 induces nuclear transcription factor-kappaB through a TRAF6-dependent pathway. *J Biol Chem* 2005;280(8):7010-21.
64. Novotny NM, Markel TA, Crisostomo PR, Meldrum DR. Differential IL-6 and VEGF secretion in adult and neonatal mesenchymal stem cells: Role of NFkB. *Cytokine* 2008;43(2):215-9.
65. Lesmeister MJ, Jorgenson RL, Young SL, Misfeldt ML. 17Beta-estradiol suppresses TLR3-induced cytokine and chemokine production in endometrial epithelial cells. *Reprod Biol Endocrinol* 2005;3:74.
66. Bhat-Nakshatri P, Newton TR, Goulet R, Jr., Nakshatri H. NF-kappaB activation and interleukin 6 production in fibroblasts by estrogen receptor-negative breast cancer cell-derived interleukin 1alpha. *Proc Natl Acad Sci U S A* 1998;95(12):6971-6.
67. Wang LH, Yang XY, Mihalic K, Xiao W, Li D, Farrar WL. Activation of estrogen receptor blocks interleukin-6-inducible cell growth of human multiple myeloma involving molecular cross-talk between estrogen receptor and STAT3 mediated by co-regulator PIAS3. *J Biol Chem* 2001;276(34):31839-44.
68. Coletta RD, Reynolds MA, Martelli-Junior H, Graner E, Almeida OP, Sauk JJ. Testosterone stimulates proliferation and inhibits interleukin-6 production of normal and hereditary gingival fibromatosis fibroblasts. *Oral Microbiol Immunol* 2002;17(3):186-92.
69. Tuck SP, Francis RM. Testosterone, bone and osteoporosis. *Front Horm Res* 2009;37:123-32.
70. Papadopoulos AD, Wardlaw SL. Testosterone suppresses the response of the hypothalamic-pituitary-adrenal axis to interleukin-6. *Neuroimmunomodulation* 2000;8(1):39-44.
71. Hershman D, Narayanan R. Prevention and management of osteoporosis in women with breast cancer and men with prostate cancer. *Current Oncology Reports* 2004;6(4):277-84.

72. Barille S, Collette M, Bataille R, Amiot M. Myeloma cells upregulate interleukin-6 secretion in osteoblastic cells through cell-to-cell contact but downregulate osteocalcin. *Blood* 1995;86(8):3151-9.
73. Blouin S, Basle MF, Chappard D. Interactions between microenvironment and cancer cells in two animal models of bone metastasis. *British journal of cancer* 2008;98(4):809-15.
74. Voorzanger-Rousselot N, Goehrig D, Journe F, *et al.* Increased Dickkopf-1 expression in breast cancer bone metastases. *British journal of cancer* 2007;97(7):964-70.
75. Deyama Y, Tei K, Yoshimura Y, *et al.* Oral squamous cell carcinomas stimulate osteoclast differentiation. *Oncol Rep* 2008;20(3):663-8.
76. Kinder M, Chislock E, Bussard KM, Shuman L, Mastro AM. Metastatic breast cancer induces an osteoblast inflammatory response. *Exp Cell Res* 2008;314(1):173-83.
77. Chen YC, Sosnoski DM, Gandhi UH, Novinger LJ, Prabhu KS, Mastro AM. Selenium modifies the osteoblast inflammatory stress response to bone metastatic breast cancer. *Carcinogenesis* 2009;30(11):1941-8.
78. Mizutani K, Sud S, Pienta KJ. Prostate cancer promotes CD11b positive cells to differentiate into osteoclasts. *J Cell Biochem* 2009.
79. Kudo O, Sabokbar A, Pocock A, Itonaga I, Fujikawa Y, Athanasou NA. Interleukin-6 and interleukin-11 support human osteoclast formation by a RANKL-independent mechanism. *Bone* 2003;32(1):1-7.
80. Schwarz EM, Ritchlin CT. Clinical development of anti-RANKL therapy. *Arthritis Res Ther* 2007;9 Suppl 1:S7.
81. Lee KM, Kang BS, Lee HL, *et al.* Spinal NF-kB activation induces COX-2 upregulation and contributes to inflammatory pain hypersensitivity. *The European journal of neuroscience* 2004;19(12):3375-81.
82. Kaji H, Sugimoto T, Kanatani M, Fukase M, Kumegawa M, Chihara K. Prostaglandin E2 stimulates osteoclast-like cell formation and bone-resorbing activity via osteoblasts: role of cAMP-dependent protein kinase. *J Bone Miner Res* 1996;11(1):62-71.
83. Kurihara N, Bertolini D, Suda T, Akiyama Y, Roodman GD. IL-6 stimulates osteoclast-like multinucleated cell formation in long term human marrow cultures by inducing IL-1 release. *J Immunol* 1990;144(11):4226-30.

84. Renard P, Zachary MD, Bougelet C, *et al.* Effects of antioxidant enzyme modulations on interleukin-1-induced nuclear factor kappa B activation. *Biochemical pharmacology* 1997;53(2):149-60.
85. Soerjomataram I, Louwman MW, Ribot JG, Roukema JA, Coebergh JW. An overview of prognostic factors for long-term survivors of breast cancer. *Breast Cancer Res Treat* 2008;107(3):309-30.
86. Lilja H, Ulmert D, Vickers AJ. Prostate-specific antigen and prostate cancer: prediction, detection and monitoring. *Nat Rev Cancer* 2008;8(4):268-78.
87. Harris L, Fritsche H, Mennel R, *et al.* American Society of Clinical Oncology 2007 update of recommendations for the use of tumor markers in breast cancer. *J Clin Oncol* 2007;25(33):5287-312.
88. Culig Z, Hobisch A. Role of IL-6 in Regulating the Androgen Receptor. *Androgen Action in Prostate Cancer*; 2009. p. 451-63.
89. Knüpfer H, Preiß R. Significance of interleukin-6 (IL-6) in breast cancer (review). *Breast Cancer Res Treat* 2007;102(2):129-35.
90. Kuroda K, Nakashima J, Kanao K, *et al.* Interleukin 6 is associated with cachexia in patients with prostate cancer. *Urology* 2007;69(1):113-7.
91. Tumminello FM, Badalamenti G, Incorvaia L, Fulfarò F, D'Amico C, Leto G. Serum interleukin-6 in patients with metastatic bone disease: correlation with cystatin C. *Med Oncol* 2008;26(1):10-5.
92. George DJ, Halabi S, Shepard TF, *et al.* The prognostic significance of plasma interleukin-6 levels in patients with metastatic hormone-refractory prostate cancer: results from cancer and leukemia group B 9480. *Clin Cancer Res* 2005;11(5):1815-20.
93. Ahmed OI, Adel AM, Diab DR, Gobran NS. Prognostic value of serum level of interleukin-6 and interleukin-8 in metastatic breast cancer patients. *Egypt J Immunol* 2006;13(2):61-8.
94. Roberto S, Sara J, Ina B, *et al.* Circulating interleukin-6 predicts survival in patients with metastatic breast cancer. *Int J Cancer* 2003;103(5):642-6.
95. Shariat SF, Andrews B, Kattan MW, Kim J, Wheeler TM, Slawin KM. Plasma levels of interleukin-6 and its soluble receptor are associated with prostate cancer progression and metastasis. *Urology* 2001;58(6):1008-15.
96. Shariat SF, Kattan MW, Traxel E, *et al.* Association of pre- and postoperative plasma levels of transforming growth factor beta(1) and interleukin 6 and its soluble receptor with prostate cancer progression. *Clin Cancer Res* 2004;10(6):1992-9.

97. Strassmann G, Fong M, Kenney JS, Jacob CO. Evidence for the involvement of interleukin 6 in experimental cancer cachexia. *The Journal of clinical investigation* 1992;89(5):1681-4.
98. Twillie DA, Eisenberger MA, Carducci MA, Hseih WS, Kim WY, Simons JW. Interleukin-6: a candidate mediator of human prostate cancer morbidity. *Urology* 1995;45(3):542-9.
99. Iwase S, Murakami T, Saito Y, Nakagawa K. Steep elevation of blood interleukin-6 (IL-6) associated only with late stages of cachexia in cancer patients. *Eur Cytokine Netw* 2004;15(4):312-6.
100. Kang SH, Kim JI, Moon HS, *et al.* Overt bone marrow metastasis from early gastric cancer. *Endoscopy* 2008;40 Suppl 2:E34-5.
101. Sudo H, Takagi Y, Katayanagi S, *et al.* [Bone metastasis of gastric cancer]. *Gan to kagaku ryoho* 2006;33(8):1058-60.
102. Ashizawa T, Okada R, Suzuki Y, *et al.* Clinical significance of interleukin-6 (IL-6) in the spread of gastric cancer: role of IL-6 as a prognostic factor. *Gastric Cancer* 2005;8(2):124-31.
103. Nakchbandi IA, Mitnick MA, Lang R, Gundberg C, Kinder B, Insogna K. Circulating levels of interleukin-6 soluble receptor predict rates of bone loss in patients with primary hyperparathyroidism. *The Journal of clinical endocrinology and metabolism* 2002;87(11):4946-51.
104. Chalaris A, Garbers C, Rabe B, Rose-John S, Scheller J. The soluble Interleukin 6 receptor: Generation and role in inflammation and cancer. *European journal of cell biology* 2010.
105. Rose-John S, Neurath MF. IL-6 trans-signaling: the heat is on. *Immunity* 2004;20(1):2-4.
106. Atreya R, Neurath MF. Signaling molecules: the pathogenic role of the IL-6/STAT-3 trans signaling pathway in intestinal inflammation and in colonic cancer. *Current drug targets* 2008;9(5):369-74.
107. Knupfer H, Preiss R. Lack of Knowledge: Breast Cancer and the Soluble Interleukin-6 Receptor. *Breast care (Basel, Switzerland)* 2010;5(3):177-80.
108. Santer FR, Malinowska K, Culig Z, Cavarretta IT. Interleukin-6 trans-signalling differentially regulates proliferation, migration, adhesion and maspin expression in human prostate cancer cells. *Endocrine-related cancer* 2009;17(1):241-53.

109. Woods Ignatoski KM, Friedman J, Escara-Wilke J, *et al.* Change in Markers of Bone Metabolism with Chemotherapy for Advanced Prostate Cancer: Interleukin-6 Response Is a Potential Early Indicator of Response to Therapy. *J Interferon Cytokine Res* 2008;29(2):105-12.
110. Wang TH, Chan YH, Chen CW, *et al.* Paclitaxel (Taxol) upregulates expression of functional interleukin-6 in human ovarian cancer cells through multiple signaling pathways. *Oncogene* 2006;25(35):4857-66.
111. Stark JR, Li H, Kraft P, *et al.* Circulating prediagnostic interleukin-6 and C-reactive protein and prostate cancer incidence and mortality. *Int J Cancer* 2009;124(11):2683-9.
112. Pinski JK, Goldman B, Dorff T, *et al.* SWOG S0354: A phase II trial of CNTO328, a monoclonal antibody against interleukin-6 (IL-6), in chemotherapy pretreated patients (pts) with castration-resistant prostate cancer (CRPC). *J Clin Oncol* 2009;27(15S):5143.
113. Luqmani YA. Mechanisms of drug resistance in cancer chemotherapy. *Med Princ Pract* 2005;14 Suppl 1:35-48.
114. Wilson TR, Johnston PG, Longley DB. Anti-apoptotic mechanisms of drug resistance in cancer. *Curr Cancer Drug Targets* 2009;9(3):307-19.
115. Rincon M, Broadwater G, Harris L, *et al.* Interleukin-6, multidrug resistance protein-1 expression and response to paclitaxel in women with metastatic breast cancer: results of cancer and leukemia group B trial 159806. *Breast Cancer Res Treat* 2006;100(3):301-8.
116. Chung TD, Yu JJ, Kong TA, Spiotto MT, Lin JM. Interleukin-6 activates phosphatidylinositol-3 kinase, which inhibits apoptosis in human prostate cancer cell lines. *The Prostate* 2000;42(1):1-7.
117. Garcia-Tunon I, Ricote M, Ruiz A, Fraile B, Paniagua R, Royuela M. IL-6, its receptors and its relationship with bcl-2 and bax proteins in infiltrating and in situ human breast carcinoma. *Histopathology* 2005;47(1):82-9.
118. Petrut B, Trinkaus M, Simmons C, Clemons M. A primer of bone metastases management in breast cancer patients. *Curr Oncol* 2008;15(Supplement 1):S50-7.
119. Coleman RE. Management of Bone Metastases. *The Oncologist* 2000;5(6):463-70.
120. Melton L, Coombs A. Actemra poised to launch IL-6 inhibitors. *Nat Biotechnol* 2008;26(9):957-9.

121. Kudo M, Jono H, Shinriki S, *et al.* Antitumor effect of humanized anti-interleukin-6 receptor antibody (tocilizumab) on glioma cell proliferation. *J Neurosurg* 2009;111(2).
122. Yoshio-Hoshino N, Adachi Y, Aoki C, Pereboev A, Curiel DT, Nishimoto N. Establishment of a new interleukin-6 (IL-6) receptor inhibitor applicable to the gene therapy for IL-6-dependent tumor. *Cancer Res* 2007;67(3):871-5.
123. Fonseca JE SM, Canhão H, Choy E. Interleukin-6 as a key player in systemic inflammation and joint destruction. *Autoimmunity Reviews* 2009;8(7):538-42.
124. Li J, Hu XF, Xing PX. CNTO-328 (Centocor). *Curr Opin Investig Drugs* 2005;6(6):639-45.
125. Puchalski T, Prabhakar U, Jiao Q, Berns B, Davis HM. Pharmacokinetic and pharmacodynamic modeling of an anti-interleukin-6 chimeric monoclonal antibody (siltuximab) in patients with metastatic renal cell carcinoma. *Clin Cancer Res* 2010;16(5):1652-61.
126. Rossi JF, Negrier S, James ND, *et al.* A phase I/II study of siltuximab (CNTO 328), an anti-interleukin-6 monoclonal antibody, in metastatic renal cell cancer. *British journal of cancer* 2010;103(8):1154-62.
127. Voorhees PM, Manges RF, Somlo G, *et al.* A phase II multicenter study of CNTO 328, an anti-IL-6 monoclonal antibody, in patients (pts) with relapsed or refractory multiple myeloma (MM). *J Clin Oncol (Meeting Abstracts)* 2009;27(15S):8527.
128. Zaki MH, Nemeth JA, Trikha M. CNTO 328, a monoclonal antibody to IL-6, inhibits human tumor-induced cachexia in nude mice. *Int J Cancer* 2004;111(4):592-5.
129. Wallner L, Dai J, Escara-Wilke J, *et al.* Inhibition of interleukin-6 with CNTO328, an anti-interleukin-6 monoclonal antibody, inhibits conversion of androgen-dependent prostate cancer to an androgen-independent phenotype in orchiectomized mice. *Cancer Res* 2006;66(6):3087-95.
130. Karkera J, Steiner H, Li W, *et al.* The anti-interleukin-6 antibody siltuximab down-regulates genes implicated in tumorigenesis in prostate cancer patients from a phase I study. *The Prostate* 2011.
131. Dorff TB, Goldman B, Pinski JK, *et al.* Clinical and Correlative Results of SWOG S0354: A Phase II Trial of CNTO328 (Siltuximab), a Monoclonal Antibody against Interleukin-6, in Chemotherapy-Pretreated Patients with Castration-Resistant Prostate Cancer. *Clin Cancer Res* 2010;16(11):3028-34.

132. Sheridan C. Pharma consolidates its grip on post-antibody landscape. *Nat Biotechnol* 2007;25(4):365-6.
133. Silverman J, Liu Q, Bakker A, *et al.* Multivalent avimer proteins evolved by exon shuffling of a family of human receptor domains. *Nat Biotechnol* 2005;23(12):1556-61.
134. Braddock M. 11th Annual Inflammatory and Immune Diseases Drug Discovery and Development Summit. *Expert Opinion on Investigational Drugs*; 2007. p. 909-17.
135. Brandt SJ, Bodine DM, Dunbar CE, Nienhuis AW. Dysregulated interleukin 6 expression produces a syndrome resembling Castleman's disease in mice. *The Journal of clinical investigation* 1990;86(2):592-9.
136. Wurch T, Lowe P, Caussanel V, Bes C, Beck A, Corvaia N. Development of Novel Protein Scaffolds as Alternatives to Whole Antibodies for Imaging and Therapy: Status on Discovery Research and Clinical Validation. *Current Pharmaceutical Biotechnology* 2008;9:502-9.
137. Gebauer M, Skerra A. Engineered protein scaffolds as next-generation antibody therapeutics. *Current Opinion in Chemical Biology* 2009;13(3):245-55.

FIGURE LEGENDS

Figure 1: *Model of Osteoclastogenesis During Bone Homeostasis and Tumor Cell Metastasis to Bone.*

(A) In normal bone, RANKL and m-CSF are produced primarily by osteoblasts. m-CSF binds to its receptor c-FMS, expressed on osteoclast progenitors, and RANKL binds to its receptor on pre-osteoclasts to promote osteoclastogenesis. Osteoprotegerin, also produced by osteoblasts, acts as a decoy receptor for RANKL and negatively regulates osteoclast differentiation. In this model, osteoblast and osteoclast activity are in homeostasis through careful regulation of osteoclastogenesis. (B) When cancer cells metastasize to the bone, increased IL-6 may be produced by both the cancer cells and the osteoblasts, as an inflammatory response to the cancer cells. IL-6 then stimulates various types of stromal cells in the bone, which include bone marrow cells, osteoblasts, and fibroblasts in the area of the metastasis, to increase the expression of RANKL and m-CSF by osteoblasts. This IL-6-mediated increase in RANKL and m-CSF also occurs with injury and inflammation to the bone, but unlike in cancer metastasis, it is transient. RANKL and m-CSF then in turn activate the osteoclast differentiation cascade, where m-CSF strongly stimulates early stages of osteoclast differentiation and RANKL stimulates late stages of osteoclast differentiation, as well as osteoclast activity. Once this occurs, osteoclast activity becomes dysregulated and reduces bone integrity.

Figure 2: *Factors That Increase IL-6 Production in Response to Various Stimuli.*

Increased IL-6 production is associated with stimuli such as infection and inflammation. Infection, injury, and cancer can all stimulate inflammation that can lead to the increase of IL-6-modulating factors such as IL-1 β , COX-2, PGE2, and TGF β . Infection can also promote lipopolysaccharide (LPS) secretion from bacteria, which increases NF- κ B-dependent IL-6 levels. There are two main IL-6 production pathways: NF- κ B-dependent and NF- κ B-independent. NF- κ B-independent pathways upregulate IL-6 secretion via TGF β or PGE2, which is produced downstream of COX-2 activation. In the NF- κ B-dependent pathway, LPS or IL-1 β stimulate NF- κ B activity that causes an increase in IL-6 production.

Figure 3: *Model of Canonical IL-6 Signaling Versus IL-6 Trans-Signaling in Tumor Progression and Metastases.*

In the canonical IL-6 signaling pathway, the IL-6 receptor subunit is membrane bound and forms a heterotrimer with two gp130 subunits. When IL-6 binds to the receptor, STAT3 is activated in a JAK-dependant manner that leads to increased RANKL expression. IL-6 may also activate AKT via increased JAK-dependent PI3K activity and results in cell survival and anti-apoptosis signaling. Concomitantly, increased MAPK activity downstream of JAK activation can lead to upregulated cell growth, proliferation, and mitosis. In the IL-6 trans-signaling pathway, IL-6 first binds to the truncated soluble IL-6R (sIL6R). The IL-6/sIL6R complex then binds to the membrane-bound gp130 dimer to form an IL-6 trans-signaling complex. Due to the fact that the sIL-6 receptor lacks a membrane signaling domain, there appears to be significant differences in the intracellular signaling pathways. While IL-6

trans-signaling also leads to phosphorylation and activation of STAT3, increased cell survival, proliferation and mitosis occurs in an AKT-and MAPK-independent manner. The exact mechanisms for IL-6 trans-signaling leading to increased cell survival, proliferation, and mitosis are not yet known.

FIGURES

FIGURE 1

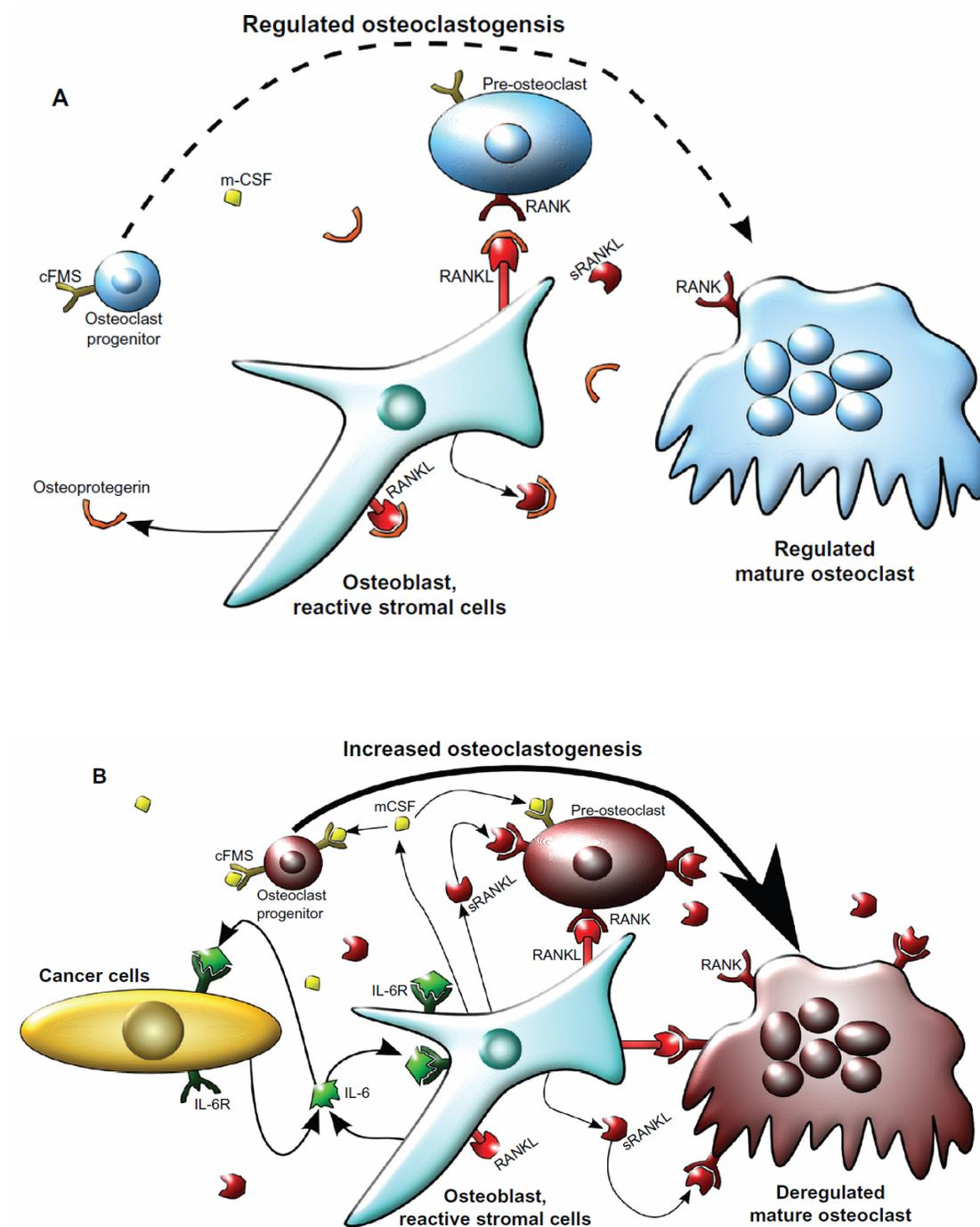


FIGURE 2

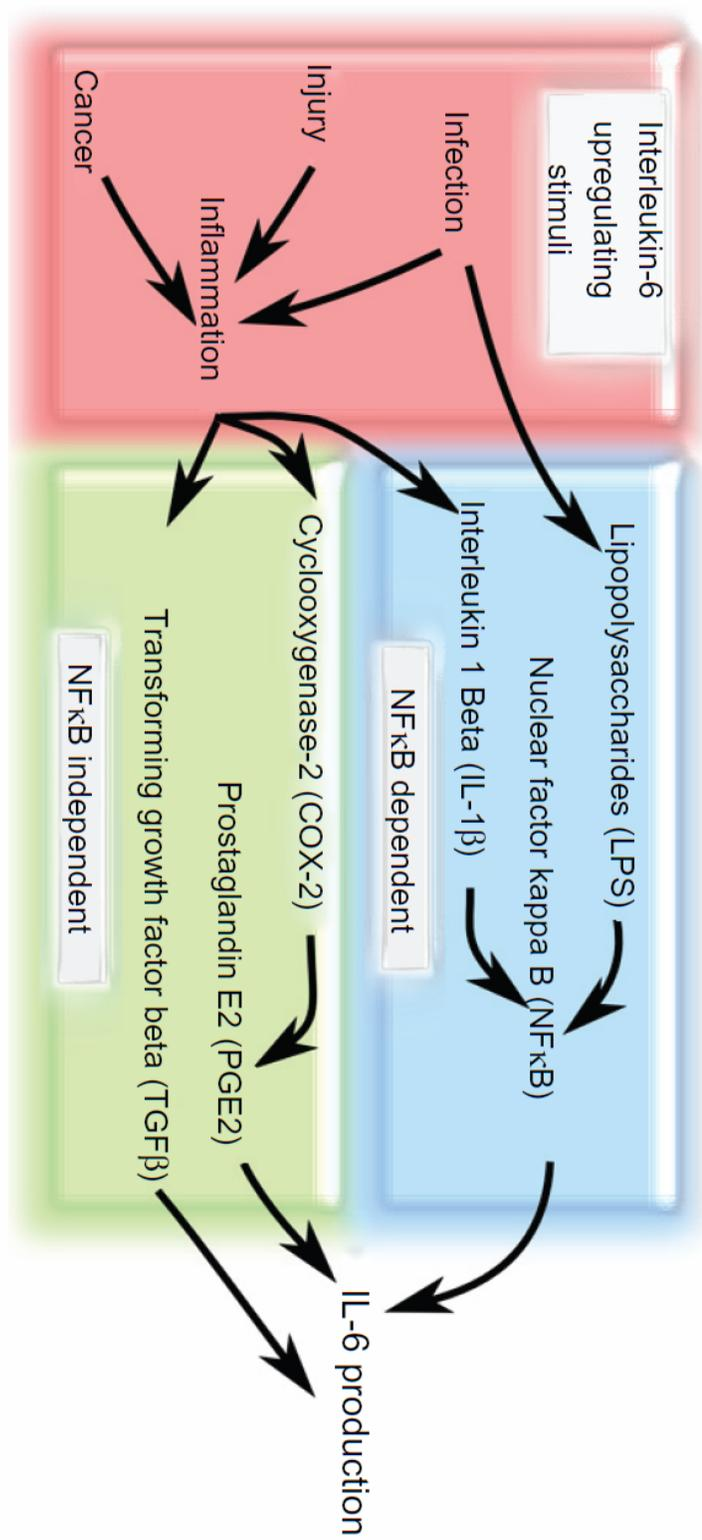
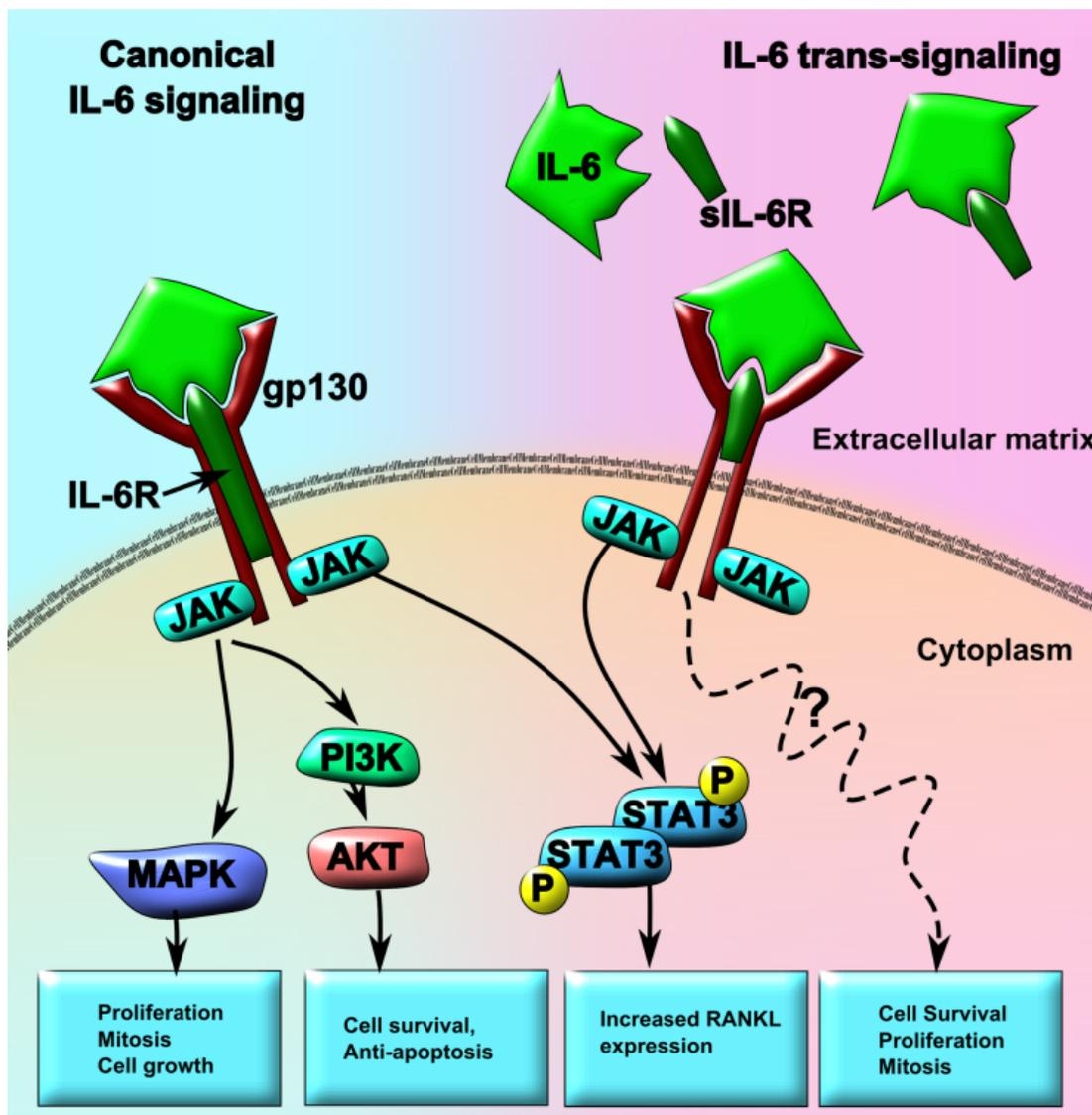


FIGURE 3



TABLES

Table 1 Targeted therapies for IL-6

FDA approval status	Drug manufacturer	Drug name	Drug type	Reference
Approved drugs				
Approved for rheumatoid arthritis	Roche and Chugai	Tocilizumab	Monoclonal humanized antibody to IL-6 receptor	Melton L et al ¹²⁰ Kudo M et al ¹²¹
Promising drugs in trials				
Phase 2 trials prostate cancer, multiple myeloma	Centocor	CNTO-328	Monoclonal chimeric antibody to IL-6	Melton L et al ¹²⁰ Zaki MH et al ¹²⁸
Phase 1 trials completed and Phase 2 trials pending	Avida, purchased by Amgen	C326 or AMG-220	Avimers	Silverman et al ¹³³ Sheridan C ¹³²